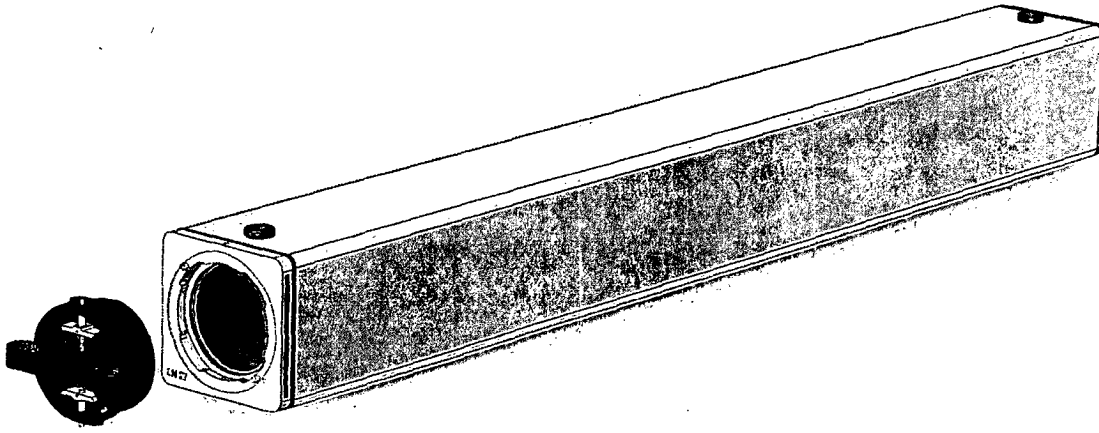


Safety Analysis Report



Advanced Test Reactor Fresh Fuel Shipping Container (ATR FFSC)

Revision 1, April 2008

Docket 71-9330



<i>Prepared by:</i>	<i>Prepared for:</i>
 AREVA AREVA Federal Services LLC	 <small>Idaho National Laboratory</small> Battelle Energy Alliance, LLC (BEA)

TABLE OF CONTENTS

1.0	General Information.....	1-1
1.1	Introduction.....	1-1
1.2	Package Description.....	1-2
1.2.1	Packaging.....	1-2
1.2.2	Contents	1-7
1.2.3	Special Requirements for Plutonium	1-9
1.2.4	Operational Features	1-9
1.3	Appendix.....	1-10
1.3.1	Glossary of Terms.....	1-10
1.3.2	Packaging and General Arrangement Drawings.....	1-10
2.0	Structural Evaluation	2-1
2.1	Structural Design	2-1
2.1.1	Discussion	2-1
2.1.2	Design Criteria	2-1
2.1.3	Weights and Centers of Gravity.....	2-3
2.1.4	Identification of Codes and Standards for Package Design.....	2-5
2.2	Materials	2-6
2.2.1	Mechanical Properties and Specifications	2-6
2.2.2	Chemical, Galvanic, or Other Reactions.....	2-7
2.2.3	Effects of Radiation on Materials	2-7
2.3	Fabrication and Examination	2-7
2.3.1	Fabrication	2-7
2.3.2	Examination	2-8
2.4	General Requirements for All Packages.....	2-8
2.4.1	Minimum Package Size	2-8
2.4.2	Tamper-Indicating Feature.....	2-8
2.4.3	Positive Closure	2-8
2.4.4	Valves	2-8
2.4.5	External Temperatures	2-9
2.5	Lifting and Tiedown Standards for All Packages.....	2-9
2.5.1	Lifting Devices.....	2-9
2.5.2	Tiedown Devices	2-11
2.5.3	Closure Handle.....	2-14
2.6	Normal Conditions of Transport.....	2-19
2.6.1	Heat.....	2-19
2.6.2	Cold.....	2-19
2.6.3	Reduced External Pressure	2-20
2.6.4	Increased External Pressure	2-20
2.6.5	Vibration	2-20
2.6.6	Water Spray	2-21
2.6.7	Free Drop	2-21
2.6.8	Corner Drop	2-22
2.6.9	Compression	2-22

2.6.10	Penetration	2-23
2.7	Hypothetical Accident Conditions	2-24
2.7.1	Free Drop	2-25
2.7.2	Crush	2-29
2.7.3	Puncture	2-29
2.7.4	Thermal	2-30
2.7.5	Immersion – Fissile Material	2-31
2.7.6	Immersion – All Packages	2-32
2.7.7	Deep Water Immersion Test	2-32
2.7.8	Summary of Damage	2-32
2.8	Accident Conditions for Air Transport Plutonium	2-40
2.9	Accident Conditions for Fissile Material Packages for Air Transport	2-40
2.10	Special From	2-40
2.11	Fuel Rods	2-40
2.12	Appendices	2-40
2.12.1	Certification Tests on CTU-1	2.12.1-1
2.12.2	Certification Tests on CTU-2	2.12.2-1
3.0	Thermal Evaluation	3-1
3.1	Description of Thermal Design	3-1
3.1.1	Design Features	3-2
3.1.2	Content's Decay Heat	3-3
3.1.3	Summary Tables of Temperatures	3-3
3.1.4	Summary Tables of Maximum Pressures	3-4
3.2	Material Properties and Component Specifications	3-6
3.2.1	Material Properties	3-6
3.2.2	Technical Specifications of Components	3-8
3.3	Thermal Evaluation for Normal Conditions of Transport	3-15
3.3.1	Heat and Cold	3-15
3.3.2	Maximum Normal Operating Pressure	3-16
3.4	Thermal Evaluation for Hypothetical Accident Conditions	3-20
3.4.1	Initial Conditions	3-20
3.4.2	Fire Test Conditions	3-21
3.4.3	Maximum Temperatures and Pressure	3-21
3.4.4	Maximum Thermal Stresses	3-23
3.5	Appendices	3-30
3.5.1	Computer Analysis Results	3-31
3.5.2	Analytical Thermal Model	3-31
4.0	Containment	4-1
4.1	Description of the Containment System	4-1
4.1.1	Type A Fissile Packages	4-1
4.1.2	Type B Packages	4-2
4.2	Containment under Normal Conditions of Transport	4-2
4.3	Containment under Hypothetical Accident Conditions	4-2
4.4	Leakage Rate Tests for Type B Packages	4-2

5.0	Shielding Evaluation.....	5-1
6.0	Criticality Evaluation.....	6-1
6.1	Description of Criticality Design.....	6-1
6.1.1	Design Features Important for Criticality.....	6-1
6.1.2	Summary Table of Criticality Evaluation.....	6-1
6.1.3	Criticality Safety Index.....	6-3
6.2	Fissile Material Contents.....	6-4
6.2.1	Fuel Element.....	6-4
6.2.2	Loose Fuel Plates.....	6-5
6.3	General Considerations.....	6-11
6.3.1	Model Configuration.....	6-11
6.3.2	Material Properties.....	6-14
6.3.3	Computer Codes and Cross-Section Libraries.....	6-15
6.3.4	Demonstration of Maximum Reactivity.....	6-15
6.4	Single Package Evaluation.....	6-24
6.4.1	Single Package Evaluation.....	6-24
6.4.2	Single Package Results.....	6-28
6.5	Evaluation of Package Arrays under Normal Conditions of Transport.....	6-33
6.5.1	NCT Array Configuration.....	6-33
6.5.2	NCT Array Results.....	6-37
6.6	Package Arrays under Hypothetical Accident Conditions.....	6-52
6.6.1	HAC Array Configuration.....	6-52
6.6.2	HAC Array Results.....	6-54
6.7	Fissile Material Packages for Air Transport.....	6-62
6.8	Benchmark Evaluations.....	6-63
6.8.1	Applicability of Benchmark Experiments.....	6-63
6.8.2	Bias Determination.....	6-64
6.9	Appendix.....	6-74
7.0	Package Operations.....	7-1
7.1	Package Loading.....	7-1
7.1.1	Preparation of Loading.....	7-1
7.1.2	Loading of Contents – ATR Fuel Assembly.....	7-1
7.1.3	Loading of Contents – Loose Fuel Plates.....	7-3
7.1.4	Preparation for Transport.....	7-4
7.2	Package Unloading.....	7-4
7.2.1	Receipt of Package from Conveyance.....	7-4
7.2.2	Removal of Contents.....	7-4
7.3	Preparation of Empty Package for Transport.....	7-5
7.4	Other Operations.....	7-5
8.0	Acceptance Tests and Maintenance Program.....	8-1
8.1	Acceptance Tests.....	8-1
8.1.1	Visual Inspections and Measurements.....	8-1
8.1.2	Weld Examinations.....	8-2

8.1.3	Structural and Pressure Tests	8-2
8.1.4	Leakage Tests.....	8-2
8.1.5	Component and Material Tests	8-2
8.1.6	Shielding Tests.....	8-2
8.1.7	Thermal Tests.....	8-2
8.1.8	Miscellaneous Tests	8-3
8.2	Maintenance Program	8-3
8.2.1	Structural and Pressure Tests	8-3
8.2.2	Leakage Rate Tests	8-3
8.2.3	Component and Material Tests	8-3
8.2.4	Thermal Tests.....	8-4
8.2.5	Miscellaneous Tests	8-4
9.0	Quality Assurance.....	9-1
9.1	Organization.....	9-1
9.1.1	ATR FFSC Project Organization	9-1
9.2	Quality Assurance Program	9-2
9.2.1	General	9-2
9.2.2	ATR FFSC-Specific Program	9-4
9.2.3	QA Levels	9-4
9.3	Package Design Control.....	9-10
9.4	Procurement Document Control	9-11
9.5	Instructions, Procedures, and Drawings.....	9-12
9.5.1	Preparation and Use	9-13
9.5.2	Operating Procedure Changes.....	9-13
9.5.3	Drawings	9-13
9.6	Document Control.....	9-13
9.7	Control Of Purchased Material, Equipment and Services	9-15
9.8	Identification And Control Of Material, Parts and Components	9-17
9.9	Control Of Special Processes.....	9-18
9.10	Internal Inspection	9-19
9.10.1	Inspections During Fabrication.....	9-20
9.10.2	Inspections During Initial Acceptance and During Service Life ..	9-21
9.11	Test Control	9-21
9.11.1	Acceptance and Periodic Tests	9-22
9.11.2	Packaging Nonconformance	9-22
9.12	Control Of Measuring and Test Equipment.....	9-22
9.13	Handling, Storage, And Shipping Control	9-23
9.14	Inspection, Test, And Operating Status	9-24
9.15	Nonconforming Materials, Parts, or Components	9-25
9.16	Corrective Action.....	9-27
9.17	Quality Assurance Records.....	9-27
9.17.1	General	9-28
9.17.2	Generating Records.....	9-29
9.17.3	Receipt, Retrieval, and Disposition of Records	9-29
9.18	Audits	9-31

1.0 GENERAL INFORMATION

This chapter of the Safety Analysis Report (SAR) presents a general introduction and description of the Advanced Test Reactor (ATR) Fresh Fuel Shipping Container (FFSC).¹ This application seeks validation of the ATR FFSC as a Type AF fissile materials shipping container in accordance with Title 10, Part 71 of the Code of Federal Regulations (10CFR71).

The major components comprising the package are discussed in Section 1.2.1, *Packaging*, and illustrated in Figure 1.2-1 through Figure 1.2-5. Detailed drawings of the package design are presented in Appendix 1.3.2, *Packaging General Arrangement Drawings*. A glossary of terms is presented in Appendix 1.3.1, *Glossary of Terms*.

1.1 Introduction

The ATR FFSC has been designed to transport unirradiated fuel. The principal payload is the ATR fuel used in the Advanced Test Reactor located in Idaho Falls, Idaho. This fuel consists of 19 aluminum-clad uranium aluminide (UAl_x) plates containing high-enriched uranium (HEU) enriched to a maximum of 94% U-235. The package can transport one ATR fuel element.

Additionally, the package is designed to transport fuel element plates that have either not yet been assembled into a fuel element or have been removed from an unirradiated fuel element. The fuel plates may be either flat or rolled to the geometry required for assembly into a fuel element.

Since the A_2 value of the payloads is low and radiation is negligible, the only safety function performed by the package is criticality control. This function is achieved, in the case of a transport accident, by confining the fuel element within the package and by maintaining separation of fuel in multiple packages. The ATR fuel itself is robust and inherently resists unfavorable geometry reconfiguration while contained within the package. For ease of handling and property protection purposes, the fuel assembly is contained within a lightweight aluminum housing referred to as the fuel handling enclosure. The loose fuel plates are contained in a loose plate basket which prevents the fuel from reconfiguring into an unfavorable geometry.

For the ATR fuel, the criticality control function is demonstrated via full-scale testing of a prototypic package followed by a criticality analysis using a model which bounds the test results, ensuring that the calculated $k_{\text{eff}} + 2\sigma$ is below the upper subcritical limit (USL) in the most limiting case. Two full-scale prototype models are used to perform a number of performance tests including normal conditions of transport (NCT) free drop and hypothetical accident condition (HAC) free drop and puncture tests.

¹ In the remainder of this Safety Analysis Report, *Advanced Test Reactor Fresh Fuel Shipping Container* will be abbreviated as *ATR FFSC*. In addition, the term 'packaging' will refer to the assembly of components necessary to ensure compliance with the regulatory requirements, but does not include the payload. The term 'package' includes both the packaging components and the payload of ATR fuel.

Authorization is sought for a Type A(F)-96, fissile material package per the definitions delineated in 10 CFR §71.4². Each ATR fuel element contains up to 1,200 grams of U-235 enriched to a maximum of 94% U-235. When shipping loose plates, the package is limited to a maximum fissile payload of 600 grams U-235.

The Criticality Safety Index (CSI) for the package, determined in accordance with the definitions of 10 CFR §71.59, is 4.0. The CSI is based on the number of packages for criticality control purposes (the method and the CSI determination are given in Chapter 6.0, *Criticality Evaluation*).

1.2 Package Description

This section presents a basic description of the ATR FFSC. General arrangement drawings are presented in Appendix 1.3.2, *Packaging General Arrangement Drawings*.

1.2.1 Packaging

1.2.1.1 Packaging Description

The ATR FFSC is designed as Type AF packaging for transportation of two payload types; ATR fuel elements and unassembled ATR fuel element plates. The packaging is rectangular in shape and is designed to be handled singly with slings, or by fork truck when racked. Package components are shown in Figure 1.2-1. Transport of the package is by highway truck. The maximum gross weight of the package loaded with an ATR fuel element is 280 pounds. The maximum gross weight of the package loaded with the ATR unassembled fuel plate payload is 290 pounds.

The ATR FFSC is a two part packaging consisting of the body and the closure. The body is single weldment that features square tubing as an outer shell and round tubing for the payload cavity. Three 1-inch thick ribs maintain spacing between the inner and outer shells. The components of the packaging are shown in Figures 1.2-2, 1.2-3, and 1.2-4 and are described in more detail in the sections which follow. With the exception of several minor components, all steel used in the ATR FFSC is ASTM Type 304 stainless steel. Components are joined using full-thickness fillet welds (i.e., fillet welds whose leg size is nominally equal to the lesser thickness of the parts joined) and full and partial penetration groove welds.

² Title 10, Code of Federal Regulations, Part 71 (10 CFR 71), *Packaging and Transportation of Radioactive Material*, 1-1-06 Edition.

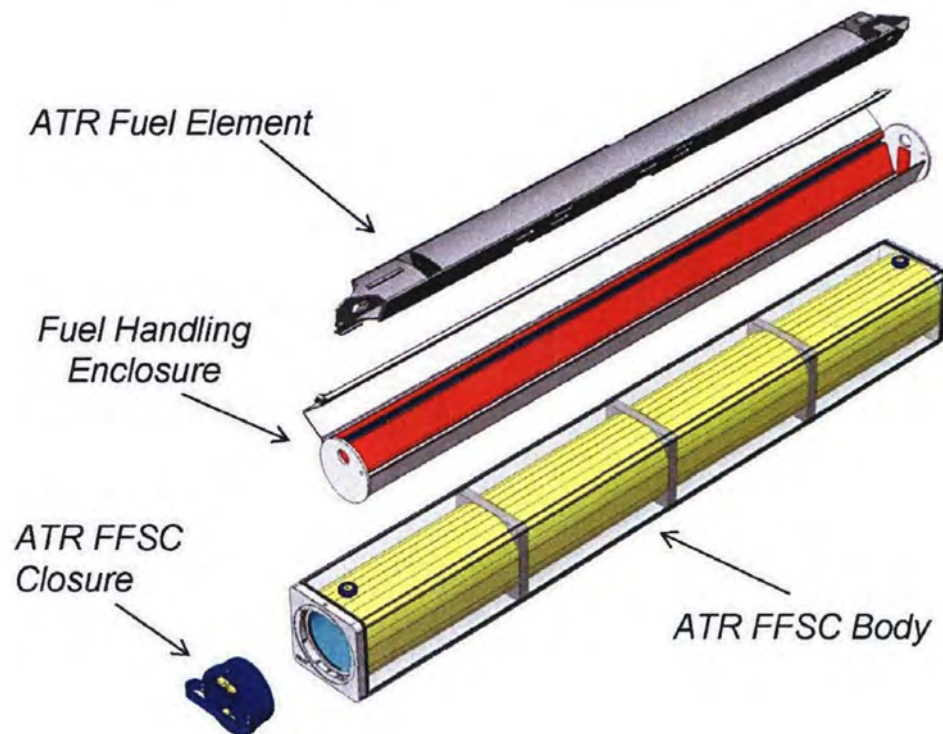


Figure 1.2-1 - Overview of the ATR FFSC (Outer Body Shell Shown Transparent)

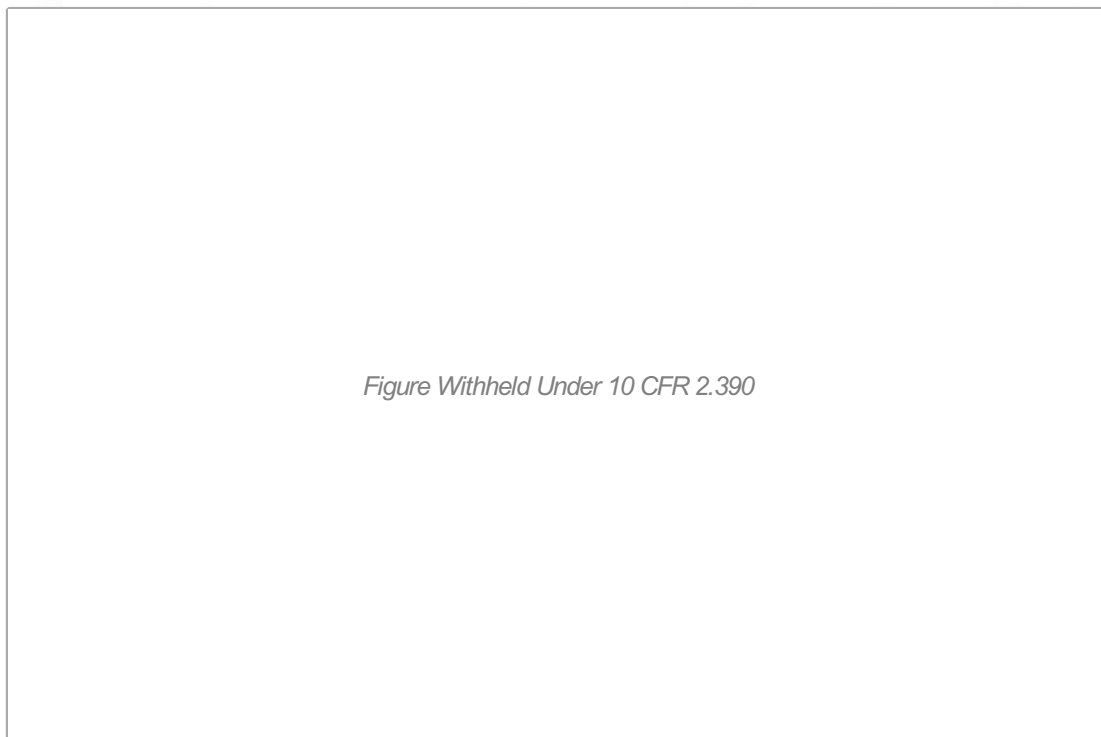


Figure 1.2-2 - Top End Body Sectional View



Figure Withheld Under 10 CFR 2.390

Figure 1.2-3 - Bottom End Body Sectional View



Figure Withheld Under 10 CFR 2.390

Figure 1.2-4 - Closure Sectional View

1.2.1.1.1 ATR FFSC Body

The ATR FFSC body is a stainless steel weldment 73 inches long and 8 inches square weighing (empty) approximately 230 lbs. It consists of two nested shells; the outer shell a square stainless steel tube with a 3/16 inch wall thickness and the inner shell a 6 inch diameter, 0.120 inch wall, stainless steel round tube. There are three 1 inch thick stiffening plates secured to the round tube by fillet welds at equally spaced intervals. The tube is wrapped with thermal insulation and the insulation is overlaid with 28 gauge stainless steel sheet. The stainless steel sheet maintains the insulation around the inner shell. This insulated weldment is then slid into the outer square tube shell and secured at both ends by groove welds. Thermal insulation is built into the bottom end of the package as shown in Figure 1.2-3, and the closure provides thermal insulation at the closure end of the package as shown in Figure 1.2-4.

1.2.1.1.2 ATR FFSC Closure

The closure is a small component designed to be easily handled by one person. It weighs approximately 10 pounds and is equipped with a handle to facilitate use with gloved hands. The closure engages with the body using a bayonet style design. There are four lugs, uniformly spaced on the closure, that engage with four slots in the mating body feature. The closure is secured by retracting two spring loaded pins, rotating the closure through approximately 45°, and releasing the spring loaded pins such that the pins engage with mating holes in the body. When the pins are properly engaged with the mating holes the closure is locked.

A small post on the closure is drilled to receive a tamper indicating device (TID) wire. An identical post is located on the body and is also drilled for the TID wire. For ease in operation, there are two TID posts on the body. There are only two possible angular orientations for the closure installation and the duplicate TID post on the body enables TID installation in both positions.

1.2.1.1.3 ATR FFSC Fuel Handling Enclosure

The Fuel Handling Enclosure (FHE) is a hinged thin gauge aluminum weldment used with the fuel assembly. The FHE is a cover used to protect the fuel from handling damage during ATR FFSC loading and unloading operations. It is a thin walled aluminum fabrication featuring a hinged lid and neoprene rub strips to minimize fretting of the fuel element side plates where they are in contact with the container.

During transport the FHE does not add strength to the package, or satisfy any safety requirement. For purposes of determining worst case reactivity, the FHE is assumed to be not present.

1.2.1.1.4 ATR FFSC Loose Fuel Plate Basket

The Loose Plate Fuel Basket is comprised of four identical machined segments joined by threaded fasteners (reference Figure 1.2-5). The fasteners joining the segments in the lengthwise direction are permanently installed. The package is opened/closed using the 8 hand tightened fasteners. For criticality control purposes during transport the loose fuel plate basket maintains the fuel plates within a defined dimensional envelope.

Additional aluminum plates may be used as dunnage to fill gaps between the fuel plates and the basket payload cavity. The dunnage is used for property protection purposes only.

1.2.1.2 Gross Weight

The maximum shipped weight of the ATR FFSC with the ATR fuel element is 280 lbs and the maximum shipped weight with the loose fuel payload is 290 lbs. Further discussion of the gross weight is presented in Section 2.1.3, *Weights and Centers of Gravity*.

1.2.1.3 Neutron Moderator/Absorption

There are no moderator or neutron absorption materials in this package.

1.2.1.4 Heat Dissipation

The uranium aluminide payload produces a negligible thermal heat load. Therefore, no special devices or features are needed or utilized in the ATR FFSC to dissipate heat. A more detailed discussion of the package thermal characteristics is provided in Chapter 3.0, *Thermal*.

1.2.1.5 Protrusions

The closure handle protrudes 1 3/8-inches from the face of the closure. The handle is secured to the closure by means of four 10-24 UNC screws. The screws will fail prior to presenting any significant loading to either the closure engagement lugs or the locking pins.

On one face of the package body, two index lugs are secured to the package to facilitate stacking of the packages. The opposite face of the package has pockets into which the index lugs nest. Each index lug is secured to the package by means of a 3/8-16 socket flat head cap screw. Under any load condition, the screw will fail prior to degrading the safety function of the package.

1.2.1.6 Lifting and Tiedown Devices

The ATR FFSC may be lifted from beneath utilizing a standard forklift truck when the package is secured to a fork pocket equipped pallet, or in a package rack. Swivel lift eyes may be installed in the package to enable package handling with overhead lifting equipment. The swivel eyes are installed after removing the 3/8-16 socket flat head cap screws and index lugs.

The threaded holes into which the swivel lift eyes are installed for the lifting the package are fitted with a 3/8-16 UNC screw and an index lug (see Figure 1.2-5) during transport. When the packages are stacked and the index lugs are nested in the mating pockets of the stacked packages, the index lugs can serve to carry shear loads between stacked packages.

1.2.1.7 Pressure Relief System

There are no pressure relief systems included in the ATR FFSC design. There are no out-gassing materials in any location of the package that are not directly vented to atmosphere. The package insulation, located in the enclosed volumes of the package, is a ceramic fiber. The insulation does not off-gas under normal or hypothetical accident conditions. The closure is not equipped with either seals or gaskets so that potential out-gassing of the ATR fuel tray neoprene material and fuel plastic bag material will readily vent without significant pressure build-up in the payload cavity.

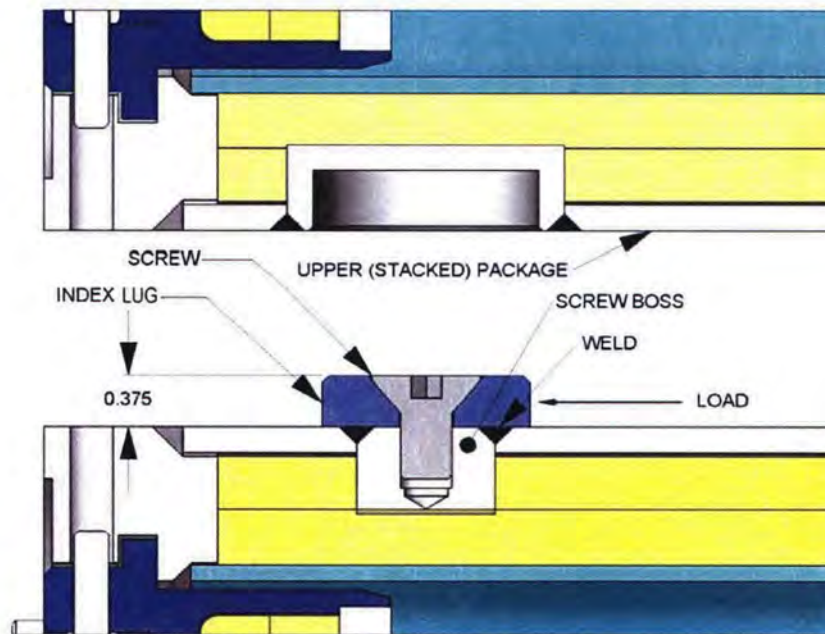


Figure 1.2-5 - Index Lug and Mating Pocket of Stacked Packages

1.2.1.8 Shielding

Due to the nature of the uranium aluminide payload, no biological shielding is necessary or specifically provided by the ATR FFSC.

1.2.2 Contents

The ATR FFSC is loaded with radioactive contents consisting of un-irradiated ATR fuel elements, enriched to a maximum of 94% U-235. The weight percents of the remaining uranium isotopes are 1.2 wt.% U-234 (max), 0.7 wt.% U-236 (max), and 5.0-7.0 wt.% U-238. Each fuel element contains a maximum of 1,200 g U-235. The fuel element (ATR Mark VII) fissile material is uranium aluminide (UAl_x). The fuel element weighs not more than 25 lbs, is bagged, and is enclosed in the FHE weighing 15 lbs.

There are four different ATR Mark VII fuel element types designated 7F, 7NB, 7NBH, and YA. The construction of these fuel elements are identical, varying only in the content of the fuel matrix. In the 7F fuel element, all 19 fuel plates are loaded with enriched uranium in an aluminum matrix with the eight outer plates (1 through 4 and 16 through 19) containing boron as a burnable poison. The fuel element with the greatest reactivity is the 7NB which contains no burnable poison. The 7NBH fuel element is similar to the 7NB fuel element except that it contains one or two borated plates. The YA fuel element is identical to the 7F fuel element except that plate 19 of the YA fuel element is an aluminum alloy plate containing neither uranium fuel nor boron burnable poison. The total U-235 and B-10 content of the YA fuel element is reduced accordingly. A second YA fuel element design (YA-M) has the side plate width reduced by 15 mils.

The ATR fuel elements contain 19 curved fuel plates. A section view of an ATR fuel element is given in Figure 1.2-6. The fuel plates are rolled to shape and swaged into the two fuel element side plates. Fuel plate 1 has the smallest radius, while fuel plate 19 has the largest radius. The fissile material (uranium aluminide) is nominally 0.02-in thick for all 19 plates. Fuel element side plates are fabricated of ASTM B 209, aluminum alloy 6061-T6 or 6061-T651 and are approximately 0.19-in thick. The fuel plates are typically spaced with a 0.08-in gap between plates.

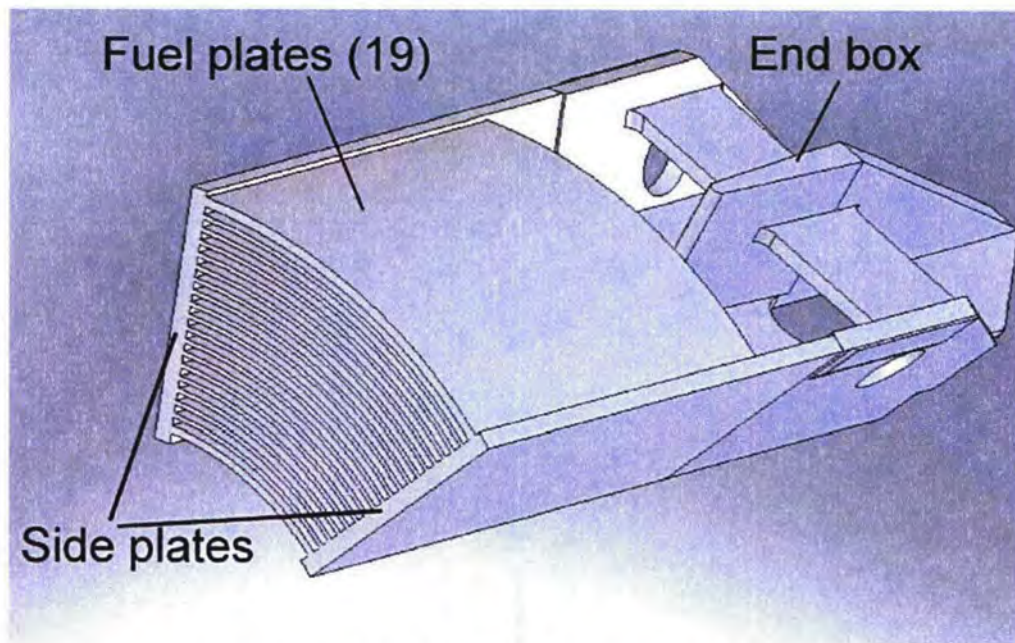


Figure 1.2-6 - ATR Fuel Element – Section View

The maximum weight of the ATR fuel loose plate payload (Figure 1.2-7) is 50 lbs. This weight is made up of the maximum basket contents weight of 20 lbs and the loose fuel plate basket weight of 30 lbs.

The loose plate payload is limited to 600 grams U-235. The plates may either be flat or rolled to the geometry required for assembly into the ATR fuel element. For handling convenience, the loose plate basket will be loaded with either flat or rolled plates. Additionally, the plates may be banded or wire tied in a bundle.

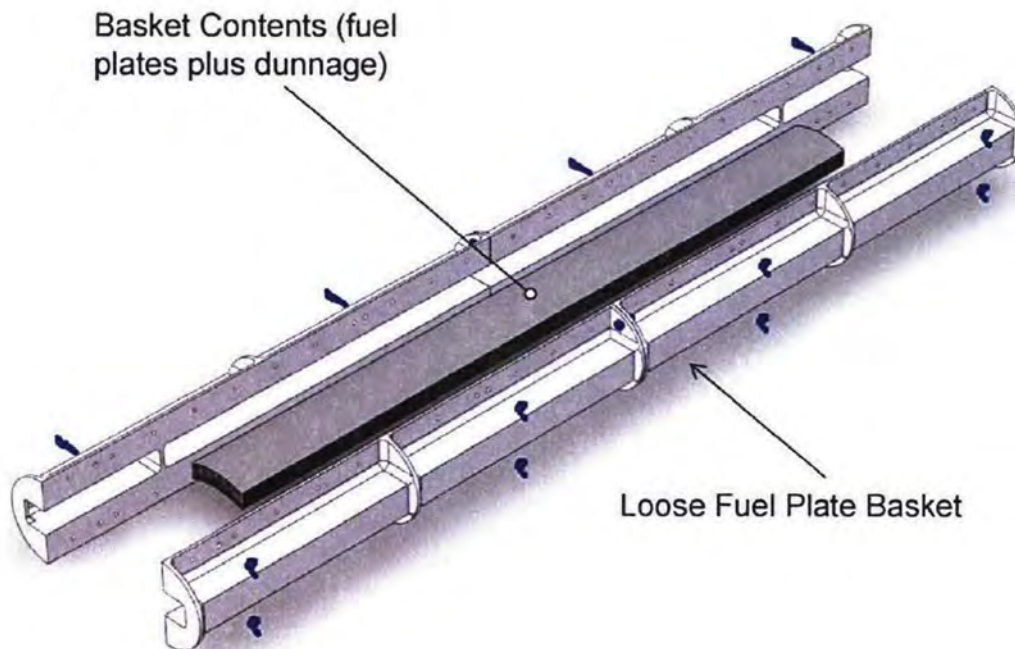


Figure 1.2-7 - Loose Fuel Plate Basket – Exploded View

1.2.3 Special Requirements for Plutonium

Because the ATR FFSC does not contain any plutonium, this section does not apply.

1.2.4 Operational Features

There are no operationally complex features in the ATR FFSC. All operational features are readily apparent from an inspection of the drawings provided in Appendix 1.3.2, *Packaging General Arrangement Drawings*. Operation procedures and instructions for loading, unloading, and preparing an empty ATR FFSC for transport are provided in Chapter 7.0, *Operating Procedures*.

1.3 Appendix

1.3.1 Glossary of Terms

ANSI –	American National Standards Institute.
ASME B&PV Code –	American Society of Mechanical Engineers Boiler and Pressure Vessel Code.
ASTM –	American Society for Testing and Materials.
AWS –	American Welding Society.
HAC –	Hypothetical Accident Conditions.
NCT –	Normal Conditions of Transport.
Closure –	The ATR FFSC package component used to close the package.
Body –	The ATR FFSC package component which houses the payload.
Index lug –	A thick washer like component secured to the package body at the lift point locations. The index lug provides shear transfer capability between stacked packages.
Pocket –	A recessed feature on the package body that accepts the index lug when packages are stacked.
Fuel Handling Enclosure (FHE)–	A sheet aluminum fabrication used to protect the ATR Fuel Element from handling damage. The enclosure is faced with neoprene at locations where the fuel element contacts the FHE to minimize fretting of the at the contact points.
Loose plate basket –	A machined aluminum container in which the unassembled ATR fuel element plates are secured during transport in the ATR FFSC. The loose plate basket is a geometry based criticality control component.

1.3.2 Packaging General Arrangement Drawings

The packaging general arrangement drawings consist of:

- 60501-10, *ATR Fresh Fuel Shipping Container SAR Drawing*, 5 sheets
- 60501-20, *Loose Plate Basket Assembly ATR Fresh Fuel Shipping Container SAR Drawing*, 1 sheet
- 60501-30, *Fuel Handling Enclosure, ATR Fresh Fuel Shipping Container SAR Drawing*, 1 sheet

Figure Withheld Under 10 CFR 2.390

Figure Withheld Under 10 CFR 2.390

Figure Withheld Under 10 CFR 2.390

Figure Withheld Under 10 CFR 2.390

Figure Withheld Under 10 CFR 2.390

Figure Withheld Under 10 CFR 2.390

Figure Withheld Under 10 CFR 2.390

2.0 STRUCTURAL EVALUATION

This section presents evaluations demonstrating that the Advanced Test Reactor (ATR) Fresh Fuel Shipping Container (FFSC) package meets all applicable structural criteria. The ATR FFSC packaging, consisting of the body and closure, is evaluated and shown to provide adequate protection for the payload. Normal conditions of transport (NCT) and hypothetical accident condition (HAC) evaluations are performed to address 10 CFR §71¹ performance requirements primarily through physical testing. Physical demonstration by testing, including the free drop and puncture events, consists of certification testing utilizing two full-scale certification test units (CTU-1 and CTU-2). CTU-1 included the ATR fuel element payload and CTU-2 included the ATR loose fuel plate basket (LFPB) and loose plates payload. Certification testing has demonstrated that the key performance objective of criticality control will be met by the ATR FFSC package. Details of the certification test program are provided in Appendix 2.12.1, *Certification Tests on CTU-1*, and Appendix 2.12.2, *Certification Tests on CTU-2*.

2.1 Structural Design

2.1.1 Discussion

The ATR FFSC is a two part packaging consisting of the body and the closure. The body is a single weldment that features square tubing as an outer shell and round tubing for the payload cavity. The closure engages with the body using a bayonet style design. There are four lugs, uniformly spaced on the closure that engages with four slots in the mating body feature. The closure is secured by retracting two spring loaded pins, rotating the closure through approximately 45°, and releasing the spring loaded pins such that the pins engage with mating holes in the body. When the pins are properly engaged with the mating holes the closure is locked.

With the exception of several minor components, all steel used in the ATR FFSC packaging is of a Type 304 stainless steel. Components are joined using full-thickness fillet welds (i.e., fillet welds whose leg size is nominally equal to the lesser thickness of the parts joined) and full and partial penetration groove welds. The fuel containers for the package, the FHE and the LFPB, are principally of aluminum construction and secured with stainless steel fasteners. The FHE is a fabrication and the LFPB consists of four machined aluminum components.

A comprehensive discussion of the ATR FFSC packaging design and configuration is provided in Section 1.2, *Package Description*.

2.1.2 Design Criteria

The ATR FFSC package has been designed to meet the majority of applicable structural requirements of 10 CFR §71 through physical testing. The design objectives for the package are threefold:

¹ Title 10, Code of Federal Regulations, Part 71 (10 CFR §71), *Packaging and Transportation of Radioactive Material*, 01-01-06 Edition.

1. For NCT, demonstrate that the ATR FFSC package contains the payload without dispersal and that it does not experience a significant reduction in its effectiveness to withstand HAC; and
2. For HAC, demonstrate that the ATR FFSC package contains the payload without dispersal, consistent with conservative bounding assumptions utilized in the criticality analysis.
3. For HAC, demonstrate that the insulation used in the ATR FFSC package remains in place, to protect the payload from excessive heat from the thermal test, within the assumptions utilized in the thermal analysis.

Consequently, the design criteria for NCT are that the ATR FFSC package exhibit only minor damage subsequent to the NCT conditions and tests, including no damage that would materially affect the outcome of the subsequent HAC tests.

For HAC, the design criteria is that the payload will be retained within the packaging subsequent to the HAC test series of free drop, puncture, thermal, and the immersion test of 10 CFR §71.73(c)(5), or subsequent to immersion of an undamaged specimen per 10 CFR §71.73(c)(6).

Material properties are controlled by the acquisition of critical components to ASTM standards, testing, and process control, as described in Section 2.2, *Materials*. Lifting devices that are a structural part of the package are designed with a minimum safety factor of three against yielding. The index lugs located at the top of the package are considered a tiedown devices and are designed to withstand the loading requirements per 10 CFR §71.45(b)(1).

2.1.2.1 Miscellaneous Structural Failure Modes

2.1.2.1.1 Brittle Fracture Assessment

The steel materials utilized in the ATR FFSC package provide adequate fracture toughness. All critical structural components of the packaging are made of Type 304 stainless steel and have a nil ductility transition temperature less than -40°F (-40°C). Therefore, brittle fracture is not a concern for the ATR FFSC packaging.

To confirm the performance of the ATR fuel element at reduced temperatures CTU-1, was subjected to two HAC drops with the payload at approximately -20°F (-29°C). Following all CTU-1 testing, as discussed in Appendix 2.12.1, *Certification Tests on CTU-1*, the package was disassembled and the payload inspected. Upon inspection, the performance of both the payload and packaging, including the reduced temperature tests, was satisfactory. Following all testing, the payload remained within the assumptions presented in Section 6.0, *Criticality Evaluation*.

2.1.2.1.2 Fatigue Assessment

Normal operating cycles do not present a fatigue concern for the ATR FFSC. The packaging does not retain pressure, and consequently fatigue due to pressure cycling cannot occur. Since all structural components of the packaging are made of the same alloy, and since thermal gradients are small, thermally-induced fatigue is not of concern. Since the packaging is normally handled on a pallet, the lifting features of the packaging are infrequently used, and fatigue of the lifting load path is not of concern.

The only components which are routinely handled are the closure and the fuel handling structures (fuel handling enclosure and loose plate basket). The closure is designed as a bayonet-type attachment with two spring-loaded locking pins which prevent rotation during transport. Neither the bayonet lugs nor the locking pins experience any significant loading (such as preload or other repeating mechanical loads) in routine usage. If damage to these components were to occur, it will be identified during the inspections discussed in Section 7.1.1, *Preparation for Loading*. Consequently, fatigue of the closure components is not of concern.

The fuel handling structures (fuel handling enclosure and loose plate basket) are simple structures that do not have significant handling loads. These structures are fully exposed to view during loading and unloading, and can be inspected to ensure integrity.

For these reasons, normal operating cycles are not a failure mode of concern for the ATR FFSC packaging. Fatigue associated with normal vibration over the road is discussed in Section 2.6.5, *Vibration*.

2.1.2.1.3 Buckling Assessment

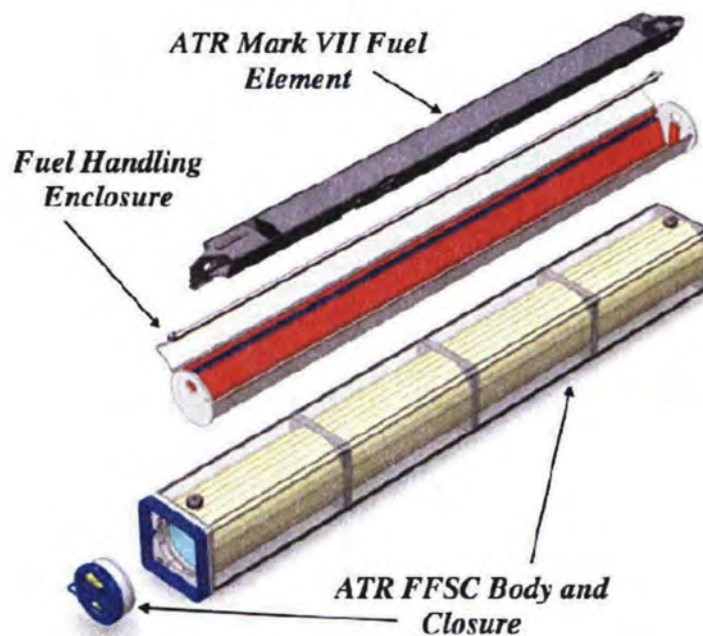
Certification testing has demonstrated that buckling of the ATR FFSC package does not occur as a result of any normal conditions of transport or as a result of the HAC primary test sequence (e.g., the free drop and puncture tests). Buckling of the ATR FFSC body is also shown to not be a concern during the 50 ft immersion test specified under 10 CFR §71.73(c)(6). A discussion of the response to the 50 ft immersion test is provided in Section 2.7.6, *Immersion – All Packages*.

2.1.3 Weights and Centers of Gravity

The maximum gross weight of the ATR FFSC package is 290 lb. The packaging component weights are summarized in Table 2.1-1. The maximum payload weight is 50 lb, for the loose plate payload, and 40 lb for the fuel assembly. Due to symmetry of design, the center of gravity (CG) of the package is located essentially at the geometric center of the package. With either payload, the center of gravity is 35 inches from the face of the closure end and 4 inches from the bottom and sides of the package. The packaging components are illustrated in Figure 2.1-1 and Figure 2.1-2.

Table 2.1-1 – ATR FFSC Component Weights

Item	Weight, lb	
	Component	Assembly
ATR FFSC Packaging	--	240
Body Assembly	230	--
Closure Assembly	10	--
Payload – Fuel Assembly	--	40
Fuel Assembly	25	--
Fuel Handling Enclosure	15	--
Payload – Fuel Plates	--	50
Loose Fuel Plates (including optional dunnage)	20	--
Loose Fuel Plate Basket	30	--
Total Loaded Package (maximum)		290

**Figure 2.1-1 – ATR FFSC Package Components (With Fuel Element)**

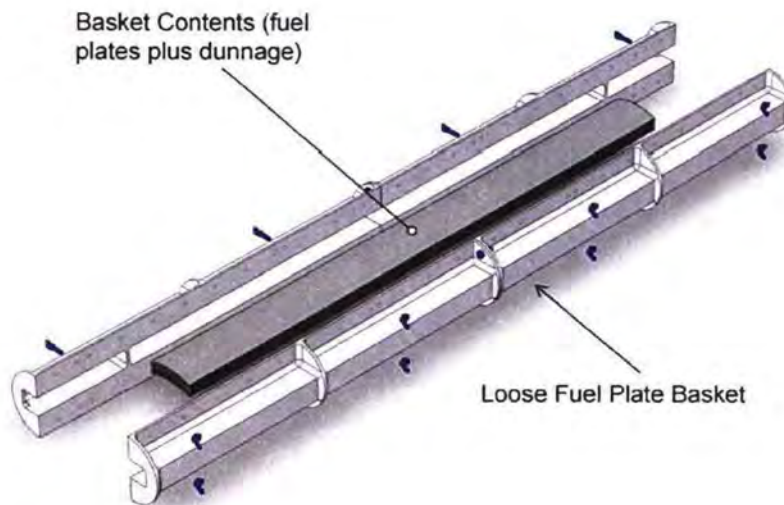


Figure 2.1-2 – ATR FFSC Loose Fuel Plate Basket Components

2.1.4 Identification of Codes and Standards for Package Design

As a Type AF package, the ATR FFSC is designed to meet the performance requirements of 10 CFR 71, Subpart E. Compliance with these requirements is demonstrated via full scale testing of the package under both NCT and HAC, as documented in Section 2.12, *Appendices*. In addition, structural materials which are important to safety are specified using American Society for Testing and Materials (ASTM) standards as shown on the drawings in Appendix 1.3.2, *Packaging General Arrangement Drawings*. Welding procedures and personnel are qualified in accordance with the ASME Code, Section IX. All welds are visually examined on each pass per the requirements of AWS D1.6:1999² for stainless steel and AWS D1.2:2003³ for aluminum. All welds which are important to safety are examined by liquid penetrant test on the final pass using procedures compliant with ASTM E165-02⁴.

² ANSI/AWS D1.6:1999, *Structural Welding Code – Stainless Steel*, American Welding Society (AWS).

³ ANSI/AWS D1.2:2003, *Structural Welding Code – Aluminum*, American Welding Society (AWS)

⁴ American Society for Testing and Materials (ASTM International), ASTM E165-02, *Standard Test Method for Liquid Penetrant Examination*, Feb 2002.

2.2 Materials

The ATR FFSC package is constructed primarily from Type 304 stainless steel structural materials. The drawings presented in Appendix 1.3.1, *Packaging General Arrangement Drawings*, delineate the specific materials used for each ATR FFSC packaging components.

2.2.1 Mechanical Properties and Specifications

Since the demonstration of compliance with the regulations is primarily via performance testing of full-scale prototypes, analytical structural evaluations are in general not performed.

Properties of structural materials are controlled either by purchase to an ASTM or other standard or via a written specification.

2.2.1.1 Stainless Steel

All of the structural steel used in the ATR FFSC packaging is an ASTM grade stainless steel. The weld consumable material is ASTM Type 308-308L, which results in weld metal deposits which have properties at least as great as the base metal. The minimum properties of the stainless steel items are given in Table 2.2-1.

Table 2.2-1 –Material Properties of Stainless Steel

Material	Yield Strength, minimum, psi	Ultimate Strength, minimum, psi
ASTM A240 Type 304	30,000	75,000
ASTM A269 Type 304	30,000	75,000
ASTM A276 Type S21800	50,000	95,000
ASTM A479 Type 304	30,000	75,000
ASTM A554 Grade MT-304	30,000	75,000

2.2.1.2 Aluminum

The internal FHE and LFPB are fabricated from aluminum alloy. Minimum material properties are given in table 2.2-2.

Table 2.2-2 –Material Properties of Aluminum

Material	Yield Strength, minimum, psi	Ultimate Strength, minimum, psi
ASTM B209, Alloy 5052 – H32	23,000	31,000
ASTM B209, Alloy 6061 – T651, 4" Plate	35,000	40,000

2.2.2 Chemical, Galvanic, or Other Reactions

The materials of construction of the ATR FFSC packaging are primarily Type 304 stainless steel and refractory insulation. Since these materials are relatively unreactive, no excessive corrosion or other reactions will occur during normal use. The package is normally transported in a closed van, and is not subject to immersion or exposure to water or chemicals other than occasional precipitation or mild cleaning agents. In addition, all of these materials have been used in Type A and Type B packagings for many years without incident. If unusual corrosion of the stainless steel components occurs, it can be readily detected during preparation of the packaging for use. The refractory insulation is sealed within the body and is not subject to chemical degradation or corrosion during normal use.

The payloads, consisting of either the FHE and fuel element or the LFPB and fuel plates, are constructed primarily of aluminum alloy. There is no galvanic or other reactions between the stainless steel package and aluminum alloy payload. Furthermore, the FHE and LFPB are inspected prior to placement within the packaging.

2.2.3 Effects of Radiation on Materials

Since the payload of the ATR FFSC consists of contact handled un-irradiated ATR fuel elements, enriched to a maximum of 94% U-235, the radiation from the payload is insignificant. Consequently, there will be no radiation effects on the materials of construction and the requirements of 10 CFR §71.43(d) are met.

2.3 Fabrication and Examination

2.3.1 Fabrication

The metallic components of the ATR FFSC packaging are fabricated using conventional metal forming and welding techniques. Structural materials which are important to safety are specified using American Society for Testing and Materials (ASTM) standards as shown on the drawings in Appendix 1.3.2, *Packaging General Arrangement Drawings*. All materials and components are procured and assembled under a 10 CFR 71, Subpart H quality assurance program. Welding procedures and personnel are qualified in accordance with the ASME Code, Section IX. Each packaging and its components are fabricated in accordance with the requirements delineated on the drawings in Appendix 1.3.2, *Packaging General Arrangement Drawings*.

2.3.2 Examination

Each packaging and its components are examined per the requirements delineated on the drawings in Appendix 1.3.2, *Packaging General Arrangement Drawings*. All welds are visually examined on each pass per the requirements of AWS D1.6:1999 for stainless steel and AWS D1.2:2003 for aluminum. All welds which are important to safety are examined by liquid penetrant test on the final pass using procedures compliant with ASTM E165-02. Personnel performing NDE shall be qualified in accordance with ASNT SNT-TC-1A⁵. Any deviations from SAR drawing requirements will be dispositioned and corrected under a 10 CFR 71, Subpart H quality assurance program prior to the application of the model number, per 10 CFR §71.85(c).

2.4 General Requirements for All Packages

This section defines the general standards for all packages. The ATR FFSC package meets all requirements of this section.

2.4.1 Minimum Package Size

The minimum dimension of the ATR FFSC package is 8 inches square. Thus, the 4 inch minimum requirement of 10 CFR §71.43(a) is satisfied.

2.4.2 Tamper-Indicating Feature

A tamper-indicating device (TID) lock wire and seal is installed through a small post on the closure provided to receive the wire. An identical post is located on the body for the TID wire. For ease in operation, there are two TID posts on the body. There are only two possible angular orientations for the closure installation and the duplicate TID post on the body enables TID installation in both positions. Thus, the requirement of 10 CFR §71.43(b) is satisfied.

2.4.3 Positive Closure

The ATR FFSC package cannot be opened unintentionally. The closure engages with the body using a bayonet style design. There are four lugs, uniformly spaced on the closure, that engage with four slots in the mating body feature. The closure is secured by retracting two spring loaded pins, rotating the closure through approximately 45°, and releasing the spring loaded pins such that the pins engage with mating holes in the body. When the pins are properly engaged with the mating holes the closure is locked. Thus, the requirements of 10 CFR §71.43(c) are satisfied.

2.4.4 Valves

The ATR FFSC does not contain any valves.

⁵ American Society for Nondestructive Testing (ASNT), Recommended Practice No. ASNT SNT-TC-1A, 2001 Edition.

2.4.5 External Temperatures

As discussed in Section 3.3.1.1, *Maximum Temperatures*, the maximum accessible surface temperature with no insolation is 100°F (38°C). Since the maximum external temperature does not exceed 122°F (50°C), the requirements of 10 CFR §71.43(g) are satisfied.

2.5 Lifting and Tiedown Standards for All Packages

2.5.1 Lifting Devices

The ATR FFSC package may be lifted from beneath utilizing a standard forklift truck when the package is secured to a fork pocket equipped pallet, or in a package rack. Swivel lift eyes can be installed in the package to enable package handling with overhead lifting equipment. The swivel eyes are installed after removing the 3/8-16 socket flat head cap screws and index lugs used for stacking.

Assuming both lift eyes carry half the load, the weight at each lug is:

$$P = \left(\frac{290}{2} \right) = 145 \text{ lbf}$$

Applying a minimum horizontal sling angle of 30°, the maximum load on each sling is:

$$T = \frac{145}{\sin(30)} = 290 \text{ lbf}$$

Therefore, all lifting devices shall have a minimum working load limit of 300 lb.

2.5.1.1 Attachment Capacity

Per 10 CFR §71.45(a) any lifting attachment that is a structural part of the package must be designed with a minimum safety factor of three against yielding. This evaluation verifies the adequacy of the groove weld securing the threaded bar to the wall of the 8 inch square tube. By inspection, the groove weld is the weakest point of the lifting point and all other items will have a greater margin of safety. The lift eye is required to have a minimum working load limit of 300 lb. The lift eye components are therefore assumed to meet the lifting requirements.

The allowable force on the groove weld is equal to the shear strength of the base material, $0.6 \cdot \sigma_{\text{yield}}$.

Allowable weld stresses:

$$\sigma_{\text{yield}} = 30,000 \text{ psi}$$

$$w_{\text{allow}} = 0.6 \cdot 30,000 = 18,000 \text{ psi}$$

Maximum tension in each of the two lift slings is 290 lbf at an angle of 30°.

$$T_y = P = 145 \text{ lbf}$$

$$T_x = 290 \cdot \cos(30) = 251 \text{ lbf}$$

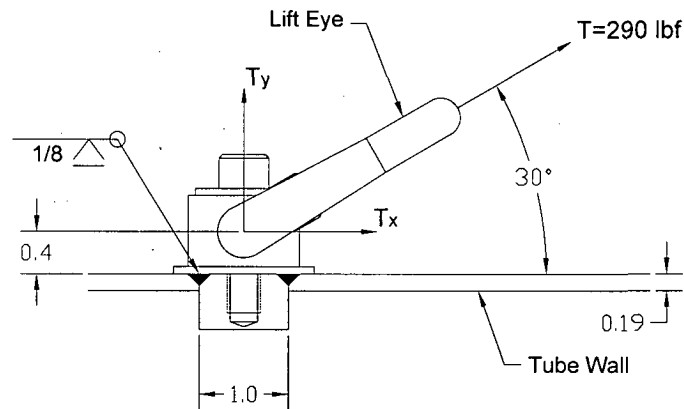


Figure 2.5-1 – Lift Attachment Diagram

Including the safety factor of three, the maximum horizontal and vertical forces are:

$$P_h = 3 \cdot T_x = 753 \text{ lbf}$$

$$P_v = 3 \cdot T_y = 435 \text{ lbf}$$

Using Blodgett⁶, the given load is divided by the length of the weld to arrive at the applied unit force, lb per linear inch of weld. From this force, the proper throat of the groove weld is determined.

The properties of the weld, treated as a line, are:

$$A_w = \pi \cdot d$$

$$S_w = \frac{\pi \cdot d^2}{4}$$

Where,

d = diameter of weld = 1.0 inch

$$A_w = \pi \cdot (1) = 3.14 \text{ in}$$

$$S_w = \frac{\pi \cdot (1)^2}{4} = 0.785 \text{ in}^2$$

Vertical tension on the weld is:

$$f_v = \frac{P_v}{A_w} = \frac{435}{3.14} = 139 \frac{\text{lbf}}{\text{in}}$$

Horizontal shear on the weld is:

⁶ Omer Blodgett, *Design of Welded Structures*, 1982, The James F. Lincoln Arc Welding Foundation, Cleveland, Ohio.

$$f_h = \frac{P_h}{A_w} = \frac{753}{3.14} = 240 \frac{\text{lb}f}{\text{in}}$$

The bending force on the weld is

h = height of applied load from lift eye = 0.4 in, plus half of the weld thickness of 0.125/2

$$h = 0.4 + (.125 / 2) = 0.463 \text{ in}$$

$$M = P_h \cdot h = 753 \cdot 0.463 = 349 \text{ in} \cdot \text{lb}$$

$$f_b = \frac{M}{S_w} = \frac{349}{0.785} = 445 \frac{\text{lb}f}{\text{in}}$$

The vertical tension and bending forces are in the same direction and additive:

$$f_{v+b} = f_v + f_b = 139 + 445 = 584 \frac{\text{lb}f}{\text{in}}$$

The vertical and horizontal loads are perpendicular, therefore the combined load is:

$$f_r = \sqrt{(f_{v+b})^2 + f_h^2} = \sqrt{(584)^2 + (240)^2} = 631 \frac{\text{lb}f}{\text{in}}$$

The required groove weld is:

$$w = \frac{f_r}{w_{allow}} = \frac{631}{18,000} = 0.035 \text{ in}$$

Thus the weld margin of safety is:

$$MS_{weld} = \frac{.125}{.035} - 1 = +2.6$$

2.5.1.2 Conclusion

From the above analyses, the lifting attachment points adequately lift the fully loaded package with a margin of safety of 2.6. The conservative minimum lifting angle of the slings is 30° above horizontal. Failure of this lifting component under excessive load would not impair the ability of this package to meet other requirements of 10 CFR §71, per the requirements of 10 CFR §71.45(a).

2.5.2 Tiedown Devices

For transport, the package will be strapped or otherwise restrained inside or on the transport vehicle. Any features used to lift the ATR FFSC will be removed or rendered unusable for tiedown. The index lugs used to align the package during stacking are evaluated for the tiedown loads. Per 10 CFR §71.45(b)(1) the tiedown system must withstand a vertical loading of 2g, horizontal for/aft loading of 10g, and horizontal lateral loading of 5g. Because there is no vertical restraint capability of the index lug, the 2g vertical load is neglected. Combining the

loads, the maximum horizontal g loading is $\sqrt{10^2 + 5^2} = 11.18g$. The loaded ATR FFSC package weighs 290 lb.

2.5.2.1 Tiedown Method

The ATR FFSC may be stacked in a 4 wide by 3 high array during transport. The packages are secured by means which resist the vertical loading. However, any axial/lateral restraint is conservatively neglected.

The index lugs at each end of the packages are used to align and secure the packages within the array and are subjected to g-loads from neighboring packages. The index lugs are attached to the package by a single flat head, socket cap screw such that horizontal loading causes shearing in the threaded area of the screw as shown in Figure 2.5-2.

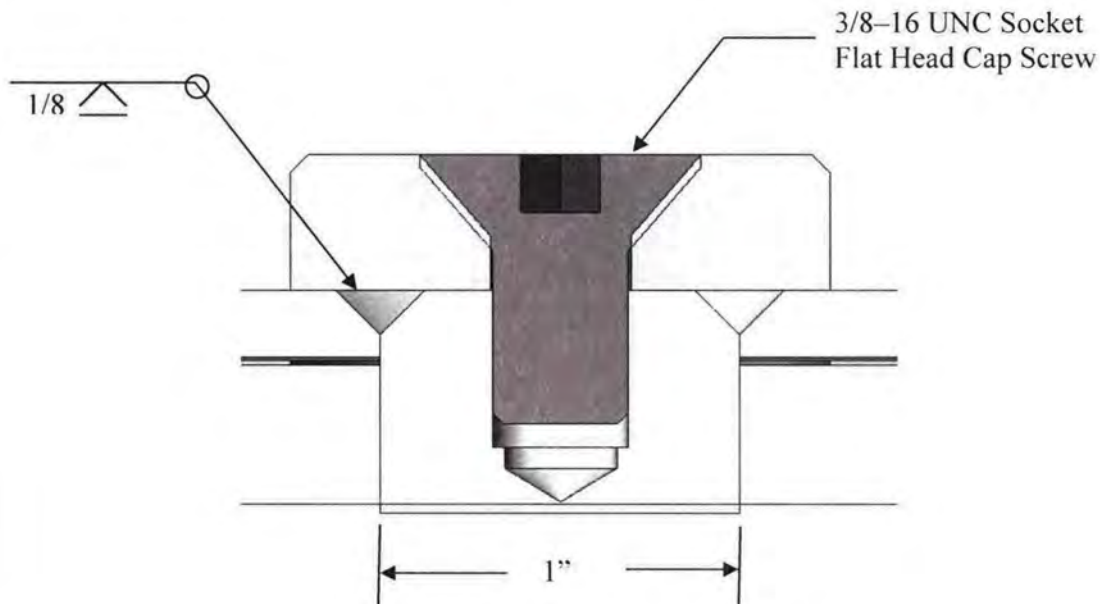


Figure 2.5-2 – Index Lug

2.5.2.2 Tiedown Capacity

By assuming the package is not restrained horizontally, the index lugs of the first tier must resist the horizontal loading of the middle and top tiers. The maximum load on each button is 2W times the g loading.

$$P_h = \frac{(2)(290)(11.18)}{2} = 3,242 \text{ lbf}$$

2.5.2.3 Fasteners

The screw thread shear area is 0.0775 in^2 and the screw material is ASTM F835 which has minimum tensile strength of 145 ksi. The yield strength is 116 ksi; conservatively assuming yield to be 80% of tensile strength for alloy steel. The shear force allowable is $0.6\sigma_{\text{yield}}$.

$$\text{Fastener shear stress} = \frac{3,242}{0.0775} = 41,832 \text{ psi}$$

$$MS = \frac{(116,000)(.6)}{41,832} - 1 = +0.66$$

The load required to fail the screw is:

$$P_{h-\text{failure}} = 0.6 \cdot \sigma_{\text{ult}} \cdot A = (0.6 \cdot 145,000) \cdot (0.0775) = 6,743 \text{ lbf}$$

2.5.2.4 Weld Structure

The allowable force on the groove weld is equal to the shear strength of the base material, $0.6\sigma_{\text{yield}}$.

Allowable weld stresses:

$$\sigma_{\text{yield}} = 30,000 \text{ psi}$$

$$w_{\text{allow}} = 0.6 \cdot 30,000 = 18,000 \text{ psi}$$

Using Blodgett, the given load is divided by the length of the weld to arrive at the applied unit force, lb per linear inch of weld. From this force, the proper throat of the groove weld is determined.

The properties of the weld, treated as a line, are:

$$A_w = \pi \cdot d$$

$$S_w = \frac{\pi \cdot d^2}{4}$$

Where,

d = diameter of weld = 1.0 inch

$$A_w = \pi \cdot (1) = 3.14 \text{ in}$$

$$S_w = \frac{\pi \cdot (1)^2}{4} = 0.785 \text{ in}^2$$

Horizontal shear on the weld is:

$$f_h = \frac{P_h}{A_w} = \frac{3,242}{3.14} = 1,033 \text{ lbf/in}$$

Assume for simplicity that the index lug diameter matches that of the weld (conservative). The moment on the weld is equal to the applied load times the distance from the weld c.g. to the mid-height of the 3/8 inch high index lug, or:

$$\frac{0.125}{2} + \frac{0.375}{2} = 0.25 \text{ in}$$

The bending force on the weld, as a vertical component, is

h = height of applied load to index lug = 0.25 in

$$M = P_h \cdot h = 3,242 \cdot 0.25 = 811 \text{ in} \cdot \text{lb}$$

$$f_b = \frac{M}{S_w} = \frac{811}{0.785} = 1,033 \text{ lbf / in}$$

The vertical and horizontal loads are perpendicular, therefore the combined load is:

$$f_r = \sqrt{f_b^2 + f_h^2} = \sqrt{(1,033)^2 + (1,033)^2} = 1,461 \text{ lbf / in}$$

The required groove weld is:

$$w = \frac{f_r}{w_{allow}} = \frac{1,461}{18,000} = .081 \text{ in}$$

Thus the weld margin of safety is:

$$MS_{weld} = \frac{.125}{.081} - 1 = +0.54$$

The load required to fail the weld is:

$$f_r = w \cdot (0.6 \cdot w_{ult}) = (0.125) \cdot (0.6 \cdot 75,000) = 5,625 \text{ lbf / in}$$

$$\text{Since } f_b = f_h: f_h = \sqrt{f_r^2 / 2} = \sqrt{(5,625)^2 / 2} = 3,977 \text{ lbf / in}$$

The load required to fail the weld is:

$$P_{h-failure} = f_h \cdot A_w = (3,977) \cdot (3.14) = 12,488 \text{ lbf}$$

2.5.2.5 Conclusion

From the above analysis, the index lugs adequately withstand the combined horizontal tiedown g-loads for the fully loaded package. Furthermore, it is shown that the index lug screw will fail prior to the weld. This satisfies the requirements of 10 CFR §71.45(b)(1).

2.5.3 Closure Handle

The closure handle is not considered a structural part of the package but is evaluated here to show that its failure will not impair the ability of the package to meet other requirements. A lifting or tiedown load applied to the closure handle is expected to deform the handle and fail the closure screws causing the handle to become detached from the closure assembly. The closure handle is used only for operator convenience in handling the 10 lb closure assembly by hand. The four small fasteners securing the handle to the closure are designed to fail under light loads

and well before impairment of any safety related packaging feature. Therefore, the closure handle is considered to be other than a structural part of the package.

This evaluation conservatively neglects any tension (pulling) on the handle and handle screws since a load in this direction would pull on the closure locking tabs and not the locking pins. A simple comparison between the area of the closure tabs and the area of the handle screws shows that the closure tabs consist of significantly more material and the screws will fail well before any significant loads are applied to the closure tabs.

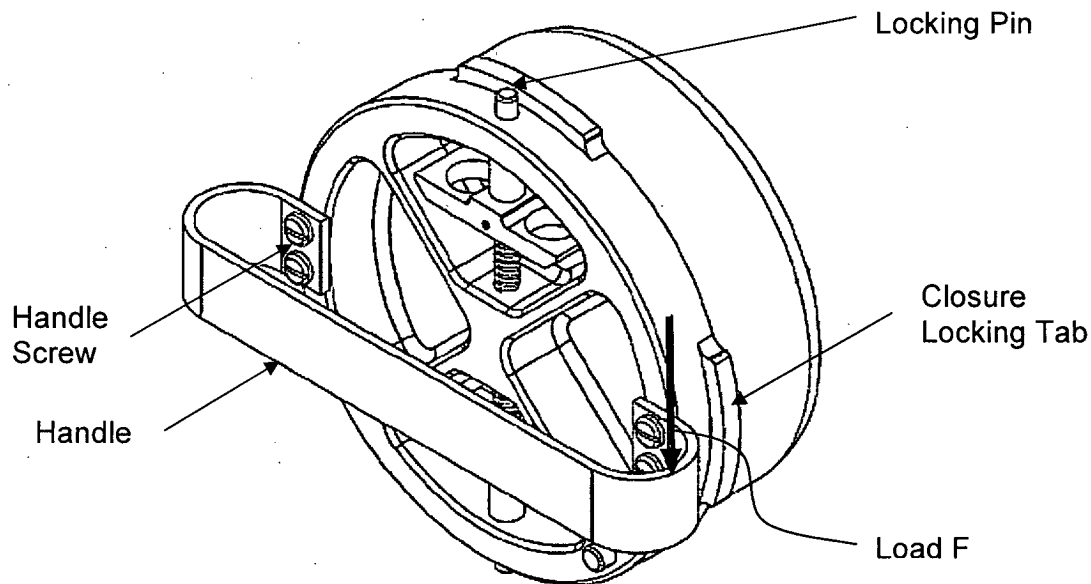


Figure 2.5-3 – Closure Assembly Handle

2.5.3.1 Handle Fasteners

The closure handle is secured by four #10-24 UNC screws (two per side). For this evaluation the load F is applied at the outside edge of the handle: 0.5 inches radially out from the screws and 0.5 inches above the face of the closure assembly.

This evaluation is based on the load F necessary to fail the handle screws. The load will be a function of the ultimate strength of the handle screws, which are given as a minimum of 72,000 psi for 18-8 material. To account for possible strain hardening due to the manufacturing process, that value will be conservatively multiplied by a factor of 2. Therefore:

$$\sigma_{\text{ultimate}} = 144,000 \text{ psi}$$

For the handle screws, the area across the threads is equal to the area of the minor diameter. For a #10-24UNC screw the minor diameter is 0.1389 inches.

$$A_s = \frac{\pi d_m^2}{4} = \frac{\pi (0.1389)^2}{4} = 0.0152 \text{ in}^2$$

The shear force in each screw is now determined. The largest forces will be at the two screws closest to the applied force. See Figure 2.5-4.

$$M = F \cdot r = 3.25 F \text{ in} \cdot \text{lb}$$

$$r = 3.25 \text{ in (dist.to centroid)}$$

The primary shear is:

$$n = 4 \text{ (number of screws)}$$

$$S' = \frac{F}{n} = \frac{F}{4} = 0.25F \text{ lb}$$

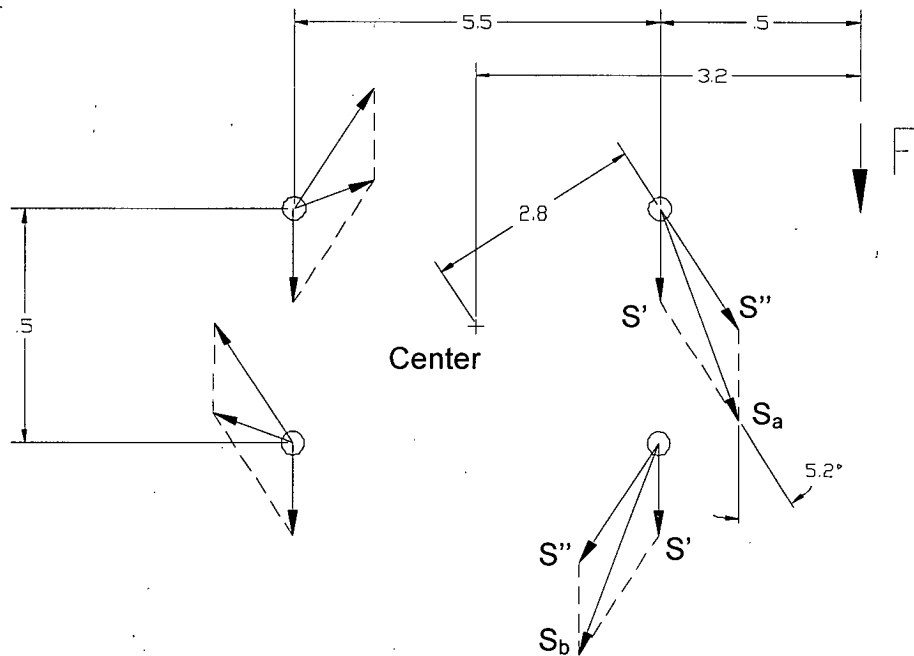


Figure 2.5-4 – Screw Pattern Diagram

The secondary shear is:

$$S'' = \frac{M}{4 \cdot R} = \frac{3.25F}{4 \cdot 2.8} = 0.29F \text{ lb}$$

$$R = 2.8 \text{ in. (dist.to centroid)}$$

The combined shear force is:

$$S_a = S_b = 0.29F + 0.25F(\cos 5.2) = 0.29F + 0.249F = 0.539F$$

The shear stress is:

$$\tau = \frac{S_a}{A_s} = \frac{0.539F}{0.0152} = 35.46F \text{ psi}$$

The tensile load on the screws due to the load F is applied to only two of the four screws, since the handle, due to its flexibility, cannot effectively transfer the load to the screws on the opposite side of the handle. The tensile load on the two screws closest to the load is:

$$\sum M_A = F \cdot (0.5) - R_1 \cdot (0.25) - R_2 \cdot (0.75) = 0$$

$$F = 0.5R_1 + 1.5R_2$$

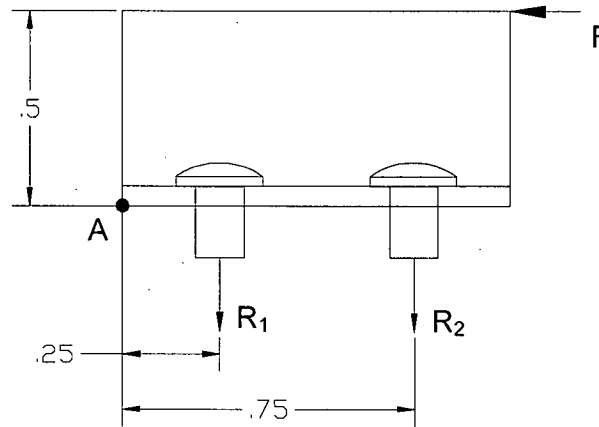


Figure 2.5-5 – Screw Prying Diagram

The relation between the screws is:

$$\frac{R_1}{R_2} = \frac{0.25}{0.75}$$

$$R_1 = \frac{1}{3} R_2$$

Substitute into the sum of moments equation:

$$F = 0.5R_1 + 1.5R_2$$

$$F = \left(\frac{1}{3} \cdot 0.5R_2\right) + 1.5R_2$$

$$R_2 = 0.6F \text{ lb}$$

$$R_1 = 0.2F \text{ lb}$$

The peak tension appears in R_2 . The maximum tensile stress is:

$$\sigma = \frac{R_2}{A_s} = \frac{0.6F}{0.0152} = 39.47F \text{ psi}$$

Combine the shear and tensile stresses to find the force necessary to fail the screws:

$$\begin{aligned}\sigma_{\text{ultimate}} &= \sqrt{\sigma^2 + 4\tau^2} = \sqrt{(39.47F)^2 + 4(35.46F)^2} \\ 144,000 &= \sqrt{6,588F^2} = 81.17F \\ F &= 1,774 \text{ lb}\end{aligned}$$

2.5.3.2 Locking Pin Loading

To show that the handle attachment fails prior to the closure components of the package, the force necessary to fail the screws is applied to the two locking pins. The yield strength of the locking pins is conservatively used in the comparison.

The locking pins are 0.25 inch in diameter and made of ASTM A276, Type S21800 material, having a yield strength of $\sigma_{\text{yield}} = 50,000$ psi. The pin area is:

$$A_p = \frac{\pi d^2}{4} = \frac{\pi (.25)^2}{4} = 0.049 \text{ in}^2$$

The load P must be calculated from the screw failure load F . The distance from the center of the closure assembly to the point of shear in the locking pin is half of the diameter of the closure at the location of the pin, or $r_p = 5.97/2 = 2.99$ inches. The distance from the center of the closure assembly to the load F is 3.25 inches.

$$P = \frac{3.25F}{2.99} = 1,928 \text{ lb}$$

The shear stress for each pin is:

$$\tau = \frac{1}{2} \cdot \frac{P}{A} = \frac{1,928}{2(.049)} = 19,673 \text{ psi}$$

The margin of safety on the locking pins (against pin yield) at the point of handle screw failure is:

$$MS = \frac{0.6\sigma_{\text{yield}}}{\tau} - 1 = \frac{0.6 \times 50,000}{19,673} - 1 = +0.52$$

where the factor of 0.6 converts the tensile yield of the pin material to shear yield. Thus, should the closure handle be incorrectly used as a tiedown device, the handle screws will break off before the pins yield.

2.5.3.3 Conclusion

From the above analysis, should the closure handle be incorrectly used as a tiedown device, the handle screws will break off before the pins yield. The analysis demonstrates that failure of the handle screws will not impair the ability of the package to meet other requirements.

2.6 Normal Conditions of Transport

2.6.1 Heat

2.6.1.1 Summary of Pressures and Temperatures

As presented in Table 3.1-1 of Section 3.1.3, *Summary Tables of Temperatures*, the maximum ATR FFSC package temperature under conditions of 100°F ambient temperature and full insolation is 186°F on the outer shell. As presented in Table 3.1-2 of Section 3.1.4, *Summary Table of Maximum Pressures*, the maximum normal operating pressure (MNOP) of the ATR FFSC package is zero. This is assured because there are no seals provided between the body and closure to retain pressure.

The ATR FFSC body cavity is also discussed in Section 3.1.4, *Summary Table of Maximum Pressures*. The maximum pressure that may develop between the inner and outer shells will be limited to that achieved due to ideal gas expansion. The maximum pressure rise within the sealed cavity under NCT will be less than 4 psi gauge.

2.6.1.2 Differential Thermal Expansion

Because of the simple design of the ATR FFSC package, there are no features, such as rigid lids and containment seals, which could be affected by the differential thermal expansion of the package components. In addition, since the package has a negligible internal decay heat, any temperature differences will arise only from the solar loading, and consequently be modest in nature.

The nominal gap between the package cavity and the FHE or the LFPB is 0.63 inches and 0.38 inches respectively. These gaps are large enough to prevent the payload from expanding enough to load the closure. Therefore, differential thermal expansion is not of concern.

2.6.1.3 Stress Calculations

Since the MNOP is zero and the maximum sealed cavity pressure is 4 psi gauge, stresses due to NCT pressures and temperatures are negligible.

2.6.1.4 Comparison with Allowable Stresses

Since NCT stresses are negligible, this section does not apply.

2.6.2 Cold

With an internal decay heat load of zero, no insolation, and an ambient temperature of -40°F, the average package temperature will be -40°F. None of the materials of construction (i.e., stainless steel) undergo a ductile-to-brittle transition at temperatures of -40 °F or higher. Therefore, the minimum NCT temperature is of negligible consequence.

2.6.3 Reduced External Pressure

As discussed in Section 2.6.1.1, *Summary of Pressures and Temperatures*, the ATR FFSC packaging is not capable of retaining pressure. Therefore, there is no effect of a reduced external pressure on the package of 3.5 lbf/in² (25 kPa) absolute, per 10 CFR §71.71(c)(3).

2.6.4 Increased External Pressure

10 CFR §71.71(c)(4) requires exposure of the ATR FFSC package to an increased external pressure of 20 psi (140 kPa) absolute. Since there are no sealing surfaces, there is no effect of an increased external pressure to the ATR FFSC package.

Section 2.7.6.1, *Cavity Evaluation*, evaluates the effect of pressure on the sealed cavity between the outer 8 inch tube and inner 6 inch diameter pipe. This cavity is welded closed during fabrication and has no relation to the payload. The cavity evaluation conservatively considers the satisfactory performance of a 22 psi gauge external pressure to the packaging.

2.6.5 Vibration

The effects of vibration normally incident to transport are not significant for the ATR FFSC packaging. Table 2 of ANSI N14.23⁷ shows peak vibration accelerations of a trailer bed as a function of package and tie-down system natural frequency. For the frequency range 0 to 5 Hz, assuming a light package, Table 2 of ANSI N14.23 gives peak accelerations (99% level) of 2g in the vertical direction, and 0.1g in both the lateral and longitudinal directions. All other frequency ranges give significantly lower acceleration levels.

The ATR FFSC is very resistant to damage from transportation vibration. The closure is subject to the $\pm 0.1g$ longitudinal (axial) loading, but since friction between the closure and its opening will exceed 0.1, the closure is not expected to apply any vibrational loadings to the bayonet lugs. The insulating material located between the inner, round tube and the outer, square tube is retained in place by a jacket of 28 gauge stainless steel. The resistance to displacement of the insulation was demonstrated in the testing program (see Section 2.12.2.5.1, *CTU Inspection*). When exposed to axial impacts which were many times larger than the vibration load of 0.1g, the insulation displaced an insignificant distance which was bounded by the assumptions made in the thermal analysis. Therefore, vibration will have no effect on the placement or condition of the insulation.

When supported on the shipping rack, the package is supported near index lugs which interface with the two pockets on the lower face of the package. Conservatively, an analysis of the package as a simply supported beam, supported at the extreme ends, is performed. The overall length of the package is $L = 72.5$ inches, and the maximum weight, from Table 2.1-1, is 290 lb. The distributed load is therefore $290/72.5 = 4$ lb/in. The outer square tube has a square

⁷ ANSI N14.23, *Design Basis for Resistance to Shock and Vibration of Radioactive Material Packages Greater Than One Ton in Truck Transport*, 1980, American National Standards Institute, Inc. (ANSI).

dimension of 8 inches and a wall thickness of 0.188 inches. AISC⁸ gives the moment of inertia of the tube as 58.2 in⁴. The c-distance is 4 inches. The bending moment is:

$$M = \frac{wL^2}{8}(2) = 5,256 \text{ in} \cdot \text{lb}$$

where the factor of 2 accounts for the inertia loading of $\pm 2g$. The reversing bending stress in the outer square tube is:

$$\sigma = \frac{Mc}{I} = 361 \text{ psi}$$

This value is well below the fatigue limit for stainless steel. Since the inner round tube is supported at three places along its length, the unsupported length is much shorter than for the outer square tube. In addition, the distributed weight, which consists of only the self-weight and payload weight, is significantly less than for the outer square tube. For these reasons, the stress in the inner round tube will be bounded by the stress in the outer square tube.

The fuel handling enclosure (FHE) and loose fuel plate basket are designed to be form fitting and supported by the inner stainless steel round tube. Furthermore, the FHE and loose fuel plate basket are completely removed and in view at both the shipping and receiving sites, and consequently, a complete fatigue failure of either basket due to transportation vibration is not to be expected.

For these reasons, the effect of vibration normally incident to transport is not of concern for the ATR FFSC package.

2.6.6 Water Spray

The external surfaces of the ATR FFSC package are made from stainless steel, whose properties are not affected by water spray. For this reason, the effect of water spray, per 10 CFR §71.71(c)(6), is not of concern for the ATR FFSC package.

2.6.7 Free Drop

10 CFR §71.71(c)(7) requires a free drop for the ATR FFSC package. Since the package gross weight is less than 11,000 lb, the applicable free drop distance is 4 ft. As discussed in Appendix 2.12.1, *Certification Tests on CTU-1*, one NCT free drop preceded the HAC drop tests performed on CTU-1. The damage from the NCT drop case was minor as illustrated in Figure 2.12.1-5 through Figure 2.12.1-7. There was no loss or dispersal of package contents, and no substantial reduction in the effectiveness of the packaging. The latter result was confirmed by the successful completion of the subsequent HAC testing.

From the test results, the amount of deformation in the top corner was approximately 1/8 inch. Because there are no crushable materials of construction, the deformation of the package in any other NCT drop orientation is assumed to be the same or less than this CG over top corner

⁸ American Institute of Steel Construction, *Manual of Steel Construction, Allowable Stress Design*, Ninth Edition, 1989.

orientation. This assumption is verified by the degree of damage recorded during the HAC drop orientations discussed in Section 2.7, *Hypothetical Accident Conditions*.

By observation the NCT damage is much less than 5% of the total effective volume of the package, approximately 230 in³, based on 5% of the volume of the 72.5-inch long, by 8-inch square tube. Therefore, the requirement of 10 CFR §71.55(d)(4)(i) is met. Further, the effective spacing between fissile contents is 8 inches, based on a center-to-center distance between packages which are in side to side and top to bottom contact. Five percent of this distance is 0.4 inches, and therefore the requirement of 10 CFR §71.55(d)(4)(ii) is met. Finally, no opening capable of admitting a 4-inch cube was created, and the requirement of 10 CFR §71.55(d)(4)(iii) is also met. Thus, the effect of the free drop test, per 10 CFR §71.71(c)(7), is not of concern.

2.6.8 Corner Drop

This test does not apply, since the ATR FFSC package is a rectangular fissile material package weighing more than 110 lb, as specified in 10 CFR §71.71(c)(8).

2.6.9 Compression

As specified in 10 CFR §71.71(c)(9), the ATR FFSC must be subjected, for a period of 24 hours, to a compressive load applied uniformly to the top and bottom of the package in the normal transport position. The greater of the following uniformly distributed loads is to be used: (a) the equivalent of 5 times the weight of the package, or (b) the equivalent of 2 lbf/in² multiplied by the vertically projected area of the package. For these two cases, the loads are:

$$P_{(a)} = 5 \cdot W = 5 \cdot 290 \text{ lbf} = 1,450 \text{ lbf}$$

$$P_{(b)} = 2 \text{ psi} \cdot L \cdot w = 2 \text{ psi} \cdot (72.5 \text{ in}) \cdot (8 \text{ in}) = 1,160 \text{ lbf}$$

Where,

W is the maximum weight of one package

w is the overall width of the package

L is the overall length of the package.

Thus, it is seen that case (a) governs with a compressive load of 1,450 lbf.

The exterior side of the ATR FFSC packaging is a reinforced 8 inch by 8 inch square stainless steel tube with a 0.188 inch wall thickness. The closure end includes a 1.5 inch thick stainless steel plate and the bottom end includes a 0.88 inch thick stainless steel plate. By observation, buckling of the outer tube is not a concern due to its reinforcement, short height, wall thickness, and the relatively small load applied. A conservative evaluation is performed in the following section to demonstrate the adequacy of the design under the compression load.

2.6.9.1 Compression Evaluation

To conservatively evaluate the compressive load, buckling of the square tube under a uniform load is evaluated neglecting the reinforcing end plates and interior ribs. The applied load, as determined in Section 2.6.9, *Compression*, is 1,450 lbf. The average stress in the 8 inch tube is:

$$\sigma_{tube} = \frac{P}{A_{tube}}$$

Where,

P = applied load = 1,450 lbf

A_{tube} = area of vertical legs of the tube = 2 x t x L = 2 · (0.19) · 72.5 = 27.6 in²

t = thickness = 0.19 in

L = length of tube = 72.5 in

Therefore:

$$\sigma_{tube} = \frac{P}{A_{tube}} = \frac{1450}{27.6} = 52.5 \text{ psi}$$

Using Roark⁹, Table 35 Case 1a, a rectangular plate under equal uniform compression, all edges simply supported, the critical unit compressive stress σ' is:

$$\sigma' = K \cdot \frac{E}{1 - \nu^2} \cdot \left(\frac{t}{L} \right)^2$$

Where,

E = modulus of elasticity for stainless steel = 27.6 Mpsi

ν = Poisson's ratio = 0.3

K = conservatively chosen as equal to 10.9

$$\sigma' = 10.9 \cdot \frac{27600000}{1 - (.3)^2} \cdot \left(\frac{0.19}{72.5} \right)^2 = 2,271 \text{ psi}$$

By comparison:

$$\sigma_{tube} \ll \sigma'$$

Therefore, buckling of the outer tube due to the compression load is not a concern.

2.6.10 Penetration

10 CFR §71.71(c)(10) requires that a bar of hemispherical end, weighing at least 13 lb be dropped from a height of 40 inches onto the most vulnerable part of the packaging. As

⁹ Young, Warren C., *Roark's Formulas for Stress and Strain*, Sixth Edition, 1989, McGraw Hill, New York, New York.

documented in Appendix 2.12.1, *Certification Tests on CTU-1*, the ATR FFSC package, weighing approximately 290 lb, was subjected to the much more demanding test of being dropped from 40 inches onto the puncture bar described in §71.73(c)(3) without experiencing any damage which could compromise confinement or criticality control. Therefore, this test does not need to be performed, and the penetration test requirement is satisfied.

2.7 Hypothetical Accident Conditions

When subjected to the hypothetical accident conditions of 10 CFR §71.73, the ATR FFSC prevents loss or dispersal of the enriched uranium payload. The analysis given in Chapter 6, *Criticality*, which includes conservative assumptions regarding damaged geometry and moderation, demonstrates the criticality safety of the ATR FFSC under hypothetical accident conditions.

10 CFR §71.55 requires that packages containing fissile material be evaluated for criticality with the inclusion of any damage resulting from the NCT tests specified in §71.71 plus the damage from the HAC tests specified in §71.73. The ATR FFSC was subjected to accident condition loadings by means of full scale certification testing. Each test specified by §71.73 was applied sequentially, as specified in Regulatory Guide 7.8¹⁰. One full scale certification test unit (CTU-1) using the ATR fuel element as the payload was subjected to the full series of free drop and puncture testing. A second full scale certification test unit (CTU-2) using the loose fuel plates as the payload was subjected to a series of worst case free drops. Puncture drops were not performed on CTU-2 because the testing focused on the performance of the insulation and payload, which would not be affected by any puncture damage. The puncture testing performed on CTU-1 demonstrated that the effects of the puncture test on the insulation and on the payload are negligible. Utilizing the results of drop testing, the fire test was evaluated analytically. The immersion tests are also evaluated analytically.

The payload for CTU-1 used during testing was an un-irradiated ATR fuel element, enriched to a maximum of 94% U-235. The ATR fuel element used was a rejected production fuel element. The defects were considered cosmetic only and had no structural significance for purposes of the certification tests. Further discussion of the CTU-1 payload is provided in Appendix 2.12.1, *Certification Tests on CTU-1*.

The simulated loose fuel plate payload for CTU-2 was a combination of 2- and 4-inch wide, 0.06-inch thick, 5052H32 aluminum flat plates. All plates were 49.5 inches long. There were 15, 2-inch wide plates and 10, 4-inch wide plates. The weight of the aluminum plates totaled 20.7 lb. Further discussion of the CTU-2 payload is provided in Appendix 2.12.2, *Certification Tests on CTU-2*.

Rationale for the selection of the test series is given below. The tests actually performed, and their sequence, are summarized in Table 2.7-1. Test results are summarized in the sections which follow and in Section 2.7.8, *Summary of Damage*, with details given in Appendix 2.12.1, *Certification Tests on CTU-1* and Appendix 2.12.2, *Certification Tests on CTU-2*.

¹⁰ U. S. Nuclear Regulatory Commission, Regulatory Guide 7.8, *Load Combinations for the Structural Analysis of Shipping Casks for Radioactive Material*, Revision 1, March 1989.

2.7.1 Free Drop

10 CFR §71.73(c)(1) requires a free drop of the specimen through a distance of 30 ft onto a flat, essentially unyielding surface in the orientation for which maximum damage is expected. The primary mode of failure of the ATR FFSC would be loss of the ability of the closure to retain the payload. This could occur through loss of the bayonet style lugs, or through failure of the retracting pins allowing the lid to rotate, or through excessive deformation of the closure area which could cause separation of the body from the closure. If a sufficient gap is formed between the body and closure, the payload may no longer be retained, consequently possibly affecting criticality safety.

The object of the free drop tests in the current instance is to create the maximum amount of damage in critical locations and components. Therefore, free drop orientations are selected which would result in the greatest amount of critical damage and which would render the package most vulnerable to damage from the puncture drop test.

The ability of the payload to remain in a critically safe geometry is also confirmed through the free drop tests. Following all drop tests, the fuel assembly in CTU-1 and the simulated loose fuel plates in CTU-2, are inspected to confirm the geometries remain within the assumptions used in Section 6.0, *Criticality Evaluation*.

To confirm the performance of the payload at reduced temperatures CTU-1 was subjected to two HAC drops with the payload temperature at approximately -20°F (-29°C). Following all CTU-1 testing, as discussed in Appendix 2.12.1, *Certification Tests on CTU-1*, the package was destructively disassembled and the payload inspected.

Upon inspection of both CTU-1 and CTU-2, the performance of both the payload and packaging, including the reduced temperature tests, was satisfactory.

2.7.1.1 Side Drop

The horizontal side drops for CTU-1 include CD1-1, CD2-1, and CD3-1. The first three HAC drops primarily address the packaging closure and shell response to the free drops. Also, the side drop orientations represent large impact loads to the ATR fuel element for geometry control. CD1-1 presents the highest acceleration to the locking pins when the pins are oriented vertically with respect to the target surface. CD2-1 is directed at challenging the outer shell in the vicinity of the index lugs. The intent is to demonstrate that the outer shell is not penetrated by the impacted index lugs which could represent a thermal concern. In CD3-1, the locking pins are oriented horizontally with respect to the target surface presenting the worst case bending load to the locking feature.

The horizontal side drops for CTU-2 include CD1-2 and CD3-2. These two HAC drops address the performance of the LFPB in maintaining the geometry of the loose plates. Furthermore, the intent is to demonstrate the similar performance of the outer packaging in response to the LFPB as the payload.

2.7.1.2 CG Over Bottom Drop

The CG over bottom drop for CTU-1 includes CD4-1. This vertical orientation is expected to have the greatest potential for deformation to the insulation cavity at the bottom end. CD4-1 is considered to present the worst case loading to the 3/8 inch thick plate located at the bottom of

the payload cavity. The intent of the drop is to demonstrate the insulation cavity at the bottom end of the package is not breached or significantly reduced. Additionally, the CD4-1 drop presents the worst case buckling load to the ATR fuel element.

For CTU-2, the CG over bottom drop includes CD4-2. As with CD4-1, this orientation is expected to have the greatest local deformation to the bottom end plate and insulation cavity and present the worst case buckling load to the LFPB and loose plates.

2.7.1.3 CG Over Corner Drop

The CG over corner drop was only performed on CTU-1. CD5-1, the CG over top corner drop, produces the greatest deformation in the closure region and also presents the greatest challenge for the closure locking tabs. The intent of the drop is to demonstrate the effectiveness of the closure in retaining the payload.

2.7.1.4 Oblique Drops

An oblique free drop orientation, also known as a slap-down drop, was not performed for this package. Consequences from the slap-down event are considered bounded by the CG over bottom (CD4-1/CD4-2) and CG over corner (CD5-1) drop tests performed. The slap-down drop challenges the closure and the fuel by producing high angular velocities and accelerations to the packaging and contents. However, in the case of the ATR FFSC, the end drops present a greater challenge to the closure and the fuel than the slap-down condition. In bolted closure designs, the slap-down side loads have the tendency to shear the closure bolts. Since the ATR FFSC closure is secured by a bayonet type design rather than bolts, this is not a concern. The axial load imparted to the closure in a slap-down drop will be lower than the axial loading developed in an end drop. And the greater the axial load, the greater the challenge to the locking tabs on the closure. The CD5-1 drop therefore presents the greatest challenge to closure retention, and the CD4-1/CD4-2 drop presents the greatest potential for fuel buckling.

2.7.1.5 Results of the Free Drop Tests

CD1-1 Flat Side Drop (CTU-1). See Figure 2.12.1-8 through Figure 2.12.1-13. The visible damage resulting from the 30 ft flat side drop, pocket side down, was negligible. There were minor visible exterior scratches resulting from the drop. The areas showing the greatest impact marks are at each end plate and near the three internal stiffening ribs. There was no significant bowing or other visible deformation. There was no visible deformation or rotation of the closure and the locking pins remained in the locked position.

Following the CD1-1 drop, CTU-1 was opened and the FHE and fuel element payload were visually inspected for damage. As illustrated in Figure 2.12.1-11 in Section 2.12.1, there were no major deformations and no cracked welds noticed. As illustrated in Figure 2.12.1-12, there was no visible damage to the fuel element.

With the closure assembly removed from the body of the CTU, one locking pin was noticeably bent approximately 1/32 inch as illustrated in Figure 2.12.1-13. It was noticed that the bent locking pin tended to bind when compressed to the open position. The other locking pin was not deformed and there was no other visible deformation of the closure assembly.

CD2-1 Flat Side Drop (CTU-1). Due to CTU-1 not impacting square on the index lugs, this orientation was tested three different times. The three tests in this orientation are identified as CD2.A-1, CD2.B-1, and CD2.C-1 throughout this section. For CD2.A-1, CTU-1 rotated during its descent and impacted at a slight angle causing the package to bounce and spin somewhat on the longitudinal axis after impact. The visible damage resulting from the CD2.A-1 drop was minor with the index lugs at each end pressed into the body approximately 1/8 inch. See Figure 2.12.1-14 through Figure 2.12.1-17.

For CD2.B-1 the package again rotated during its decent and impacted at an angle causing the package to bounce and spin on the longitudinal axis after impact. Also, a gust of wind blew the rigging straps into the adjacent stadia board during the drop. The visible damage resulting from the CD2.B-1 drop was minor with the index lugs at each end now pressed into the body approximately 3/16 inch. See Figure 2.12.1-18 through Figure 2.12.1-20.

CD2.C-1, which was performed after CD5-1, impacted in the correct orientation directly on the index lugs; see Figure 2.12.1-37 through Figure 2.12.1-40. The index lug near the closure end was flush with the original surface, pressed in approximately 3/8 inch (the height of the lug) as seen in Figure 2.12.1-39. The index lug at the bottom end was pushed in to approximately 1/8 inch from the original surface. A cracked weld was found under the index lug near the closure end as shown in Figure 2.12.1-40. The length of the cracked weld was approximately 1/2 inch.

CD3-1 Flat Side Drop – Reduced Temperature (CTU-1). See Figure 2.12.1-22 through Figure 2.12.1-25. The visible damage resulting from the 30 ft flat side drop performed with the payload at reduced temperature (-20°F) was negligible. Similar to CD1-1, the impact side exhibited scratches and impact marks near the locations of the internal ribs. Upon inspection of the closure assembly, one of the two locking pins was found sheared off from the outside edge of the closure as it interfaces with the package body. There was no other visible damage or any signs of rotation to the closure assembly as the second locking pin remained in the locked position.

CD4-1 CG Over Bottom End – Reduced Temperature (CTU-1). See Figure 2.12.1-26 through Figure 2.12.1-28. The visible damage resulting from the 30 ft CG over bottom end drop performed with the payload at reduced temperature (-20°F) was minor. The outer shell of CTU-1 exhibited minor bowing near the impact end with the greatest deformation measuring approximately 1/8 inch on one side. The overall length of the package body was compared with the initial measurements at eight locations and found to have compressed a maximum of approximately 1/8 inch. There was no visible deformation or rotation of the closure following the drop and the remaining locking pin remained in the locked position.

CD5-1 CG Over Top Corner Drop (CTU-1). See Figure 2.12.1-32 through Figure 2.12.1-36. The visible damage resulting from the 30 ft CG over top corner drop was prominent in the closure area. The impact corner was deformed in approximately 5/8 inch. There was modest deformation on the sides of the package near the impact location bulging in approximately 1/2 inch near the index lug pocket and bulged out approximately 5/8 inches on the adjoining side.

Following the drop, the closure assembly exhibited deformation with the end of the package and was unable to be rotated more than 1/8 inch in either direction. The locking pins showed no visible signs of deformation and the remaining locking pin remained in the locked position.

CD1-2 Flat Side Drop (CTU-2). See Figure 2.12.2-5 through Figure 2.12.2-7. This drop is a repeat of CD1-1 using the loose fuel plate payload rather than the ATR fuel element. The

orientation of the LFPB parting lines is shown in Figure 2.12.2-3 through Figure 2.12.2-4. There was minor visible exterior damage, principally scuff marks, resulting from the drop. There was no bowing or other significant visible deformation. There was no visible deformation or rotation of the closure assembly, and the locking pins were unaffected by the drop.

Following the CD1-2 drop, CTU-2 was opened and the LFPB and payload were inspected. The basket was not affected by the drop, however the finger operated screws securing the two basket halves were loosened slightly. One tie wrap was broken but the simulated loose fuel plates were not damaged. The broken tie wrap was not replaced for the subsequent drops.

CD3-2 Flat Side Drop (CTU-2). See Figure 2.12.2-8 through Figure 2.12.2-10. This drop is a repeat of CD3-1 but at ambient temperature and using the loose fuel plate payload rather than the ATR fuel element. As with the other side drop events, the outer shell exhibited minor impact marks at the stiffening rib locations. There was no visible deformation or rotation of the closure assembly, and the locking pins were undamaged and in good working order.

The closure was opened and the payload inspected following the CD3-2 drop. The basket exhibited no signs of deformation and again the basket screws were loosened slightly. The second plastic tie wrap was broken and the simulated fuel plates exhibited no significant damage as seen in Figure 2.12.2-10. The broken tie wrap was not replaced for the subsequent drop.

CD4-2 CG Over Bottom End (CTU-2). See Figure 2.12.2-11 through Figure 2.12.2-16. This drop orientation is a repeat of CD4-1 but at ambient temperature and using the loose fuel plate payload rather than the ATR fuel element. CTU-2 appeared to impact slightly off of true vertical and impacted near one corner of the package. The impact caused one side to dent inward approximately ½ inch and the adjacent side to bulge out approximately ½ inch. There was no overall bowing of the package or other significant visible deformation. There was no visible damage to the closure or the locking pins.

The closure was removed and the basket extracted following the CD4-2 drop. The basket damage was minor and limited to a small dent at the end of the basket that was situated closest to the package bottom and a small deformation to the basket end plate from the package inner shell. As illustrated in Figure 2.12.2-15 and Figure 2.12.2-16, the simulated fuel plates experienced localized deformation at the end of the basket closest to the package bottom. The remaining area above the localized deformation was not deformed.

The gap between the thermal shield and the stiffening rib, where the shield pulls away from the rib was found to be less than 1/16-inch during the disassembly of CTU-2 discussed in Section 2.7.8.2, *CTU-2 Package Disassembly – Results*. With the thermal shields removed the maximum compaction for all insulation sections ranged from 1 inch to 1¾ inches.

2.7.2 Crush

10 CFR §71.73(c)(2) requires that the crush test be performed on fissile material packages which have a mass not greater than 1,100 lb and a density not greater than 62.4 lb/ft³. The ATR FFSC package has a maximum weight of 290 lb and a volume of 2.69 ft³ (based on outside dimensions of 8 in x 8 in x 72.5 in), leading to a maximum density of $290/2.69 = 108 \text{ lb/ft}^3$. Therefore, the crush test is not applicable.

2.7.3 Puncture

10 CFR §71.73(c)(3) requires the drop of the package onto a 6-inch diameter steel bar from a height of 40 inches. The primary modes of failure of the ATR FFSC would be closure damage, closure rotation, and penetration of the outer shell. The object of the puncture drop tests in the current instance is to create the maximum amount of damage in critical locations and components. Therefore, drop orientations are selected which would result in the greatest amount of critical damage and which would render the package most vulnerable to the thermal event. For the ATR FFSC, these are the CG over center of closure, 30° oblique CG over side, and an oblique drop onto the closure.

The CG over center of closure position was chosen to confirm the performance of the closure assembly and verify at least one locking pin remained locked to prevent rotation. The 30° oblique CG over side was chosen to confirm the resistance of the outer shell to penetration from the puncture bar. The oblique drop onto the closure assembly confirms that the puncture bar can not cause rotation of the closure and was added after the CD3-1 drop sheared one of the locking pins.

CTU-2 was not subjected to puncture, since the purpose of the CTU-2 test unit was to demonstrate the effectiveness of the LFPB and the performance of the thermal insulation. The puncture test would have no impact on these features.

2.7.3.1 Results of the Puncture Tests

CG Over Center of Closure, Vertical (CP1-1). See Figure 2.12.1-44 through Figure 2.12.1-46. The puncture bar impacted directly on the closure assembly (the handle was removed during previous free drop tests). The drop resulted in only minor damage with the TID post deformed into the closure and the closure assembly exhibiting minor scratches from the puncture bar. The locking pins showed no visible signs of deformation and the remaining functional locking pin remained in the locked position.

CG Over Side, 30° Oblique (CP2-1). See Figure 2.12.1-41 through Figure 2.12.1-43. The initial impact caused a deformation of approximately 1/2 inch deep by 5 inches across with a radius the same as the puncture bar. There were no tears or fissures in the ATR FFSC outer skin and there was no change to the closure assembly.

Oblique Drop onto Closure (CP3-1). See Figure 2.12.1-29 through Figure 2.12.1-31. CP3-1 was an unscheduled puncture drop with the purpose of causing rotation to the closure assembly. This extra drop was chosen due to the failure of one of two locking pins during CD3-1. The puncture bar squarely impacted the closure rib and the CTU bounced away from the puncture bar onto the

drop pad. Following the drop, the closure assembly rib exhibited minor deformations at the impact point made by the puncture bar. There was no rotation of the closure, and the remaining functional locking pin remained in the locked position and showed no visible signs of deformation.

2.7.4 Thermal

10 CFR §71.73(c)(4) requires the exposure of the ATR FFSC packaging to a hypothetical fire event. Performance of the package under the thermal event is addressed analytically in Chapter 3, *Thermal Evaluation*. Disassembly of the package following the structural tests confirmed that the compaction to the insulation features, as assumed in the thermal analyses, was shown to still perform in a satisfactory manner.

2.7.4.1 Summary of Pressures and Temperatures

As shown in Section 3.4.3, *Maximum Temperatures and Pressures*, the maximum peak temperature of the outer shell was evaluated to be 1,427°F. The annular space between the outer shell and inner shell pressurized to a maximum 38 psi gauge during the HAC thermal event. The payload cavity of the ATR FFSC is vented to the atmosphere and therefore the inner shell (6 inch diameter pipe) experiences an external pressure of 38 psi gauge. Since the ATR FFSC does not provide leaktight containment, this pressure is not significant to the package.

2.7.4.2 Differential Thermal Expansion

The thermal analysis presented in Section 3.4.4, *Thermal Evaluation under Hypothetical Accident Conditions*, identifies that the peak temperature difference between the inner and outer shells occurs approximately six minutes into the thermal event and results in a free differential thermal expansion of approximately 0.9-inches between the two shells. This places the outer shell in compression and the inner shell in tension. The packaging could respond structurally to the forces developed by this differential expansion by:

- failure of one of the two inner shell to end plate welds (allowing free expansion of the outer shell relative to the inner shell), or
- no weld failure, but buckling of the outer shell, or
- a combination of the above two scenarios.

In any case, none of these scenarios results in a geometry change to the packaging that leads to an increase in reactivity. The only concern is a condition that could allow an increase in heat transfer to the fuel such that the fuel approaches the melting point.

As identified in Section 3.4.4, *Thermal Evaluation under Hypothetical Accident Conditions*, the thermal consequences of the above events results in insignificant changes to the fuel temperature. The fuel does not approach the melting point and therefore there will be no impact to reactivity. The effect of differential thermal expansion on the various packaging components is therefore considered negligible.

At 72°F, the nominal length of the packaging cavity is 67.88 inches, the nominal length of the FHE is 67.25 inches and the nominal length of the LFPB is 67.5 inches. Both the LFPB and the FHE are fabricated from aluminum so the worst case for potential interference due to thermal

expansion is with the LFPB. From Figure 3.4-5 it can be seen that above 700°F the inner shell temperature is much greater than the LFPB temperature and so the inner shell thermal expansion rate exceeds that of the LFPB. During the cooling period below 700°F, the temperatures of the two components track within about 50 °F with the inner shell temperature always less than the LFPB. The worst condition for potential thermal expansion interference is near the peak temperature of the LFPB. For this evaluation, conservatively assume the LFPB temperature is 700°F and the inner shell is at 650°F. The length of the two components at these temperatures is calculated as follows:

$$L = \alpha \cdot L_{Original} \cdot (\Delta T) + L_{Original}$$

Where,

$L_{Original}$ = the original length of the component at 72°F

α = the coefficient of thermal expansion¹¹

For aluminum: $\alpha_{Al} = 14.5(10^{-6})$ in/in/°F at 700 °F

For stainless steel: $\alpha_{SST} = 9.9(10^{-6})$ in/in/°F at 650 °F

ΔT = the change in temperature from 72°F

L = the length of the component at the elevated temperature

Loose fuel plate basket length at 700°F is:

$$L_{LFPB} = 14.5(10^{-6})(67.5)(700 - 72) + 67.5 = 68.11 \text{ inches}$$

Inner shell length at 650°F is:

$$L_{IS} = 9.9(10^{-6})(67.88)(650 - 72) + 67.88 = 68.27 \text{ inches}$$

$L_{IS} > L_{LFPB}$, therefore there is no interference under worst case conditions.

2.7.4.3 Stress Calculations

Since there is no differential thermal expansion interference between FHE or LFPB and the packaging, and since the packaging internal pressure is zero, there are no stresses to report.

2.7.4.4 Comparison with Allowable Stresses

Since there are no stresses to report, this section does not apply.

2.7.5 Immersion – Fissile Material

10 CFR §71.73(c)(5) requires performance of the immersion test for packages containing fissile material. The criticality evaluation presented in Chapter 6.0, *Criticality Evaluation*, assumes optimum hydrogenous moderation of single ATR FFSC packages and arrays of packages. Since

¹¹ Coefficients of thermal expansion are taken from ASME B&PV Code, Section II, Part D, coefficient B. For aluminum, Table TE-2, and for stainless steel, Table TE-1, Group 3.

the criticality consequences of water in-leakage are accounted for, and leakage of the payload from the packaging did not occur, the immersion test of 10 CFR §71.73(c)(5) is not of concern.

2.7.6 Immersion – All Packages

10 CFR §71.73(c)(6) requires performance of an immersion test on an undamaged specimen under a head of water of at least 50 ft or 21.7 psig. The package payload cavity does not provide a leak tight containment. Since the criticality consequences of water in-leakage are accounted for, and leakage of the payload from the packaging did not occur, the immersion test of 10 CFR §71.73(c)(6) is not of concern.

The ATR FFSC does contain a sealed annular space between the outer square tube and the inner pipe where the insulation is located. The possible consequence of a 21.7 psig pressure applied to the outside surface of the square tube and the inside surface of the 6 inch diameter tube are considered insignificant to both the packaging and the payload.

2.7.7 Deep Water Immersion Test

The ATR FFSC package is a Type A Fissile package; hence, this requirement does not apply.

2.7.8 Summary of Damage

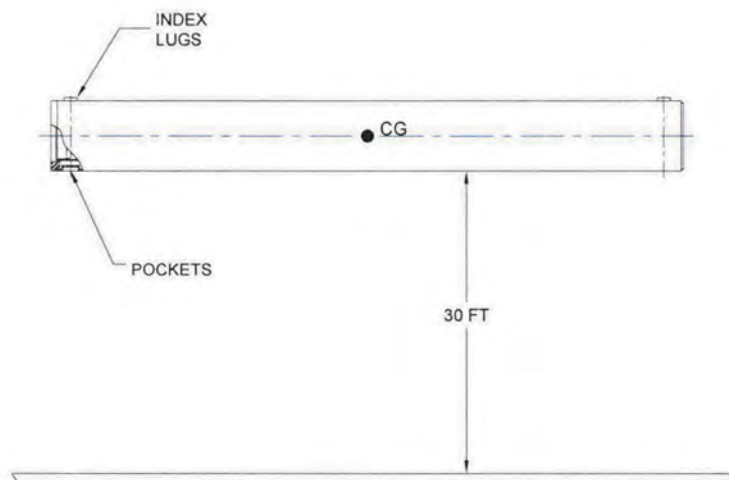
The discussions of sections 2.7.1, *Free Drop*, through 2.7.7, *Deep Water Immersion Test*, demonstrate that the ATR FFSC package prevents loss or dispersal of the payload when subjected to all applicable hypothetical accident tests. In addition, the ATR fuel element and loose fuel plates retain a geometry consistent with the analysis presented in Section 6.0, *Criticality Evaluation*. The physical test series consisted of multiple 30 ft free drop and puncture drop tests conservatively applied to two CTUs. Following the drop tests, each CTU was destructively disassembled to inspect various aspects of the packaging. Table 2.7-1 presents the certification drop test series in the sequential order performed for both CTU-1 and CTU-2.

Table 2.7-1 – ATR FFSC Certification Drop Test Series

Test No.	Test Description	Purpose of Test
CN1-1 (CTU-1)	CG over top corner	Confirm: <ul style="list-style-type: none"> Fuel element does not penetrate the closure insulation pocket. Fuel retains geometry necessary to maintain sub-criticality. Closure is retained on the body and has not rotated relative to the package body.
CD1-1 (CTU-1)	Flat side drop, pocket side down.	Confirm: <ul style="list-style-type: none"> Closure is retained and has not rotated relative to the package body. Fuel retains geometry necessary to maintain sub-criticality.
CD2.A-1 (CTU-1)	Flat side drop, index lugs down	Confirm: <ul style="list-style-type: none"> Impact on index lugs does not cause a fracture in the outer shell. Closure is retained and has not rotated relative to the package body.
CD2.B-1 (CTU-1)	Flat side drop, index lugs down	Same purpose as CD2.A-1. This test was repeated due to the impact during CD2.A-1 being slightly rotated on the longitudinal axis and not fully impacting the index lugs.
CD3-1 (CTU-1)	Flat side drop, pocket and index lugs on side (-20°F)	Confirm: <ul style="list-style-type: none"> Closure is retained and does not rotate relative to the package body. Fuel element performance at cold temperature. Fuel retains geometry necessary to maintain sub-criticality.
CD4-1 (CTU-1)	CG over bottom end (-20°F)	Confirm: <ul style="list-style-type: none"> Fuel element does not penetrate into the packaging bottom end insulation pocket. This is a thermal performance requirement. Fuel element performance at cold temperature. Fuel retains geometry necessary to maintain sub-criticality.
CP3-1 (CTU-1)	Oblique drop onto closure assembly	Confirm: <ul style="list-style-type: none"> Closure is retained on the body and does not rotate relative to the package body. This was an unscheduled test to confirm the performance of the remaining locking pin after the failure of the other pin during CD3-1.

Table 2.7-1 – ATR FFSC Certification Drop Test Series (continued)

Test No.	Test Description	Purpose of Test
CD5-1 (CTU-1)	CG over top corner (same orientation as CN1)	Confirm: <ul style="list-style-type: none"> Fuel element does not penetrate the closure insulation pocket. Fuel retains geometry necessary to maintain sub-criticality. Closure is retained and does not rotate relative to the package body.
CD2.C-1 (CTU-1)	Flat side drop, index lugs down	Same purpose as CD2.A-1. This test was repeated for a third time due to the impact during CD2.B-1 being slightly rotated on the longitudinal axis and not fully impacting the index lugs.
CP2-1 (CTU-1)	CG over side, 30° oblique	Confirm: <ul style="list-style-type: none"> Resistance of outer shell to puncture bar penetration.
CP1-1 (CTU-1)	CG over center of closure (Vertical)	Confirm: <ul style="list-style-type: none"> Closure is retained and does not rotate relative to the package body.
CD1-2 (CTU-2)	Flat side drop, pocket side down.	Confirm: <ul style="list-style-type: none"> Closure is retained and has not rotated relative to the package body. Simulated fuel plates and basket retain geometry necessary to maintain sub-criticality.
CD3-2 (CTU-2)	Flat side drop, pocket and index lugs on side	Confirm: <ul style="list-style-type: none"> Closure is retained and does not rotate relative to the package body. Simulated fuel plates and basket retain geometry necessary to maintain sub-criticality.
CD4-2 (CTU-2)	CG over bottom end	Confirm: <ul style="list-style-type: none"> Simulated fuel plates or basket do not penetrate into the packaging bottom end insulation pocket. This is a thermal performance requirement. The insulation is not excessively compacted along the axial length of the package at the inner tube. Simulated fuel plates and basket retain geometry necessary to maintain sub-criticality.



Index lugs and pockets rotated depending on drop series.

Figure 2.7-1 – ATR FFSC Certification Tests CD1-1, CD2-1, CD3-1, CD1-2, & CD3-2 (Test CD1-1 Shown)

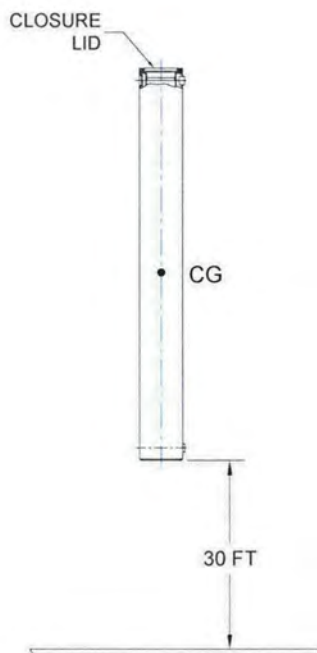


Figure 2.7-2– ATR FFSC Certification Tests CD4-1 & CD4-2

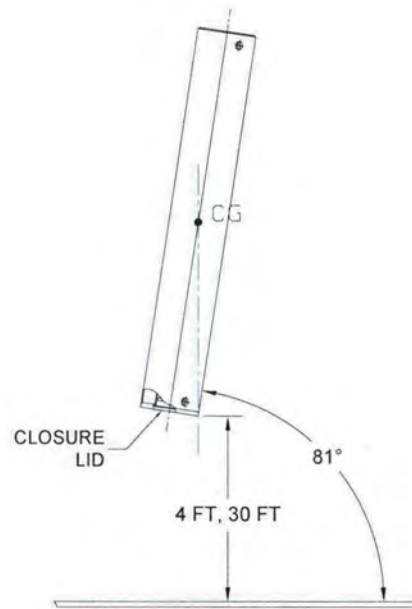


Figure 2.7-3 – ATR FFSC Certification Tests CN1-1 & CD5-1

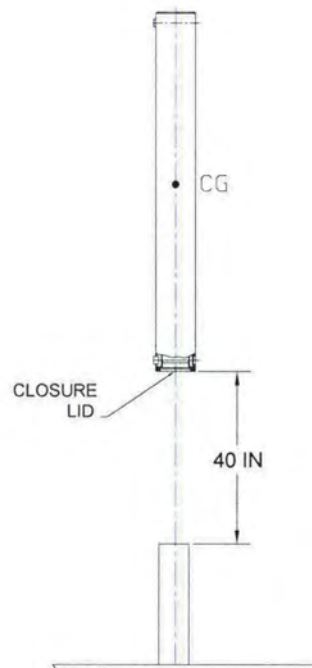


Figure 2.7-4– ATR FFSC Certification Test CP1-1

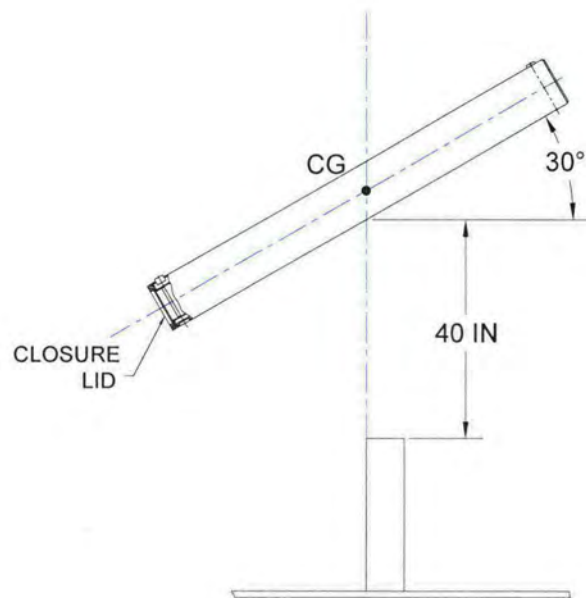


Figure 2.7-5— ATR FFSC Certification Test CP2-1

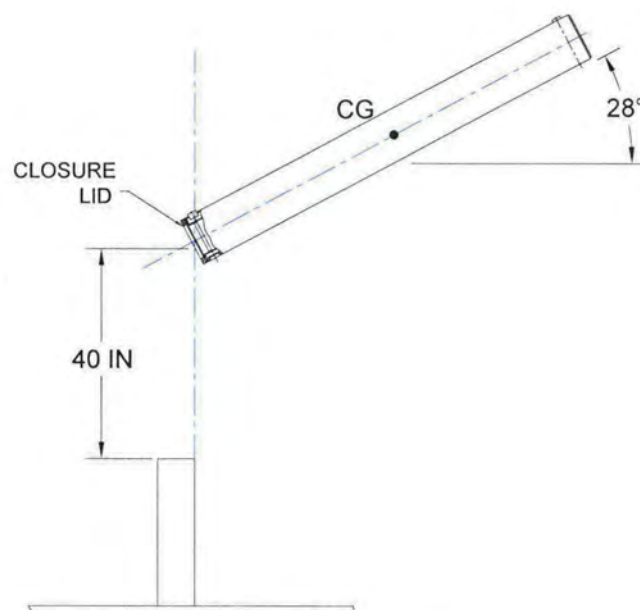


Figure 2.7-6— ATR FFSC Certification Test CP3-1

2.7.8.1 CTU-1 Package Disassembly - Results

Following the nine free drop tests and three punctures, CTU-1 was disassembled to examine the internal features. The items of critical importance focused on during the disassembly included:

- Loss or dispersal of any radioactive/fissile material
- Movement or compaction of the insulation material wrapped around the inner shell and condition of each end plate as related to the thermal evaluation.
- Deformations associated with the position and geometry of the ATR fuel element as related to the criticality evaluation.

To confirm the thermal performance features of the package the inner shell insulation and the insulation pockets at each end were visually inspected. The inner thermal shields remained in place and the maximum compaction for all insulation sections ranged from 1-1/8 inches to 1-1/2 inches. The closure end and bottom end insulation pockets were not penetrated and exhibited only minor deformation. For photographs of the disassembly see Figure 2.12.1-47 through Figure 2.12.1-51.

The inner tube was inspected as shown in Figure 2.12.1-52 and Figure 2.12.1-53. Due to the CG over corner drop deformation, CD5-1, the inner tube bowed out approximately 1/4 inch in one localized area near the closure end. In the same area the inner tube also bowed inward approximately 3/16 inch slightly deforming the FHE aluminum end plate. There were no visible signs of any weld failures associated with the inner tube.

The FHE was removed from the inner shell and visually inspected as shown in Figure 2.12.1-56. The welds joining the endplates to the FHE body had failed at both ends. There was minor bowing and deformation located near the closure end of the package and some of the neoprene padding on the inside had become detached.

The ATR fuel element end boxes were shattered as expected. The geometry of the fissile material within the fuel element was not significantly altered and clearly was within the assumptions used in the criticality analysis as illustrated in Figure 2.12.1-57 through Figure 2.12.1-62. The post test inspection of the fuel element revealed large impact marks in the fuel plates as shown in Figure 2.12.1-58 through Figure 2.12.1-59 from fragments of the fuel element end boxes deforming the ends of the fuel plates. However, the uranium aluminide fissile material within each fuel plate was not exposed and the deformations at each end did not extend to the fissile material within each fuel plate. A comparison between the pre-test and post-test inspections of the fuel element is provided in Table 2.7-2. The measurements were generally taken at five locations along the length of the fuel plates. Note that, due to the numerous free drops and punctures applied to CTU-1, the damage experienced by the ATR fuel element was much greater than is to be expected for a single, 30 ft free drop and 40-inch puncture drop. Further detail is provided in Appendix 2.12.1, *Certification Tests on CTU-1*.

Table 2.7-2 – ATR Fuel Element Measurements

Measurement Area	Pre-Test Range (in)	Post-Test Range (in)
Side Plate Flatness	±0.010	±0.075
In-Plane Bending of Side Plates	±0.011	±0.025
Side Plate Spacing - Top	4.113 – 4.130	4.015 – 4.131
Side Plate Spacing - Bottom	1.840 – 1.845	1.837 – 1.845
Height of Top Fuel Plate from Table (top side up)	2.675 – 2.691	2.655 – 2.785
Height of Bottom Fuel Plate from Table (bottom side up)	2.500 – 2.540	2.415 – 2.508
Fuel Plate to Fuel Plate Spacing	0.075 to 0.080	0.023 to 0.098 ^①

^① The minimum and maximum fuel plate spacing measurements were in localized areas near the side vents and not representative of the general spacing.

2.7.8.2 CTU-2 Package Disassembly - Results

Following the three free drop tests, CTU-2 was disassembled to examine the internal features. The items of critical importance focused on during the disassembly included:

- Loss or dispersal of any parts of the simulated loose fuel plate payload.
- Movement or compaction of the insulation material wrapped around the inner shell and condition of each end plate as related to the thermal evaluation.
- Deformations associated with the position and geometry of the simulated loose fuel plates as related to the criticality evaluation.

To confirm the thermal performance features of the package the inner shell insulation and the insulation pockets at each end were visually inspected. The gap between the thermal shield and the stiffening rib, where the shield pulls away from the rib, is less than 1/16-inch. With the thermal shields removed the maximum compaction for all insulation sections ranged from 1 inch to 1 ¾ inches. The closure end and bottom end insulation pockets were not penetrated and exhibited only minor deformation. The bottom end plate was cut open and there was no indication of compression of the insulation in that region. For photographs of the disassembly see Figure 2.12.2-18 through Figure 2.12.2-27.

The inner tube was inspected and a minor deformation occurred near the bottom end of the package as shown in Figure 2.12.2-28 and Figure 2.12.2-29. The tube was bulged out approximately 1/16-inch and, closer to the end, an inward deformation of approximately ¼ inch.

These deformations were localized and did not impair free movement of the basket in the payload cavity. There were no visible signs of any weld failures associated with the inner tube.

Following each of the three drop tests the package was opened and both the LFPB and simulated fuel plates visually inspected. The damage to the LFPB was limited to a small dent at the end of the basket that was situated closest to the package bottom and the impact point as shown in Figure 2.12.2-14. The damage was minor and did not impair the ability of the LFPB to retain the simulated fuel plates.

The simulated fuel plates within the LFPB experienced visible deformation only during the CD4-2 drop. The plates experienced localized deformation at the end of the basket closest to the package bottom as seen in Figure 2.12.2-15 and Figure 2.12.2-16. Above this area the simulated fuel plates were not deformed. Further details can be found in Appendix 2.12.2, *Certification Tests on CTU-2*.

By meeting all of the structural approval standards of Subpart E of 10 CFR §71, the ATR FFSC ensures criticality safety of the package under normal conditions of transport and hypothetical accident conditions.

2.8 Accident Conditions for Air Transport of Plutonium

The ATR FFSC package does not transport plutonium; hence, this section does not apply.

2.9 Accident Conditions for Fissile Material Packages for Air Transport

The ATR FFSC package is not transported by air; hence, this section does not apply.

2.10 Special Form

The ATR FFSC payload is not in special form; hence, this section does not apply.

2.11 Fuel Rods

The ATR FFSC package does not carry irradiated fuel rods; hence, this section does not apply.

2.12 Appendices

2.12.1 Certification Tests on CTU-1

2.12.2 Certification Tests on CTU-2

2.12.1 Certification Tests on CTU-1

This report describes the methods and results of a series of tests performed on the Advanced Test Reactor (ATR) Fresh Fuel Shipping Container (FFSC) transportation package shown in Figure 2.12.1-1. The objective of testing was to conduct drop tests in accordance with the requirements of 10 CFR 71, §71.71 Normal Conditions of Transport (NCT), and §71.73 Hypothetical Accident Conditions (HAC). The verification of the loose fuel plate basket structural integrity and the performance of the package insulation are supported by the tests described in Section 2.12.1, *Certification Tests on CTU-2*.

Testing was performed at Sandia National Laboratories (SNL) in Albuquerque, New Mexico between May 21 and May 23, 2007. Data logs were maintained to track the testing that was performed. In addition, color photographs and videos were taken to document relevant events.

2.12.1.1 Overview

There are three primary objectives for the certification test program:

1. To demonstrate that, after a worst-case series of NCT and HAC free drop and puncture events, the package maintains containment of radioactive contents.
2. To demonstrate that, after a worst-case series of NCT and HAC free drop and puncture events, geometry of both the fuel and package are controlled as necessary to maintain subcriticality.
3. To demonstrate that, after the free drop and puncture bar events, the package retains the thermal protection necessary to maintain the fuel below its melting point during the thermal evaluation.

Several orientations were tested to ensure that the worst-case series of free and puncture drop events had been considered. Post-impact examination demonstrated that the package sufficiently met the design objectives. The design objectives include:

- The package closure remained attached to the body and did not become unlocked as evidenced by no rotation of the closure, thus maintaining containment.
- The package dimensions remained essentially the same providing adequate geometry control.
- Punctures and tears in the outer shell were prevented and thermal insulation was retained for protection during the fire event.
- Reconfiguration of the ATR fuel element and/or Fuel Handling Enclosure (FHE) is bounded by the criticality analysis.

2.12.1.2 Pretest Measurements and Inspections

The ATR FFSC packaging, the FHE, and ATR fuel element were received at SNL and identified as the ATR Fuel Element Certification Test Unit (CTU). The components arrived fully constructed, although not assembled, and ready for testing. The fabrication serial

number of the ATR FFSC test unit is CTU3. The serial number for the FHE is FHA 2. The packaging and payload are identified as ATR FFSC Certification Test Unit CTU-1.

The ATR fuel element is an ATR Mark VII high enriched uranium (HEU) fuel element. The ATR fuel element, serial number XA-877R, is a rejected production fuel element based on minor dimensional discrepancies. Prior to assembly of the CTU, some basic dimensions from the fuel element were recorded for post-test comparison. Figure 2.12.1-2 is a photograph of the ATR fuel element prior to testing.

The CTU was dimensionally inspected to the drawings at the fabricator and the fabrication records forwarded to PacTec. A Certificate of Compliance was issued by the fabricator of the CTUs documenting compliance with the fabrication drawings. Minor discrepancies between the drawings and the CTUs were identified and independently evaluated. The evaluations concluded that the discrepancies were minor and would not significantly affect the CTU during testing.

There were four fabrication deviations associated with the serial number CTU3 package fabrication:

- The 3/8-16 UNC index lug screws were obtained without specified ASTM F-879 certifications.
- The #10-24 UNC closure handle screws were obtained without specified ASTM F-879 certifications.
- Chemical over testing of the package body closure plate material identified manganese content 0.02% above the ASTM A479 maximum allowable.
- The handle width is specified to be 7.5 \pm 3-inches. When measured in the free state (not secured to the closure), the handle width was undersized by approximately 0.1-inches.

Other deviations relative to the CTU are the absence of the stainless nameplate and the use of temporary rigging attachments. These items are also insignificant relative to the weight of the CTU and their impact upon the drop tests.

2.12.1.2.1 Component Weights

Component weights were measured and recorded as shown in Table 2.12.1-1.

2.12.1.2.2 Drop Test Pad and Puncture Bar Measurement and Description

The drop pad consists of a 10.2 x 28-ft x 4 to 8-in. steel plate firmly anchored to a 300 inch reinforced concrete slab embedded in the ground. The estimated weight of the pad is greater than 2 million lbs. Thus the test pad was qualified as an essentially unyielding surface for the approximately 300 lb CTU. The puncture bar measured 6 in. (150 mm) in diameter and was 36 inches above the drop pad for the puncture drops CP1 and CP2. The puncture bar was securely mounted to the drop pad by welding.

2.12.1.2.3 Equipment and Instruments

Instrumentation used for the component weights and drop tests is given in Table 2.12.1-2. All applicable test and measurement equipment were calibrated in accordance with SNL procedures. The instrumentation used was associated with physical measurements, drop height, angle of the package, and temperature. It is noted that the SNL calibration procedures require National Institute of Standards and Technology (NIST) traceability and that SNL records adequately demonstrated that the calibrations were NIST traceable.

A few different methods were used to confirm the drop height of the package including:

- A plumb bob with a stretch resistant string.
- A tape measure.
- A surveyor theodolite.

SNL project personnel under the supervision of PacTec personnel verified the correct height prior to each drop. The angle of the CTU prior to each drop was measured using a digital level.

Photographic backdrops were fabricated and erected 54 ¼ inches away to the North and 103 ½ inches to the West from the center of the drop pad. The squares on the backdrop are approximately 10.5 inches horizontal and 14.4 inches vertical on the North stadia and 12 inches square on the West stadia.

Two high speed digital video cameras were used to record the drop events. The video views were from the front and side of the drop pad, 90 degrees apart. In addition, color photographs were taken to document the testing.

2.12.1.3 Summary of Tests and Results

2.12.1.3.1 Initial Conditions

The initial conditions for the two HAC drops CD3-1 and CD4-1 were performed at reduced temperature. All other NCT drops, HAC drops, and puncture drops were performed at ambient temperature. Figure 2.12.1-3 shows the chilling unit used to chill the CTU. The chilling unit internal temperature cycled between approximately -25 to -75°F as it circulated cold air. The CTU was in the chiller for 15 hours and 17 minutes. Just prior to removing the CTU from the chiller, the surface temperature was approximately -60°F. The target temperature for the ATR fuel element at the time of drop was -20°F. The surface temperature was recorded before CD3-1 and CD4-1 and varied due to the length of time between removal from the chilling unit to the drop. It is estimated that although the surface temperature raised quickly, the internal temperature of the fuel element was close to the target temperature.

2.12.1.3.2 Summary of Testing

Table 2.12.1-3 identifies the sequential order and testing performed on the ATR FFSC CTU.

2.12.1.4 Certification Tests

2.12.1.4.1 Drop Tests

Only one NCT drop was performed followed by seven HAC drops and three drops onto a puncture bar. The testing conditions are considered conservative due to the large number of HAC drops in various orientations on the single CTU. Relatively minor deformations were recorded due to impact attenuating devices (impact limiters) not being used in the design.

Two 30 ft HAC drops performed on the ATR fuel element CTU were at reduced temperature. These two drops were considered the worst case for the ATR fuel element payload with a targeted temperature of -20°F. The other orientations confirmed the performance of the packaging.

Figure 2.12.1-4 illustrates the orientation markings on the CTU to aid in the descriptions provided throughout this report. The test identification numbering reflects the same drop orientation as performed in CTU-2. For example, CD3-1 is the same orientation as the third HAC drop in CTU-2, test CD3-2. The "-1" identifies this drop as a CTU-1 test.

2.12.1.4.1.1 CN1-1 – CG Over Top Corner NCT Drop

A rigging attachment was welded to the bottom end of the CTU to attain the proper orientation. The drop configuration for CN1-1 was with the CG over the top corner of the closure end.

Figure 2.12.1-5 illustrates the drop orientation. Initial conditions were as follows:

- Ambient temperature: 71°F
- Avg. surface temperature: 71°F
- Time: 11:21 a.m. 5/21/2007
- Drop height: 4 ft

The impact location was at corner number 5 identified in Figure 2.12.1-4. Following impact, the CTU bounced slightly and tipped over onto its side. There was minor visible exterior damage at the impact corner. The maximum deformation at the corner was approximately 1/8 inch. The closure handle was also deformed as a result of the drop. The overall length of the package did not change other than the 1/8 inch at the impact corner and compression of the closure handle of approximately 1/2 inch on one side. There was also a 1/8 inch deformation on the side corner approximately 1 ¼ inch from the impact corner. There was no visible deformation or rotation of the closure, other than the handle. Figure 2.12.1-6 and Figure 2.12.1-7 show the CTU following the NCT drop.

2.12.1.4.1.2 CD1-1 – Flat Side, Pockets Down, HAC Drop

Following CN1-1, the temporary rigging attachments were removed. To rig CD1-1 the index lugs on the CTU were removed and lifting eyes installed in their place. The drop configuration for CD1-1 was with the CTU in the typical lifting orientation, horizontal position, with the alignment pockets facing down. Figure 2.12.1-8 illustrates the drop orientation. Initial conditions were as follows:

- Ambient temperature: 76°F

- Avg. surface temperature: 78°F
- Time: 12:20 p.m. 5/21/2007
- Drop height: 30 ft

Following impact, the CTU bounced and rotated slightly in the air. The high speed video was reviewed and the impact was determined to be sufficiently flat. The justification for the determination was the large number of drops planned for the CTU, and that there were two more similar flat side drops. Also, data gathered during engineering test were consistent with the deformation exhibited from the CD1-1 drop.

There were minor visible exterior scratches resulting from the drop. The areas showing the greatest impact marks are at each end plate and near the three internal stiffening ribs. There was no significant bowing or other visible deformation. There was no visible deformation or rotation of the closure and the locking pins remained in the locked position. Figure 2.12.1-9 shows the CTU following the drop.

Upon inspection of the CTU the closure assembly was fully functional and able to be opened as illustrated in Figure 2.12.1-10. The FHE was removed and visually inspected as illustrated in Figure 2.12.1-11. There were no major deformations or cracked welds noticed. One of the spring plungers on the FHE lid was bent slightly but still functional.

As illustrated in Figure 2.12.1-12, there was no visible damage to the fuel element. The fuel element was not removed from the FHE but both end boxes were clearly visible and fully intact.

With the closure assembly removed from the body of the CTU, the locking pin was noticeably bent approximately 1/32 inch as illustrated in Figure 2.12.1-13. This locking pin was located near position number 8 identified in Figure 2.12.1-4. The other locking pin was not deformed and there was no other visible deformation of the closure assembly. It was noticed that the bent locking pin tended to bind when compressed to the open position.

2.12.1.4.1.3 CD2.A-1 – Flat Side, Index Lugs Down, HAC Drop

Following CD1-1, the FHE was reinserted with the hinged lid facing up towards the index lugs and then temporary rigging attachments were welded to the CTU to orient the package in the horizontal position with the index lugs facing down. The lifting eyes used in CD1-1 were removed and the index lugs re-installed with a 22 ft-lb torque applied to the screws. The drop configuration for CD2-1 was with the CTU in the horizontal position, with the index lugs facing down. Figure 2.12.1-14 illustrates the drop orientation. Initial conditions were as follows:

- Ambient temperature: 80°F
- Avg. surface temperature: 82°F
- Time: 2:59 p.m. 5/21/2007
- Drop height: 30 ft

Following impact, the CTU bounced and spun in the air about its longitudinal axis. After viewing the high speed video it was confirmed that the CTU impacted the drop pad at a slight angle on the longitudinal axis which caused the CTU to spin during the rebound. The index lugs did receive much of the impact but due to the angle it may not have been the worst case impact to the index lugs. There was visible exterior damage resulting from the drop at the index lugs. The index lugs were both pressed inward approximately 1/8 inch. There were no visible signs of broken welds.

The center of the package had an inward bow of about 1/16 inch. There was no other significant visible deformation. There was no visible rotation of the closure. Figure 2.12.1-15 and Figure 2.12.1-16 show the CTU following the drop. Following CD2.A-1 the closure could no longer be opened due to the body opening becoming slightly out-of-round. As illustrated in Figure 2.12.1-17, the body and closure assembly pinched in two locations.

The locking pin on the left side (near #8) of Figure 2.12.1-17 is shown stuck in the open – unlocked position. This happened during the inspection and not as a result of the drop. As the locking pins and closure assembly were inspected functionally by the test engineer, the one locking pin would bind in the open position and require a light tap from a hammer to become unstuck. The photo however, was taken before the locking pin was returned to the locked position.

2.12.1.4.2 CD2.B-1 – Flat Side, Index Lugs Down, HAC Drop

Following CD2.A-1, a second drop in the same orientation, package in the horizontal position with the index lugs facing down, was performed. The purpose of the re-test was to confirm the performance of the package in this orientation. It was felt that due to the slight incline of the package at impact, the maximum load on the index lugs was not experienced. Figure 2.12.1-18 illustrates the drop orientation which was rotated slightly to account for rotation during the drop. Initial conditions were as follows:

- Ambient temperature: 77°F
- Avg. surface temperature: 80°F
- Time: 4:07 p.m. 5/21/2007
- Drop height: 30 ft

During the drop the high speed video showed that the CTU rotated past the horizontal position in the air and impacted at an incline again. Furthermore, the rigging caught a gust of wind and blew to the side and caught the North stadia board. Following impact, the CTU bounced and spun in the air about the longitudinal axis indicating a non-flat impact. The index lugs were both pressed inward approximately 3/16 inch, at the greatest point, from the original surface of the tube. There were no visible signs of broken welds. The handle of the closure assembly broke loose at point #6 shown in Figure 2.12.1-4. The two screws both sheared off and the opposite side remained attached. There was no other significant visible deformation. There was no visible deformation or rotation of the closure and the locking pins remained in the locked position following the drop. During a functional test of the closure assembly the locking pins functioned well (with the locking pin near #8 binding in the open position) and the closure could rotate approximately ¼ inch. Figure 2.12.1-19 and Figure 2.12.1-20 show the CTU following the drop.

2.12.1.4.3 CD3-1 –Flat Side HAC Drop

The CTU was fitted with temporary rigging attachments for both CD3-1 and CD4-1 prior to chilling to minimize warming of the CTU prior to the drops. The CTU was removed from the chilling unit after 15 hours and 17 minutes with the average surface temperature reading -57°F, 14 minutes prior to CD3-1. Figure 2.12.1-21 shows the CTU in the chiller prior to removal. The CTU was oriented for a drop onto the long side with the pockets and index lugs oriented at 90° to the drop pad. The drop configuration was with the CTU's side parallel to the horizontal. Figure 2.12.1-22 illustrates the drop orientation. Initial conditions were as follows:

- Ambient temperature: 67°F
- Avg. surface temperature: +13°F
- Time: 9:31 a.m. 5/22/2007
- Drop height: 30 ft

Following impact, the CTU bounced slightly and came to rest in its standard position with the index lugs facing up. The impact side showed just minor scratches and impact marks from the drop. Figure 2.12.1-23 and Figure 2.12.1-24 show the CTU following the drop. The impact side showed a slight bowing of the ends. Using a straight edge, the maximum gap at each end was approximately 1/8 inch. There was no visible rotation of the closure and the locking pins remained in the locked position following the CD3-1 drop.

As illustrated in Figure 2.12.1-25, the closure assembly was functionally tested and upon close inspection it was found that the locking pin near point #4 (bottom of picture) had sheared off between the closure assembly and body preventing the locking pin from engaging in the body. The locking pin near point #8 was engaged following the drop but continued to bind in the open - unlocked position when depressed by hand. Figure 2.12.1-25 shows this locking pin in the open position following the attempt to open the closure. The closure assembly could partially rotate approximately 1/4 inch but was unable to fully rotate to the open position. The locking pin near point #8 was returned to the locked position following the inspection. The dull gray color seen on the photographs is frost.

2.12.1.4.4 CD4-1 –CG Over Bottom End HAC Drop

Immediately after CD3-1, rigging was attached to the pre-welded lugs near the closure and the CTU prepared for the CD4-1 drop. The time between CD3-1 and CD4-1 was 33 minutes. During that time the CTU was kept elevated above the drop pad. The drop configuration was with the CTU in the vertical position, with the bottom end down (closure end up). Figure 2.12.1-26 illustrates the drop orientation. Initial conditions were as follows:

- Ambient temperature: 64°F
- Avg. surface temperature: 42°F
- Time: 10:04 a.m. 5/22/2007
- Drop height: 30 ft

Following impact the outer shell of the CTU exhibited minor bowing near the impact end with the greatest deformation measuring approximately 1/8 inch on the 90° side per Figure 2.12.1-4. The overall length of the package body was compared with the initial measurements at the eight locations and found to have compressed a maximum of approximately 1/8 inch. There was no visible deformation or rotation of the closure following the drop and the functionality of the closure assembly did not change. Figure 2.12.1-27 and Figure 2.12.1-28 show the CTU following the drop.

2.12.1.4.5 CP3-1 – Oblique, CTU Closure Over Puncture Bar

Following CD4-1 the CTU was positioned for an unscheduled puncture bar drop onto the closure. The purpose for this drop was to attempt to rotate the closure assembly prior to the CD5-1 drop which would severely deform the closure area of the body preventing any chance of

rotation. The temporary rigging attachments from CD3-1 and CD4-1 were removed and new attachments welded for this drop. The puncture bar, 36 inches in height, was welded to the drop pad. For CP3-1, the CTU was hoisted at a 28.3° orientation from horizontal and a 225° twist on the longitudinal axis so the puncture bar would impact one of the ribs in the closure assembly. The closure handle, which had broke off from one side during CD2.B-1, was bend outward to keep from interfering with the targeted impact location. Figure 2.12.1-29 and Figure 2.12.1-30 illustrate the drop orientation. Initial conditions were as follows:

- Ambient temperature: 72°F
- Avg. surface temperature: 73°F
- Time: 11:50 a.m. 5/22/2007
- Drop height: 40 inches

The puncture bar squarely impacted the closure rib and the CTU bounced away from the puncture bar onto the drop pad. Following the drop, the closure assembly rib exhibited minor deformations at the impact point made by the puncture bar. There was no rotation of the closure assembly and the locking pins showed no visible signs of deformation. The locking pin by #8 remained in the locked position. Both locking pins were functioning and able to be moved and compressed against the spring when tested by hand. Note that the locking pin by #4 was previously sheared during the CD3-1 drop. Figure 2.12.1-31 shows the CTU closure following CP3-1.

2.12.1.4.6 CD5-1 – CG Over Top Corner HAC Drop

For CD5-1, the CTU was hoisted in the same orientation as CN1 with the CG over the top corner; point #5 in Figure 2.12.1-4. The closure handle was removed for convenience since it was loose and obstructing the drops. Figure 2.12.1-32 illustrates the drop orientation. Initial conditions were as follows:

- Ambient temperature: 76°F
- Avg. surface temperature: 81°F
- Time: 1:54 p.m. 5/22/2007
- Drop height: 30 ft

Following impact, the CTU bounced slightly and tipped over onto its side. The impact corner was deformed in approximately 5/8 inch. There was modest deformation on the sides of the package near the impact location bulging in approximately 1/2 inch near the index lug pocket and bulged out approximately 5/8 inches on the adjoining side. The impacted corner deformed in approximately 5/8 inch and the opposite corner, #1, had no change in length. Figure 2.12.1-33 through Figure 2.12.1-36 show the CTU following CD5-1.

Following the drop, the closure assembly exhibited deformation with the end of the package and was unable to be rotated more than 1/8 inch in either direction. The locking pins showed no visible signs of deformation and the pin by #8 remained in the locked position. Both locking pins were functioning and able to be moved and compressed against the spring when tested by hand.

2.12.1.4.7 CD2.C-1 – Flat Side, Index Lugs Down, HAC Drop

Following CD5-1 a third drop in the same CD2 orientation, package in the horizontal position with the index lugs facing down, was performed. The purpose of third re-test was to confirm the performance of the package in this orientation. It was felt that due to the incline of the package at impact during the previous drops, the maximum load on the index lugs was not experienced. Both the release mechanism and rigging cables were changed to aid the drop. Figure 2.12.1-37 illustrates the drop orientation. Initial conditions were as follows:

- Ambient temperature: 79°F
- Avg. surface temperature: 79°F
- Time: 2:37 p.m. 5/22/2007
- Drop height: 30 ft

The third try produced a satisfactory drop orientation. Following impact, the CTU bounced and spun just slightly indicating the impact was directly on the index lugs. The index lugs were both pressed inward. The index lug at the closure end was flush with the general surface. The index lug at the bottom end was pushed in to approximately 1/8 inch from the general surface. Figure 2.12.1-38 and Figure 2.12.1-39 show the index lugs following the drop. The index lugs were removed and a cracked weld was revealed under the index lug near the closure end as shown in Figure 2.12.1-40. The length of the cracked weld was approximately 1/2 inch. There was no other significant visible deformation. There was no visible deformation or rotation of the closure as a result of the drop.

2.12.1.4.8 CP2-1 – CG Over Side, 30° Oblique, HAC Puncture Drop

For CP2-1, the CTU was hoisted at a 30° oblique angle with the CG over the edge of the puncture bar. Figure 2.12.1-41 illustrates the drop orientation. Initial conditions were as follows:

- Ambient temperature: 76°F
- Avg. surface temperature: 77°F
- Time: 3:19 p.m. 5/22/2007
- Drop height: 40 inches

As the CTU impacted the puncture bar, there was no tearing or severe deformation. The initial impact caused a deformation of approximately 1/2 inch deep by 5 inches across with a radius the same as the puncture bar. There was no fracture of the outer shell. Figure 2.12.1-42 and Figure 2.12.1-43 show the CTU following the CP2-1 drop.

2.12.1.4.9 CP1-1 – CG Over Center of Closure HAC Puncture Drop

For CP1-1, the CTU was hoisted in the vertical orientation with the closure directly over the puncture bar. Figure 2.12.1-44 illustrates the drop orientation. Initial conditions were as follows:

- Ambient temperature: 79°F
- Avg. surface temperature: 81°F
- Time: 4:06 p.m. 5/22/2007

- Drop height: 40 inches

Following impact, the CTU bounced slightly on the puncture bar, as verified by high speed video, and came to rest in the vertical position on top of the puncture bar as seen in Figure 2.12.1-45. Following the drop, the tamper indicating device (TID) post was deformed into the closure. The closure assembly exhibited minor scratches from the puncture bar. The locking pins showed no visible signs of deformation and the remaining locking pin by #8 remained in the locked position. Both locking pins were functioning and able to be moved and compressed against the spring when tested by hand. Figure 2.12.1-46 shows the CTU in the up-side-down position following CP1-1. Note that both locking pins were binding somewhat following testing and shown in the photographs in the open – unlocked position following the functional tests.

2.12.1.5 Post-test Disassembly and Inspection

The final acceptance criteria for the ATR FFSC package lies with the criticality and thermal evaluations. Any increase in reactivity of the contents resulting from the certification tests must not exceed the allowable as defined in the criticality evaluation. The inspections required to support determination of compliance with the acceptance criteria are identified as follows:

- Inspect the outer shell to verify the thermal performance of the package is unimpaired by the free drop and puncture events. The thermal analysis assumes that the outer shell is intact such that there is no significant communication between the environment and the outer/inner shell annular space during the thermal event.
- Inspect the insulation to verify compliance with the assumptions of the thermal analysis.
- Inspect the overall package to verify that the package geometry remains within the criticality analyses assumptions.
- Inspect the Mark VII fuel element to verify that the fuel geometry remains within the assumptions of the criticality analyses.

Any deviation of the test results from these acceptance criteria must be reconciled with the criticality or thermal evaluations.

2.12.1.5.1 CTU Inspection

Radiological surveys were performed after each drop test and during the disassembly of the package. The radiological survey reports confirm that there was no loss or dispersal of radioactive material from the package or from the ATR fuel element.

The ATR fuel element CTU was disassembled and inspected on May 23, 2007. Prior to disassembly the exterior dimensions were recorded for comparison to the pre-test condition. Table 2.12.1-4 lists the measured dimensions and Figure 2.12.1-4 identifies the location of the identified measurements.

The closure handle was flattened, loosened, and finally removed during testing for convenience. Due to the relatively weak nature of the handle, its presence or absence had no significant effect on any test outcome. The height of the handle changed from 1 3/8 inches to 1/2 inch on one side before being removed. There was very little bowing or change in shape of the package. The maximum

bowing of the package over its length is estimated at approximately $\frac{1}{4}$ inch. During the CD5-1, CG over corner HAC drop, deformation of the outer wall caused the width of the package to increase from 8 inches to approximately 8 $\frac{5}{8}$ inches. The same CD5-1 impact caused the outer wall to deform inward approximately $\frac{1}{2}$ inch.

The CTU was disassembled systematically by cutting away the outer layers of the packaging using an abrasive saw. The destructive examination was necessary due to the deformation of the closure and the need to inspect the interior insulation. Figure 2.12.1-47 illustrates the unsuccessful attempt to rotate the closure assembly and open the package with a steel bar and 5 lb hammer. The closure could not be rotated more than approximately $\frac{3}{8}$ inch using the bar and hammer.

The package was cut with an abrasive saw lengthwise along two opposite corners and at the ends to expose the thermal shield. Figure 2.12.1-48 through Figure 2.12.1-50 show the condition of the thermal shields and insulation. The thermal shields were in relatively good shape with dents from both the index lug bosses and pockets on the shields. There was also some minor deformation at each end of the shields by the stiffening rib plates.

The insulation tended to compact towards the closure end except for the bottom end which compacted towards the bottom. The compaction was not uniform but varied around the circumference of the internal pipe. The maximum compaction for all section ranged from 1- $\frac{1}{8}$ inches to 1- $\frac{1}{2}$ inches.

Two thermal shield designs were used; one with a simple overlapping design and the other secured by rivets. There was no appreciable difference between the performance of either design. Both experienced minor deformation at the pockets and index lugs, and at the ends due to impacting the adjoining plates. Furthermore, the compaction of the insulation under each shield was very similar. On the riveted design, there was no failure of any rivet.

The thermal shields and insulation were removed and using an abrasive saw the bottom end plate was removed by cutting the inner tube. Figure 2.12.1-51 illustrates the condition of the bottom end plate. There were no large deformations or punctures of the stainless steel plate. There were no visual indications of broken welds or other damage near the end plate.

As shown in Figure 2.12.1-52 and Figure 2.12.1-53, the inner tube was inspected and the photographs show the areas of greatest deformation. Due to the CG over corner drop deformation, CD5-1, the inner tube bowed out approximately $\frac{1}{4}$ inch. The inner tube also bowed inward approximately $\frac{3}{16}$ inch slightly deforming the FHE aluminum end plate. There were no visible signs of any weld failures associated with the inner tube.

Figure 2.12.1-54 illustrates the relatively unchanged position of the FHE and fuel element within the CTU. Also seen in this figure are pieces of the broken end box at the bottom end and also pieces of neoprene padding from the FHE during removal. The FHE was somewhat difficult to remove and the aluminum end plate had broken off so the ATR fuel element was carefully pulled from the bottom end of the package as illustrated in Figure 2.12.1-55. Both end boxes of the fuel element had shattered into several pieces. These pieces were collected and kept with the fuel element. There were no pieces of the fuel element end boxes found outside the FHE. Once the fuel element was removed, the FHE was pulled from the inner tube. The welds securing each FHE end plate to the body were completely broken and both the end plates were loose. Figure 2.12.1-56 illustrates the area of greatest deformation to the FHE which was at the closure end.

2.12.1.5.2 ATR Fuel Element Inspection

The ATR fuel element was placed on an inspection table and compared against the same pre-test measurements for the fuel plates. Because the fuel element end boxes had shattered and bent the ends of the side plates, some of the fuel plate measurements taken from the side plates could be slightly exaggerated. The measurements included side plate flatness, in plane bending of the side plates, side plate spacing, overall fuel plate spacing, and fuel plate to fuel plate spacing. Table 2.12.1-5 provides the general change in dimensions to the fuel plates. Measurements were generally taken at five locations along the length of the fuel element. The five locations include 1 inch from the end of the fuel plate (neglecting the end boxes), 12 inches from each end of the fuel plate, and at the center of the fuel plate.

Figure 2.12.1-57 through Figure 2.12.1-62 illustrate the condition of the ATR fuel element. As shown in Figure 2.12.1-58 and Figure 2.12.1-59, fragments from the fuel element end boxes deformed and cut into the ends of the fuel plates during testing. At no point did the fuel meat, the embedded uranium within the aluminum cladding, become exposed.

In conclusion, the CTU satisfied the acceptance criteria of preventing loss or dispersal of the contents, the outer shell remained intact, the insulation remained within the assumptions of the thermal analysis, and the package and fuel geometry remained greatly unchanged. The deformations of the package and condition of the ATR fuel element were evaluated against the criticality and thermal evaluations and determined to be within the bounds of the assumptions and conditions used to ensure safety.

Table 2.12.1-1 - Component Weights

Component	Weight (lbs)
Body Assembly	225.0
Closure Assembly	9.0
Fuel Handling Enclosure	14.3
ATR Fuel Element	22.1
Package (fully loaded)	270.4

Table 2.12.1-2 - Instrumentation for Drop Tests

Item Description	Model	Serial Number	Calibration Due Date	Comments
Drop Height Indicators	N/A	N/A	N/A	String plumb bobs made specifically for this testing. The length was established using a metal tape measure.
Tape Measure	Stanley	N/A	N/A	35-ft. steel tape
Digital Level 2'	M-D Building Products	SNL 3665	1/23/09	Used to identify CTU orientation
Digital Level 4'	M-D Building Products	SNL 3666	1/23/09	Used to identify CTU orientation
Scale	NCI	D798311	2/12/08	Used to measure weights of CTU components
Hook Scale	Dively	60418/46180	Aug 2007	Used to measure the weight of the ATR FFSC body
Multilogger Thermometer	Omega Engineering	06000855	10/19/07	Handheld temperature reader for measuring ambient temperature and CTU surface temperature
Temperature Probe	N/A	56194	10/19/07	Probe which attaches to multimeter
Torque Wrench 0-25 ft-lbs	N/A	SNL 1933	2/26/09	Used to apply measured torque to index lug screws

Table 2.12.1.3 - Summary of Testing

Test No.	Test Description	Comments
CN1-1	CG over top corner	CG over top corner drop from 4 ft. Minor deformation at impact corner. Maximum change in length approximately 1/8 inch at impact point only. Closure handle deformed. Closure functions properly.
CD1-1	Flat side drop, pocket side down	Flat side drop from 30 ft. Minor visible scratches and impact marks. Closure functions properly. Package opened and inspected. One locking pin on closure bent slightly but still operable. No visible damage to fuel element.
CD2.A-1	Flat side drop, index lugs facing down	Flat side drop from 30 ft. Impact pushed index lugs into package approximately 1/8 inch. CTU impact was not level on the longitudinal axis causing the package to bounce and spin after impact. A second drop in the same orientation was chosen.
CD2.B-1	Flat side drop, index lugs facing down	Flat side drop from 30 ft. Impact pushed index lugs into package approximately 3/16 inch. CTU impact again was not level due to a gust of wind blowing the rigging straps into the stadia board.
CD3-1	Flat side drop, pockets and index lugs on side, reduced temperature	Flat side drop from 30 ft. Minor visible scratches and impact marks. One locking pin sheared during impact. No rotation of closure. Surface temperature approximately 13°F.
CD4-1	CG over bottom end (vertical), reduced temperature	Flat bottom drop from 30 ft. No appreciable deformation on impact side but minor bowing outward on side near impact end. Maximum change in length approximately 1/8 inch. Surface temperature approximately 41°F.
CP3-1	Closure assembly over puncture bar	Unscheduled drop chosen to ensure performance of closure assembly due to broken locking pin from CD3. Impact caused small deformation to closure assembly rib. There was no rotation of the closure and no other visible damage.
CD5-1	CG over top corner (same orientation as CN1)	CG over top corner drop from 30 ft. Deformation of the corner, including adjoining sides, and minor bending of the closure assembly. Maximum change in length at impact point approximately 5/8 inches.
CD2.C-1	Flat side drop, index lugs facing down	Flat side drop from 30 ft. This third drop on the index lugs was chosen to ensure performance of the outer skin and index lugs in this orientation. The previous two drops did not impact flat on the lugs. Index lug at closure end pushed in flush with general package surface, approximately 1/2 inch. A small crack in the weld between the index lug boss and square tube was recorded.
CP2-1	CG over side, 30° oblique	CG over side puncture drop from 40 in. Minor deformation from impact. Depth of impact approximately 1/2 inch. Width of impact approximately 5" across.

Table 2.12.1.3 - Summary of Testing

Test No.	Test Description	Comments
CP1-1	CG over center of closure (Vertical)	Vertical puncture drop on closure from 40 in.. The tamper indicating device stud pushed into closure assembly. No other visible damage. No rotation of closure assembly.

Table 2.12.1-4 – Package Length Measurements

Test ID	1	2	3	4	5	6	7	8
Pre-Test (in.)	72 ½	72 ½	72 ½	72 ½	72 ½	72 ½	72 ½	72 ½
Post-Test (in.)	72 5/16*	72 ½	72 7/16	72 ¼	71 11/16*	72 ¼	72 ½	72 7/16

*These locations were modified slightly due to the welding and removal of temporary rigging attachments. The change to position #5 was approximately -1/16 inch. There was approximately no change to position #1.

Table 2.12.1-5 - ATR Fuel Element Measurements

Measurement Area	Pre-Test Range (in)	Post-Test Range (in)
Side Plate Flatness	±0.010	±0.075
In-Plane Bending of Side Plates	±0.011	±0.025
Side Plate Spacing - Top	4.113 – 4.130	4.015 – 4.131
Side Plate Spacing - Bottom	1.840 – 1.845	1.837 – 1.845
Height of Top Fuel Plate from Table (top side up)	2.675 – 2.691	2.655 – 2.785
Height of Bottom Fuel Plate from Table (bottom side up)	2.500 – 2.540	2.415 – 2.508
Fuel Plate to Fuel Plate Spacing	0.075 to 0.080	0.023 to 0.098*

* The minimum and maximum fuel plate spacing were in localized areas near the side vents and not representative of the general spacing.

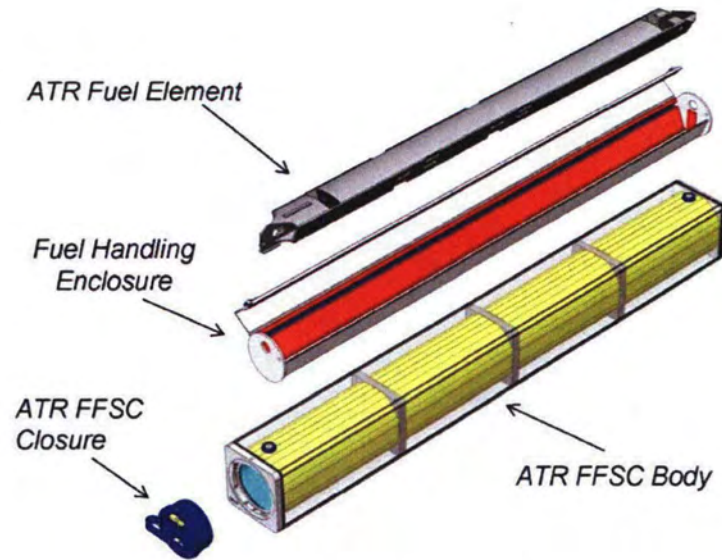


Figure 2.12.1-1 - ATR FFSC

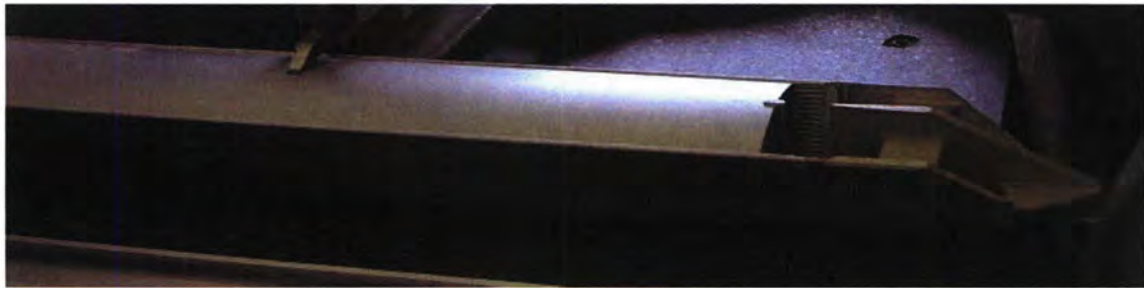


Figure 2.12.1-2 – ATR Fuel Element



Figure 2.12.1-3 – Chilling Unit

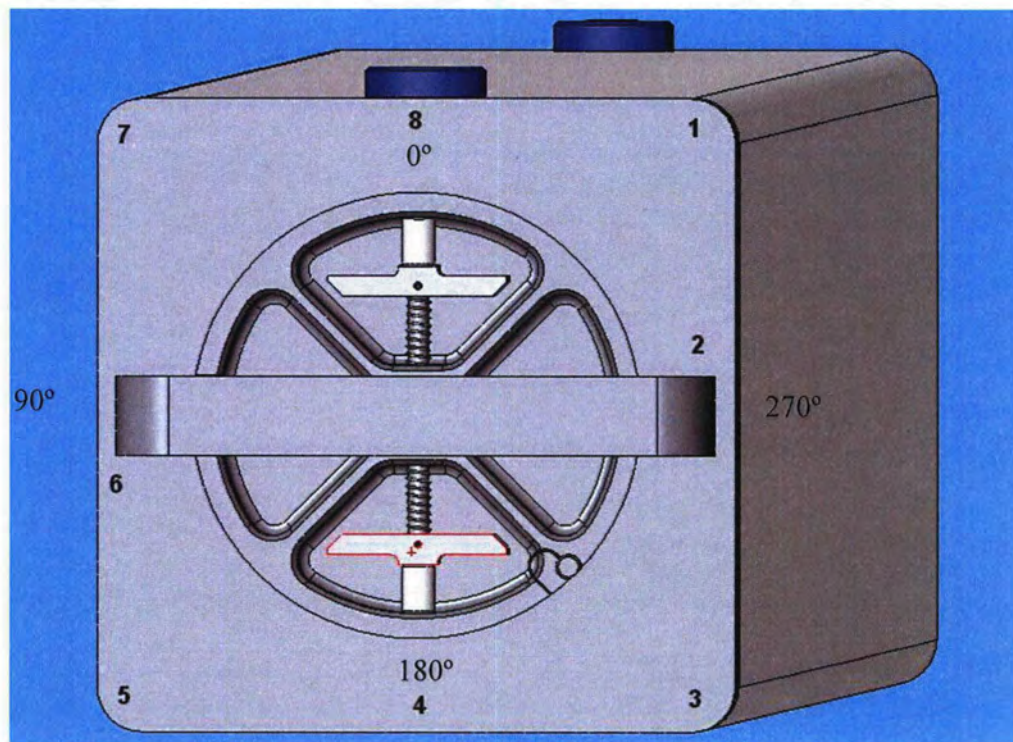


Figure 2.12.1-4 – ATR Package Orientation Markings



Figure 2.12.1-5 - CN1-1 Drop Orientation

Impact
corner



Figure 2.12.1-6 - CN1-1 Impact Damage



Figure 2.12.1-7 - CN1-1 Impact on Closure Handle

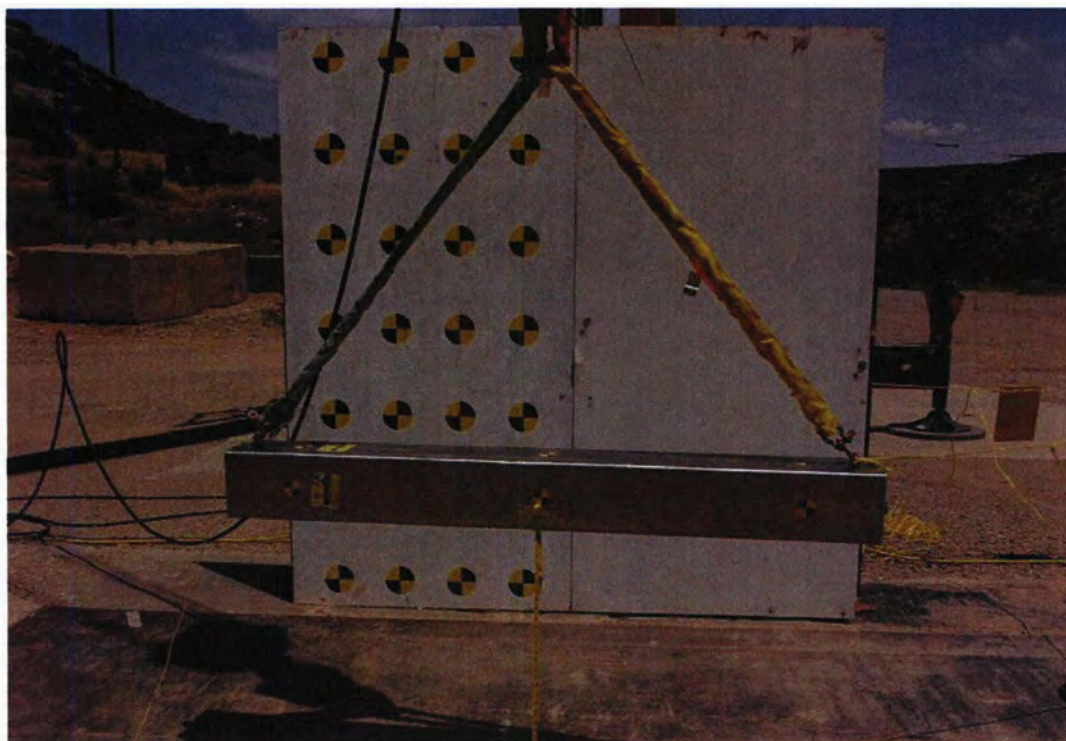


Figure 2.12.1-8 – CD1-1 Drop Orientation

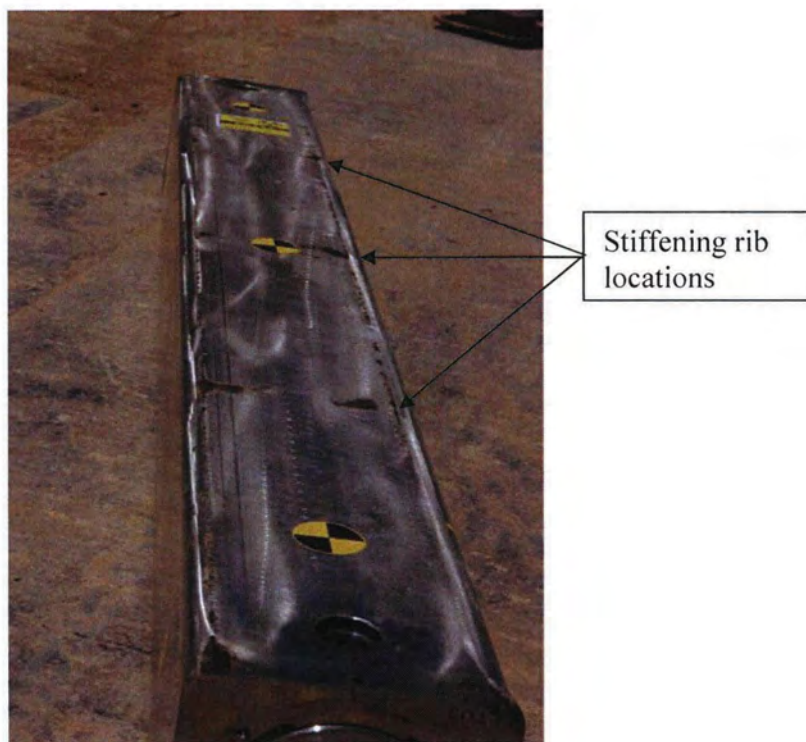


Figure 2.12.1-9 – CD1-1 Impact Side

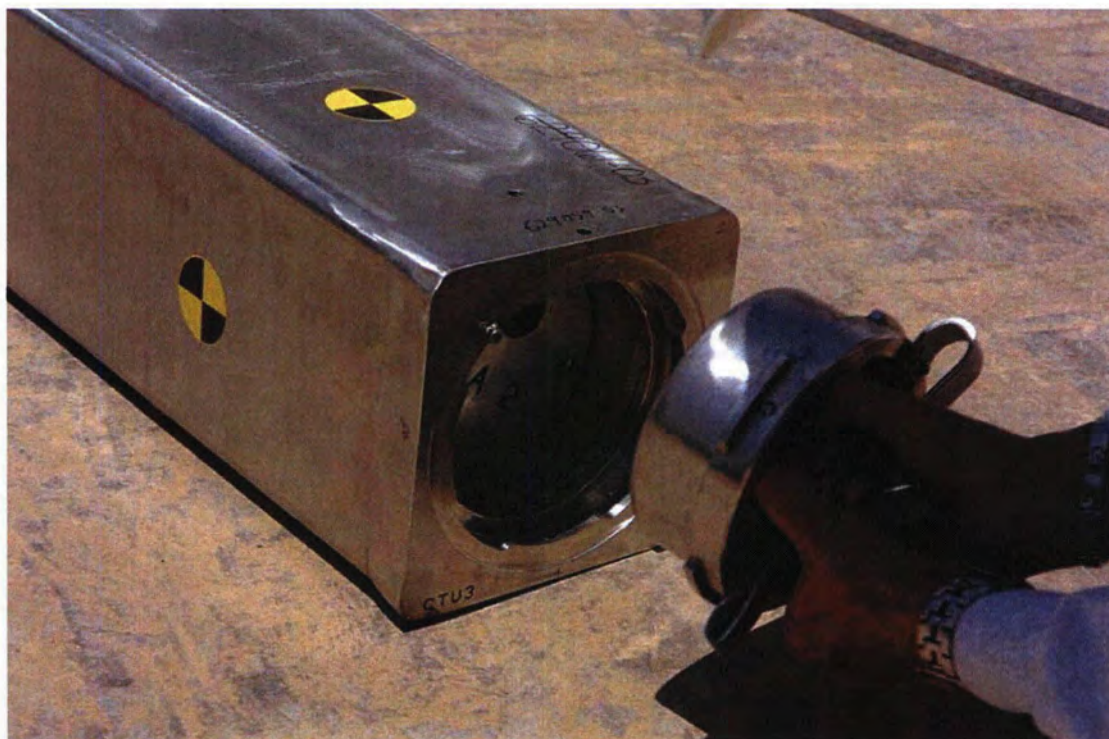


Figure 2.12.1-10 - Opening of CTU Following CD1-1

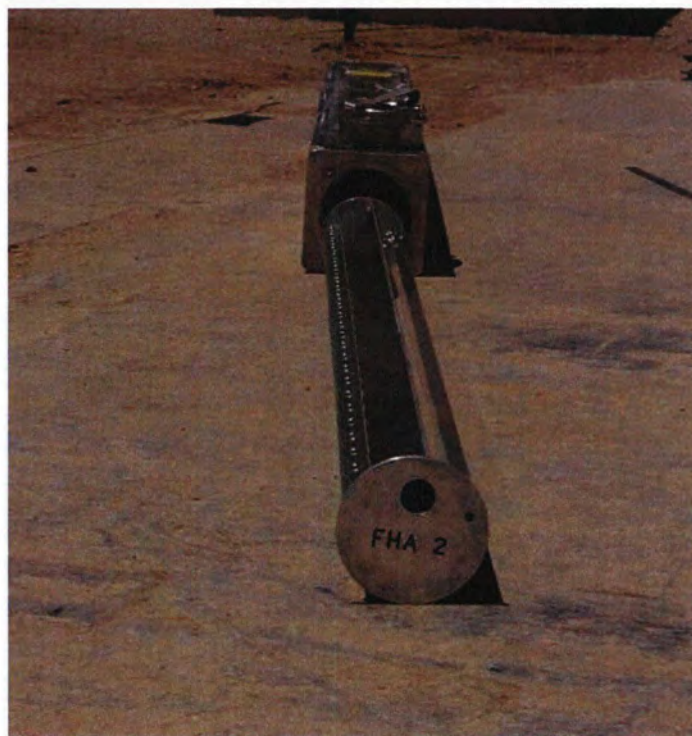


Figure 2.12.1-11 - Inspection of Payload Following CD1-1

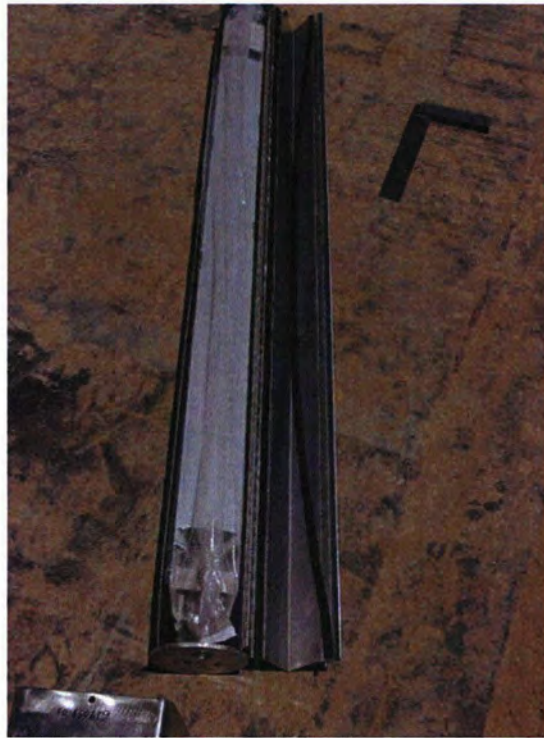


Figure 2.12.1-12 - Inspection of Fuel Element Following CD1-1

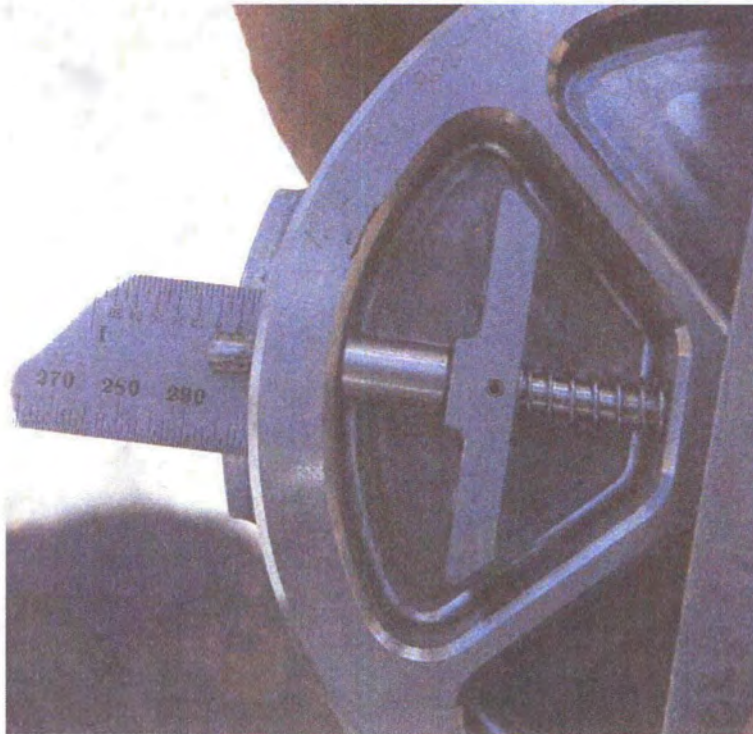


Figure 2.12.1-13 - Inspection of Closure Assembly Following CD1-1

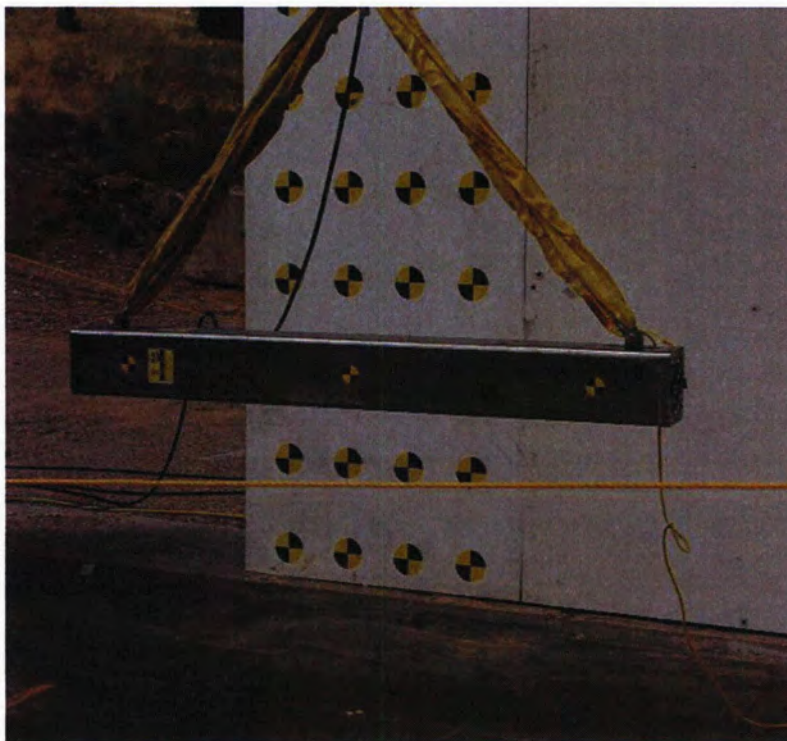


Figure 2.12.1-14 – CD2.A-1

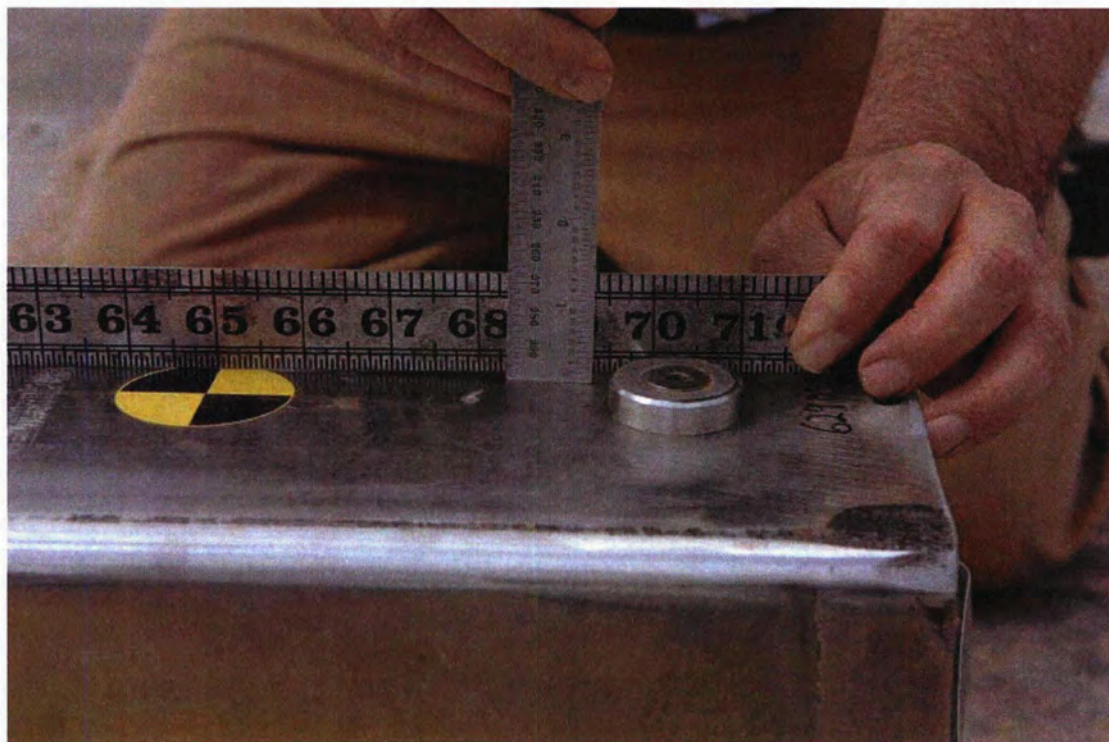


Figure 2.12.1-15 - Index Lug Near Closure End, CD2.A-1

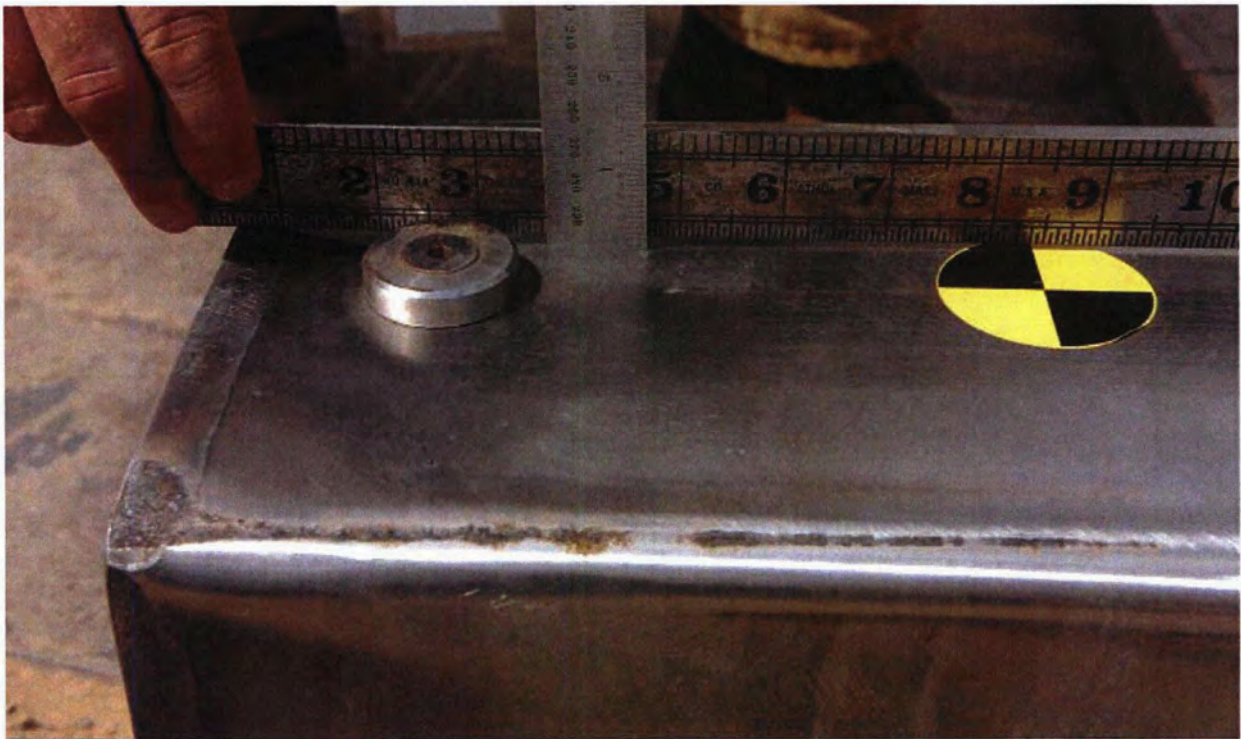


Figure 2.12.1-16 - Index Lug Near Bottom End, CD2.A-1

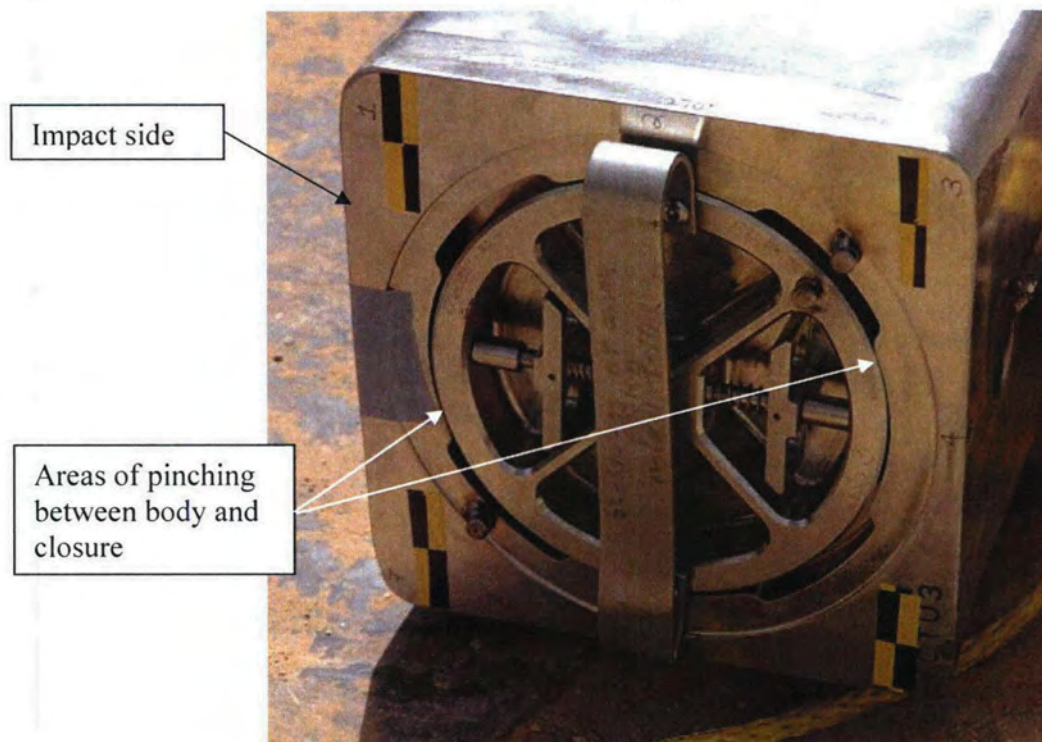


Figure 2.12.1-17 - View of Closure Following CD2.A-1

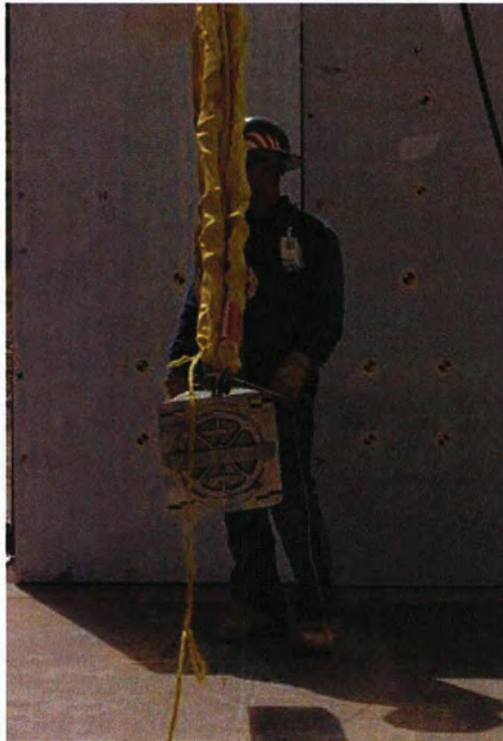


Figure 2.12.1-18 - CD2.B-1 Drop Orientation



Figure 2.12.1-19 - CTU Position Following CD2.B-1 Drop

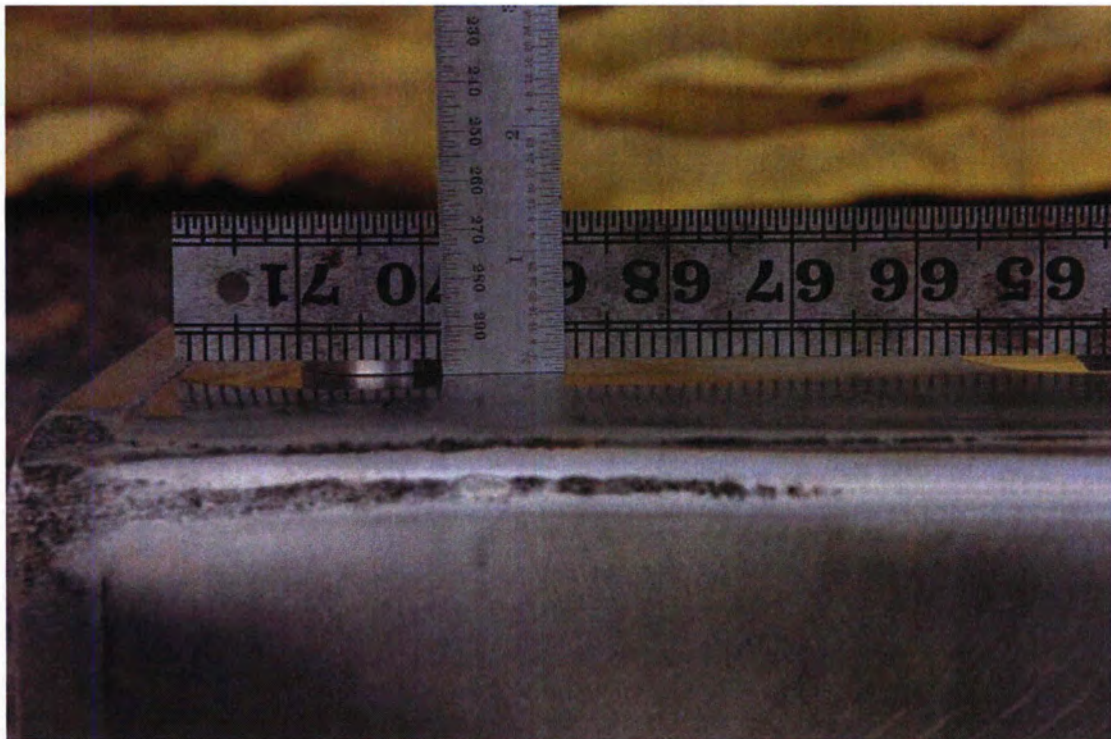


Figure 2.12.1-20 - Index Lug Near Bottom End, CD2.B-1



Figure 2.12.1-21 - CTU in Chiller Unit

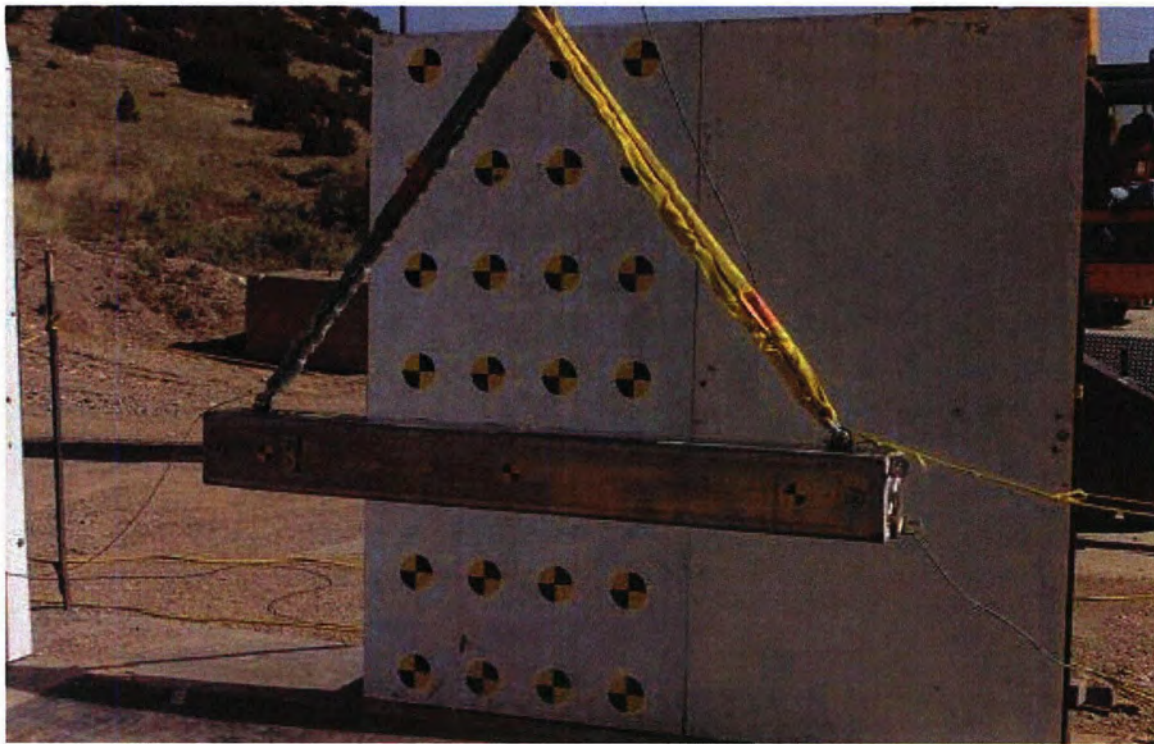


Figure 2.12.1-22 - CD3-1 Drop Orientation

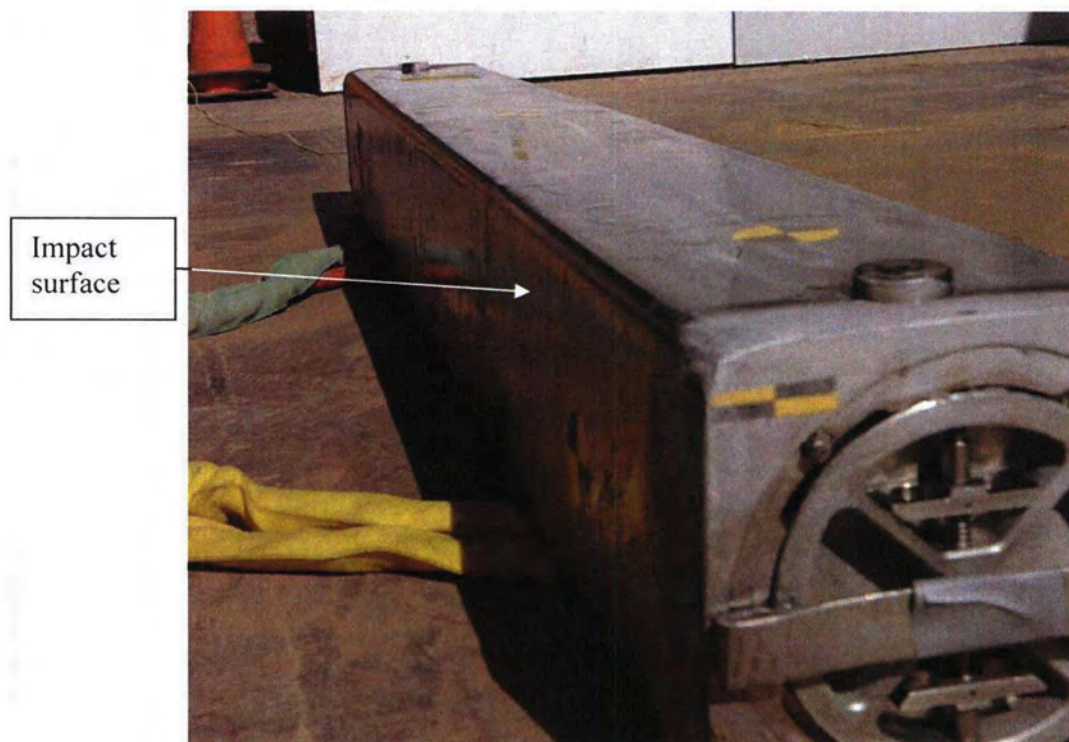


Figure 2.12.1-23 - CTU Following CD3-1 Impact

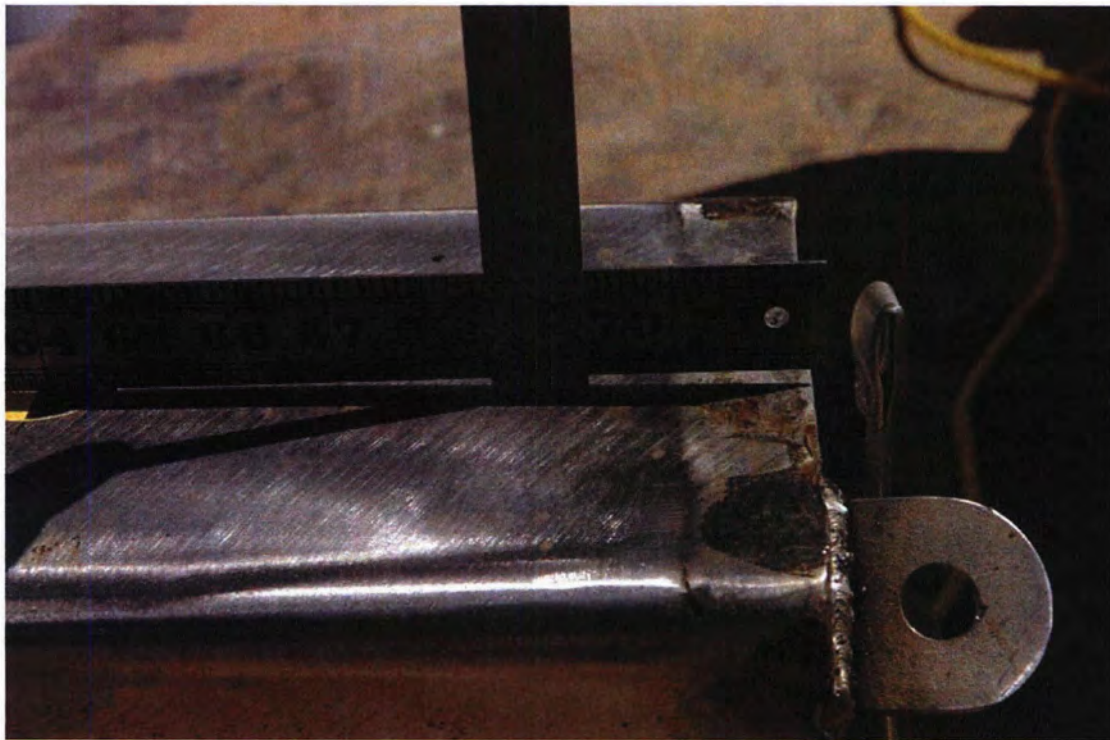


Figure 2.12.1-24 - Deformation Near Closure End Following CD3-1

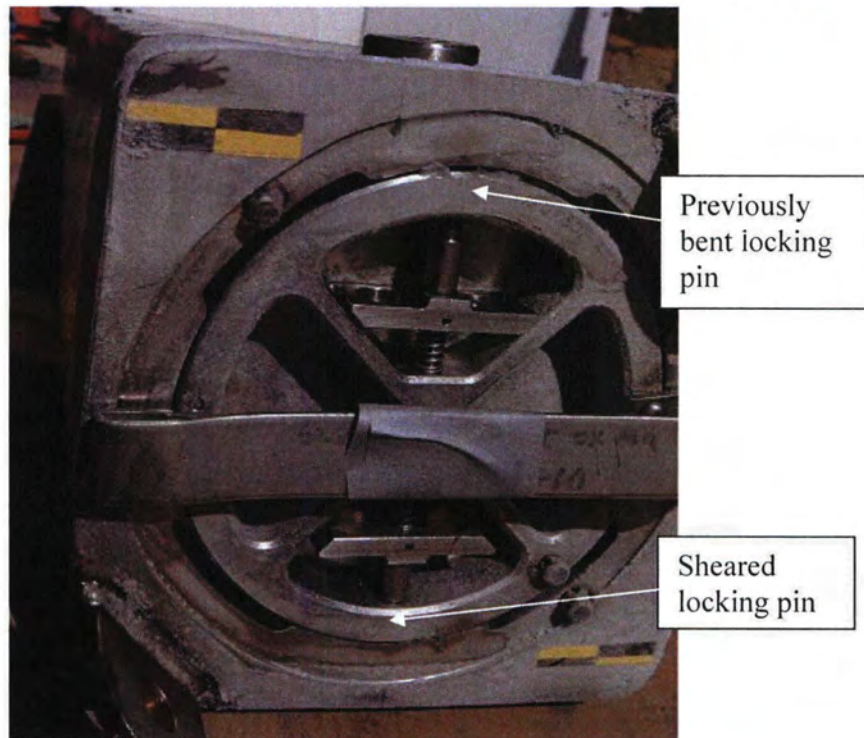


Figure 2.12.1-25 - View of Closure Following CD3-1



Figure 2.12.1-26 - CD4-1 Drop Orientation

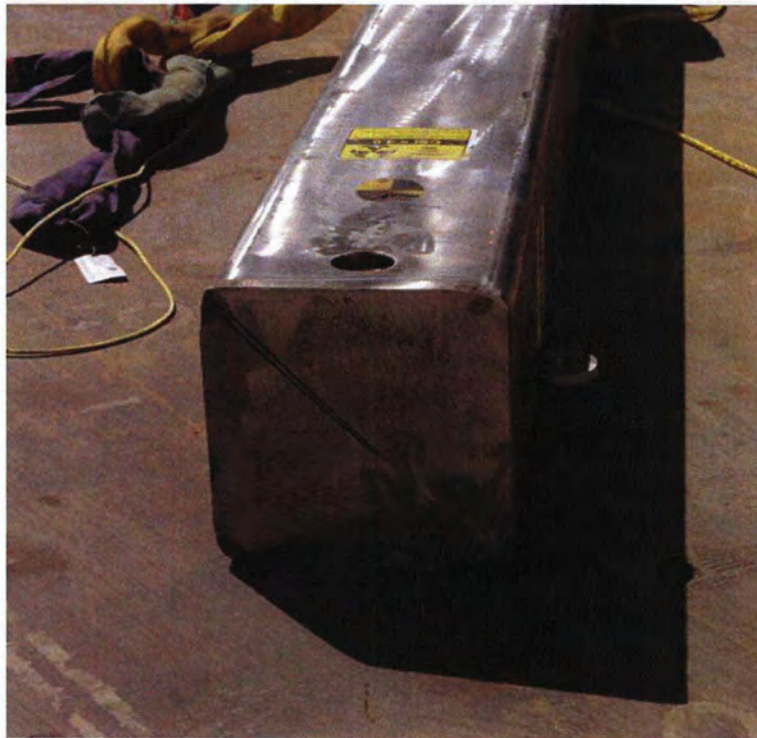


Figure 2.12.1-27 - View of Impact End Following CD4-1

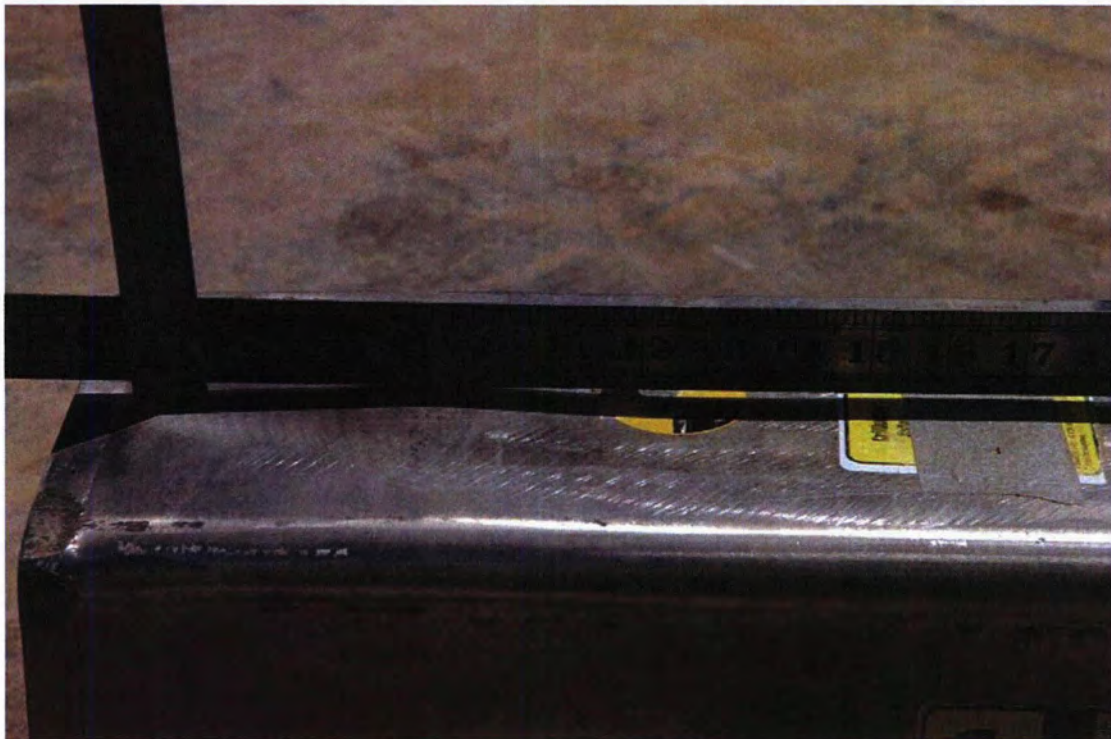


Figure 2.12.1-28 - View of Side Bowing Following CD4-1

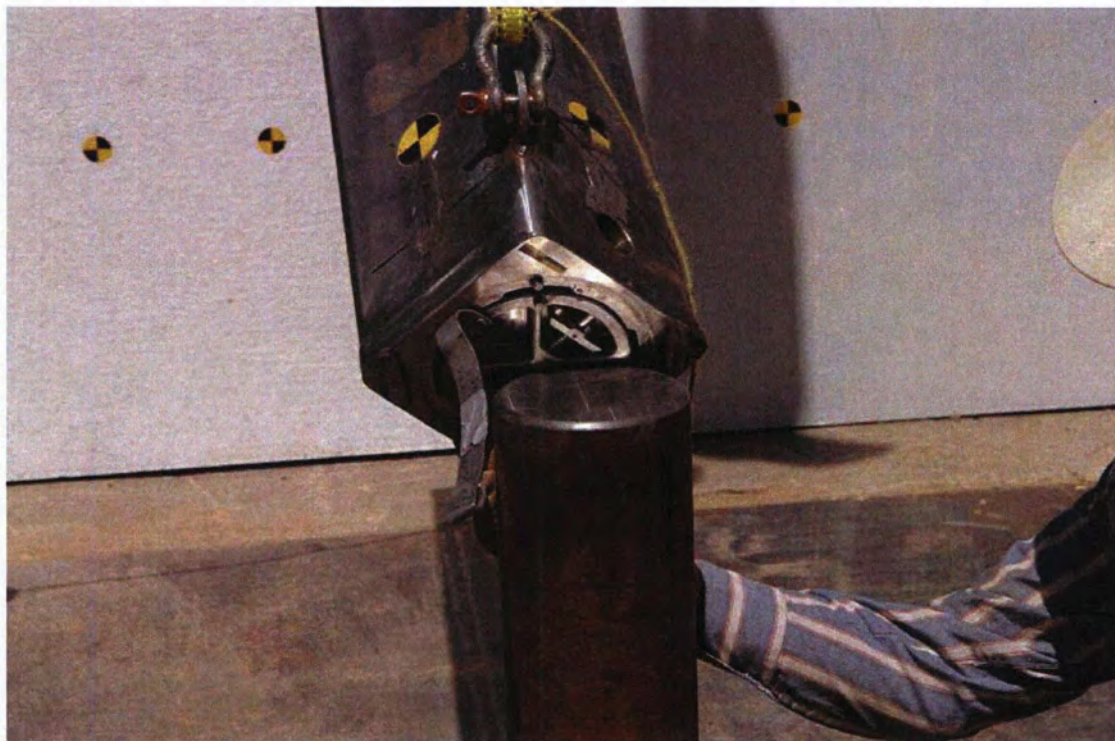


Figure 2.12.1-29 - CP3-1 Drop Orientation – Front



Figure 2.12.1-30 - CP3-1 Drop Orientation – Front

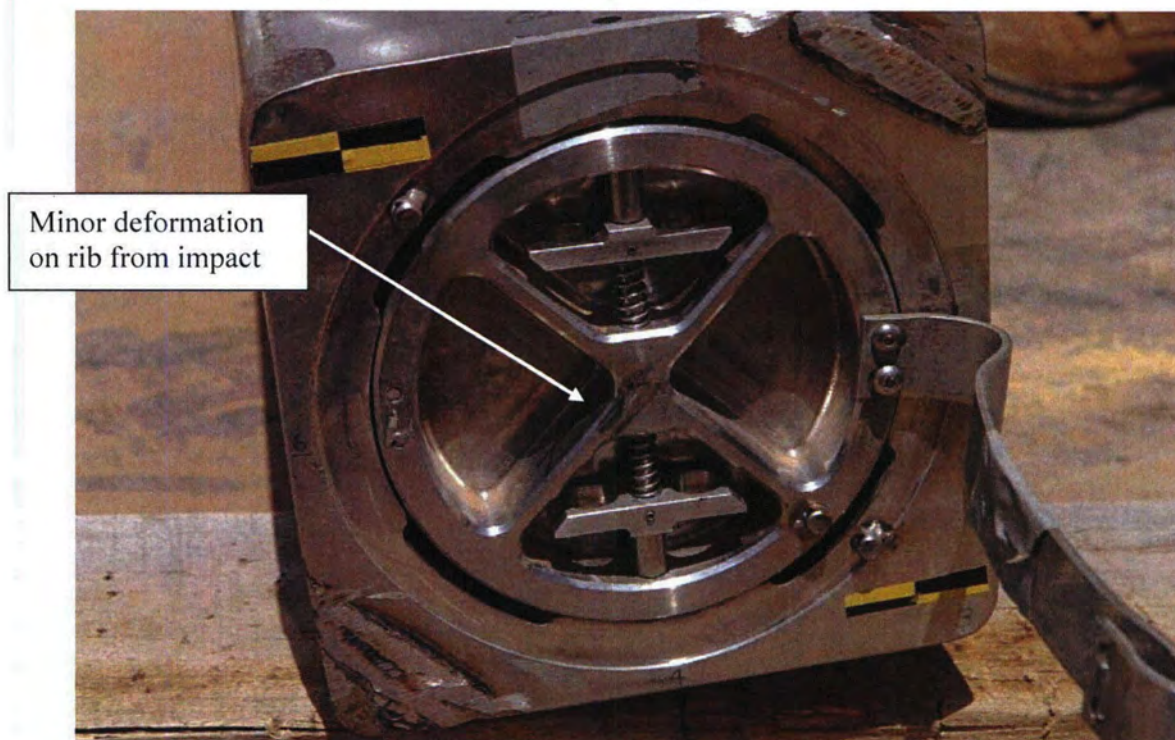


Figure 2.12.1-31 - CTU Following CP3-1 Impact



Figure 2.12.1-32 - CD5-1 Drop Orientation

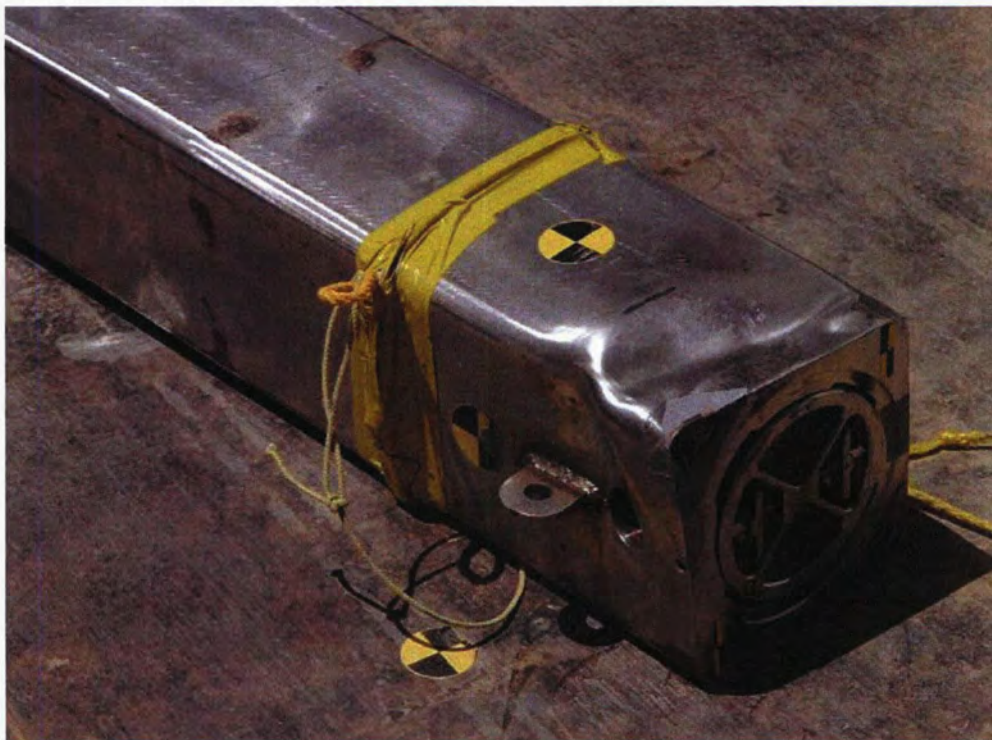


Figure 2.12.1-33 - CTU Following CD5-1 Impact

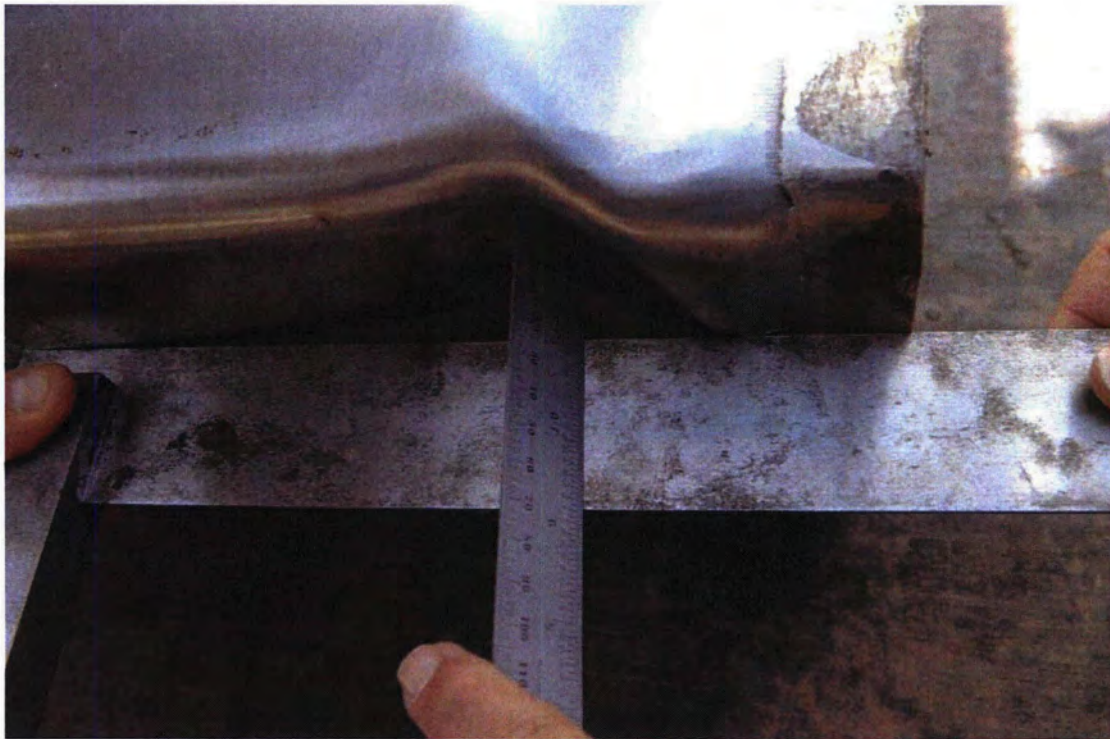


Figure 2.12.1-34 - CD5-1 Impact Damage on Bottom 180° Side



Figure 2.12.1-35 - CD5-1 Impact Damage on Closure End



Figure 2.12.1-36 - CD5-1 Impact Damage on Closure Area

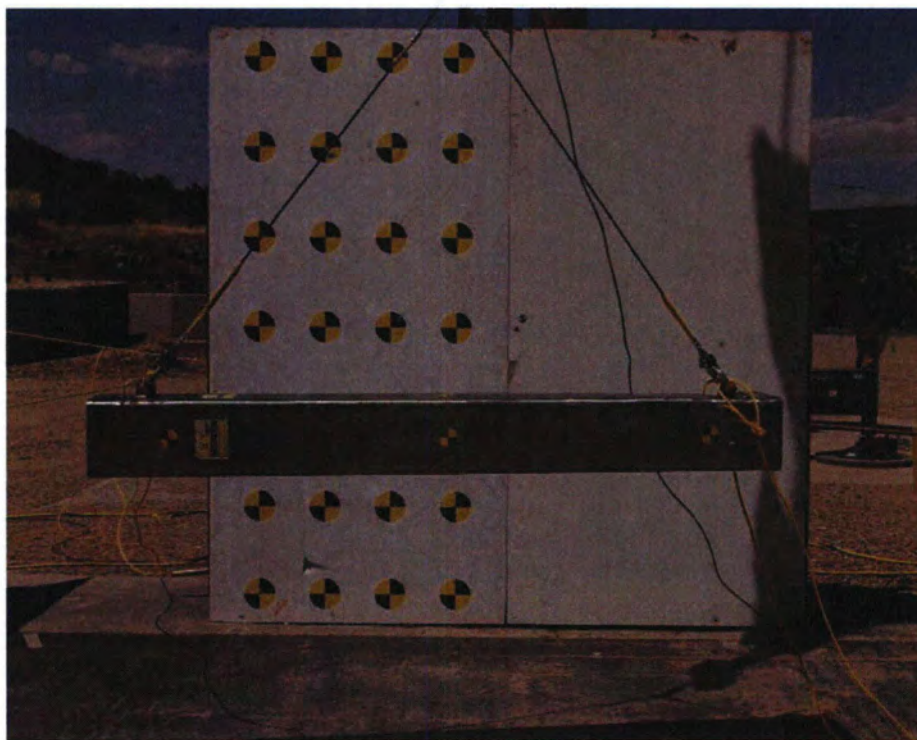


Figure 2.12.1-37 - CD2.C-1 Drop Orientation



Figure 2.12.1-38 - Side View of CTU Following CD2.C-1 Drop

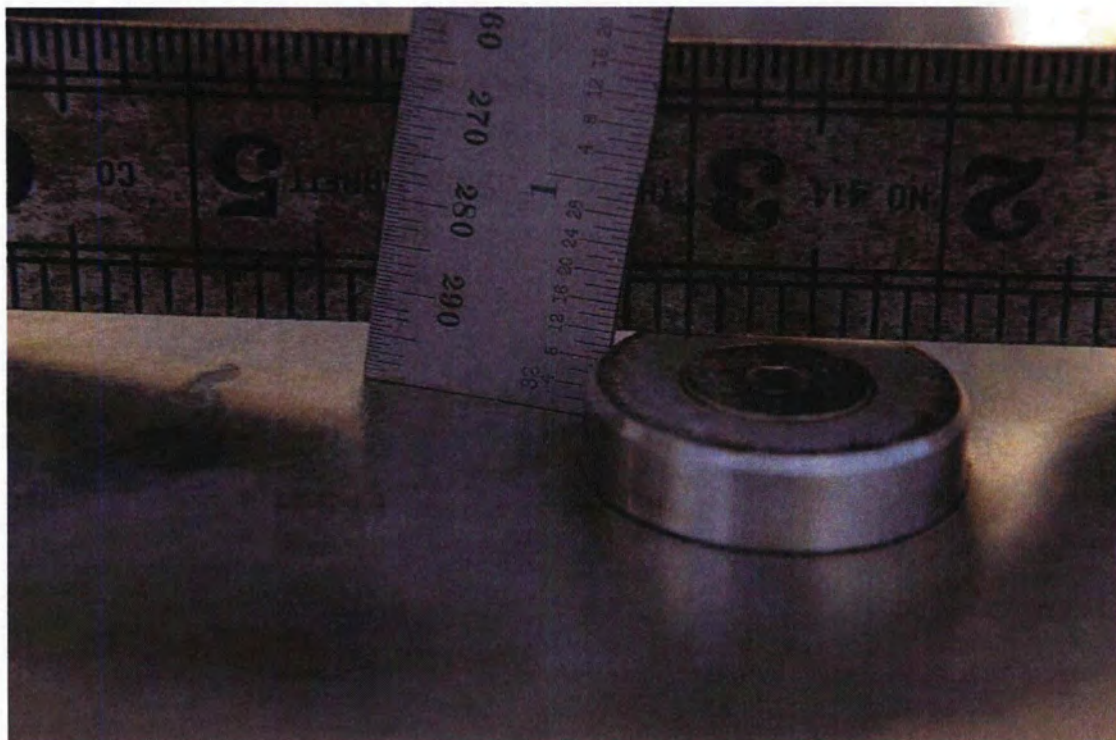


Figure 2.12.1-39 - Index Lug Near Closure End, CD2.C-1

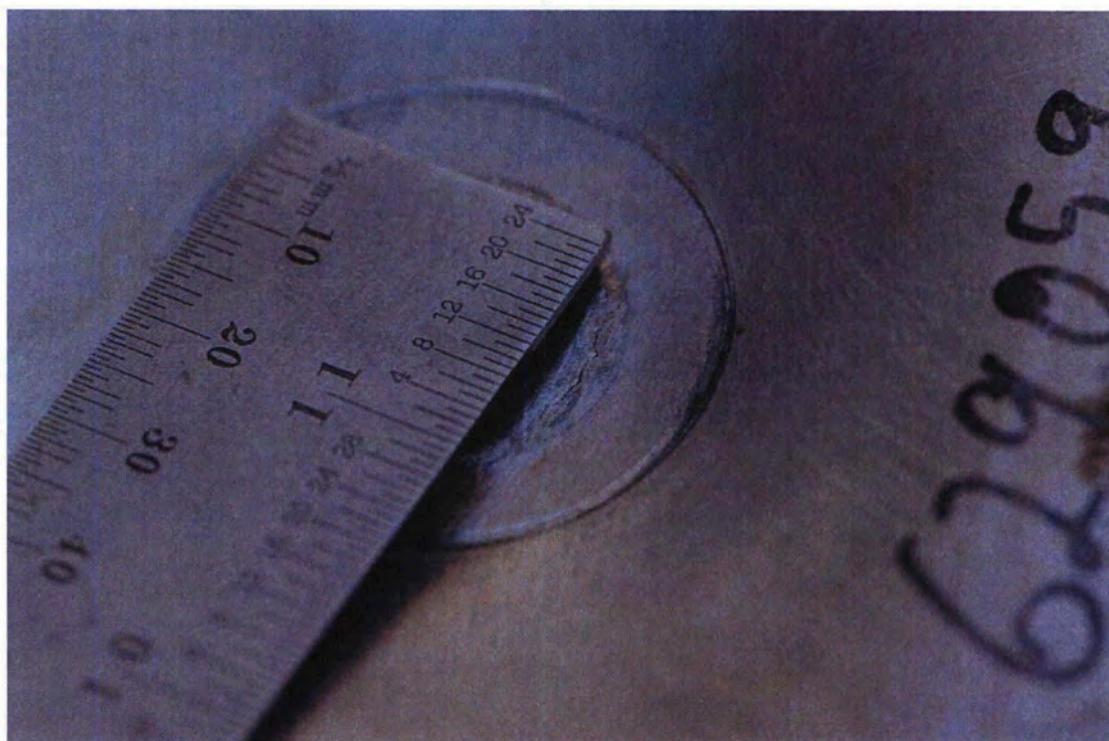


Figure 2.12.1-40 - Cracked Weld Under Index Lug, CD2.C-1

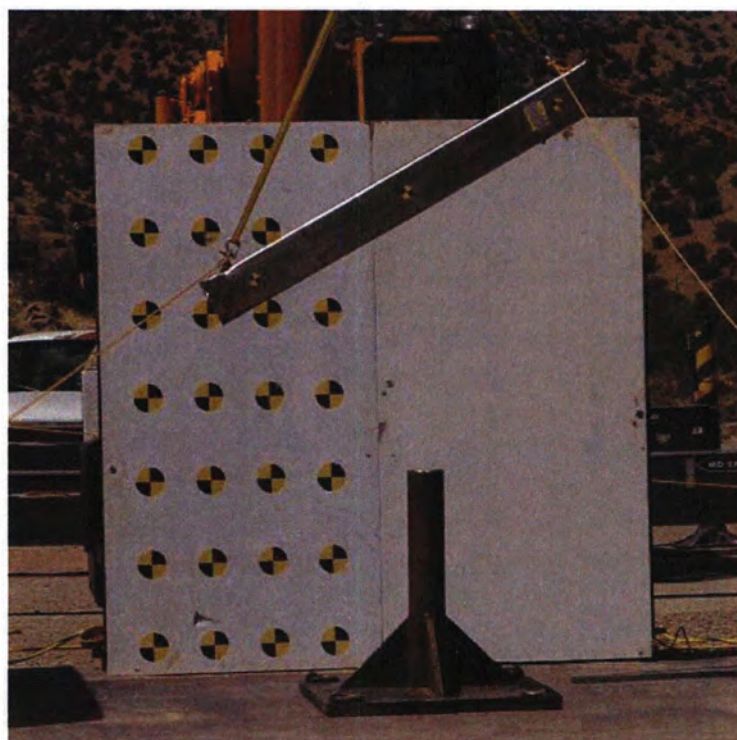


Figure 2.12.1-41 - CP2-1 Drop Orientation

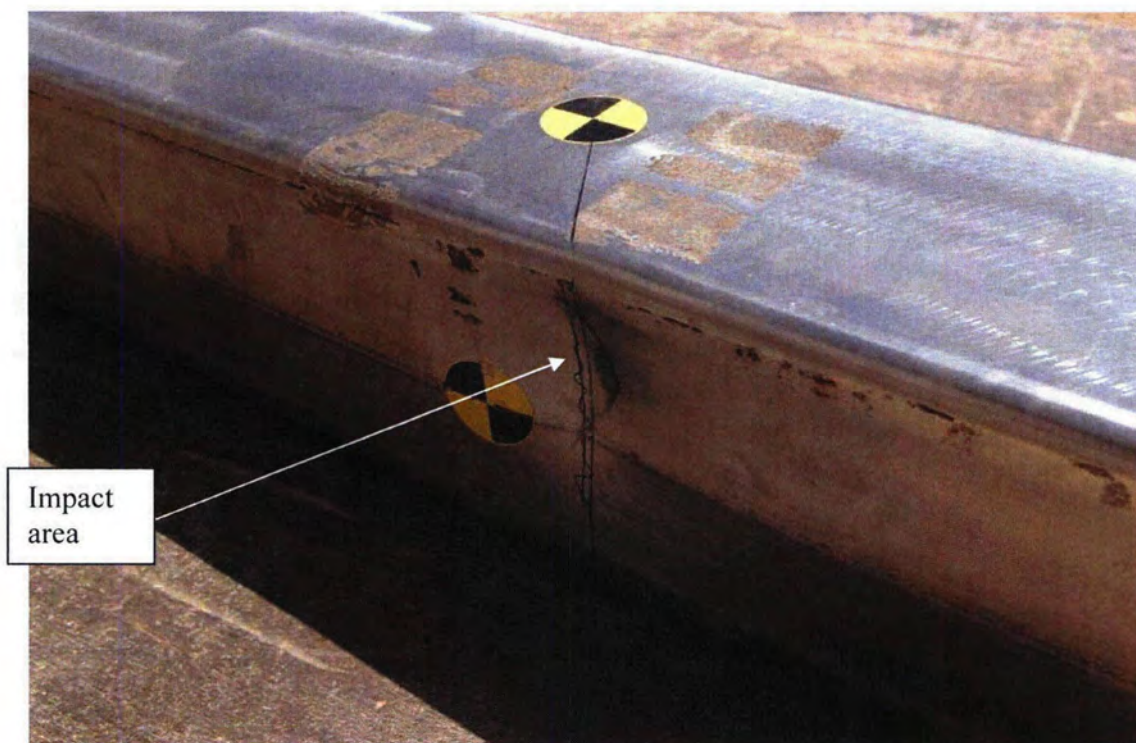


Figure 2.12.1-42 - CTU Following CP2-1 Impact

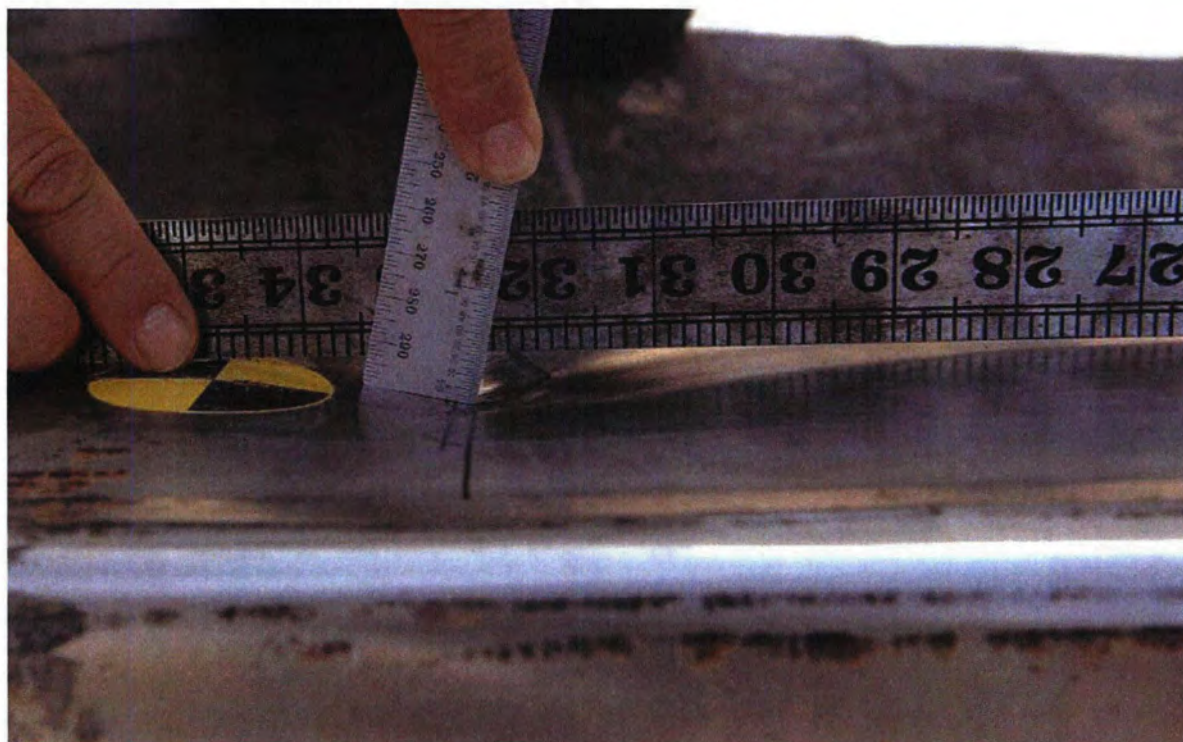


Figure 2.12.1-43 - CP2-1 Impact Damage

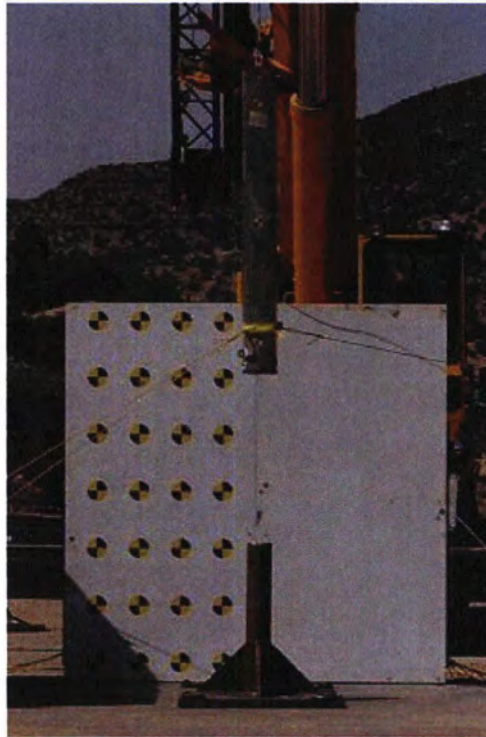


Figure 2.12.1-44 - CP1-1 Drop Orientation

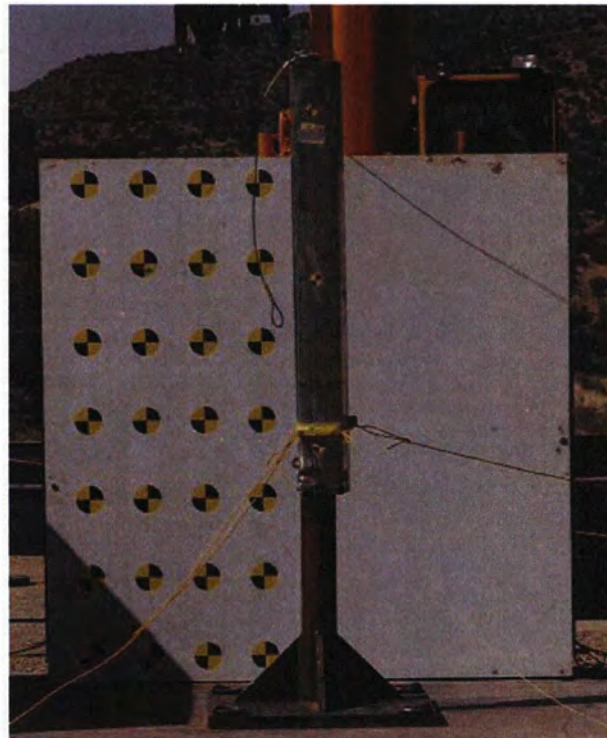


Figure 2.12.1-45 - CTU Following CP1-1 Impact

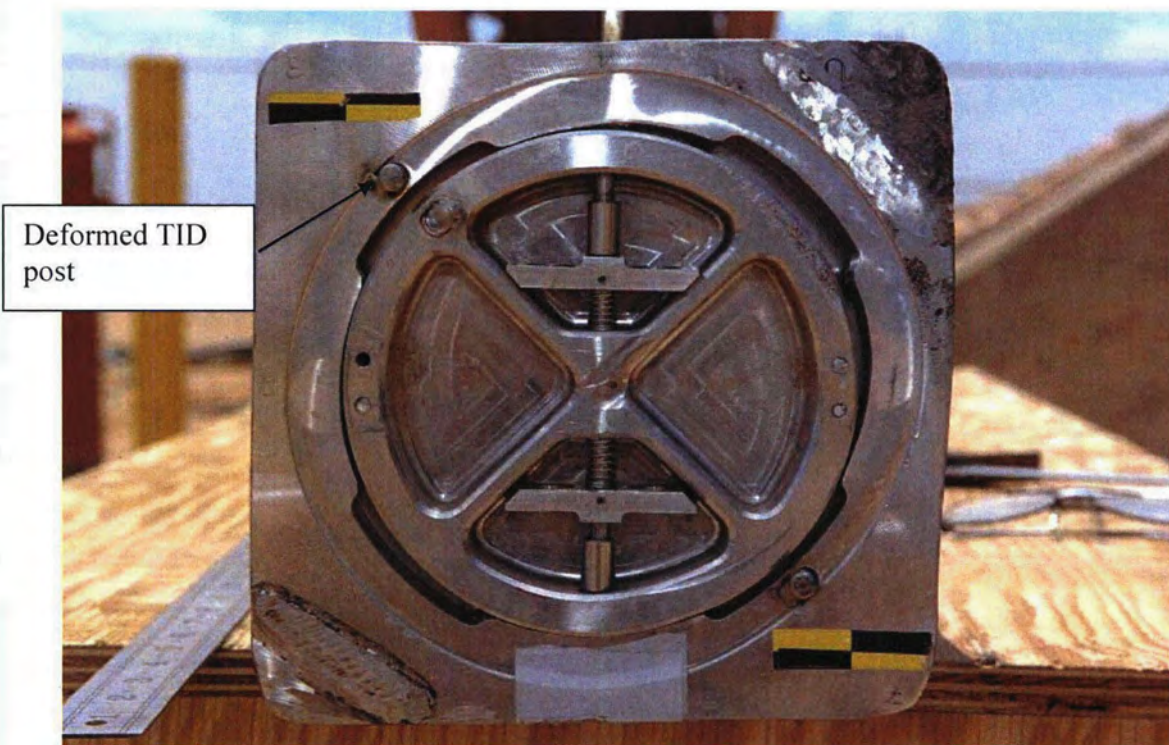


Figure 2.12.1-46 - CP1-1 Impact Damage (Shown Index Lugs Down)



Figure 2.12.1-47 - Attempted Closure Removal



Figure 2.12.1-48 - Exposure of Thermal Shield



Figure 2.12.1-49 - Insulation After Removal of Thermal Shield



Figure 2.12.1-50 - Middle Insulation After Removal of Thermal Shield



Figure 2.12.1-51 - Bottom End Plate Condition

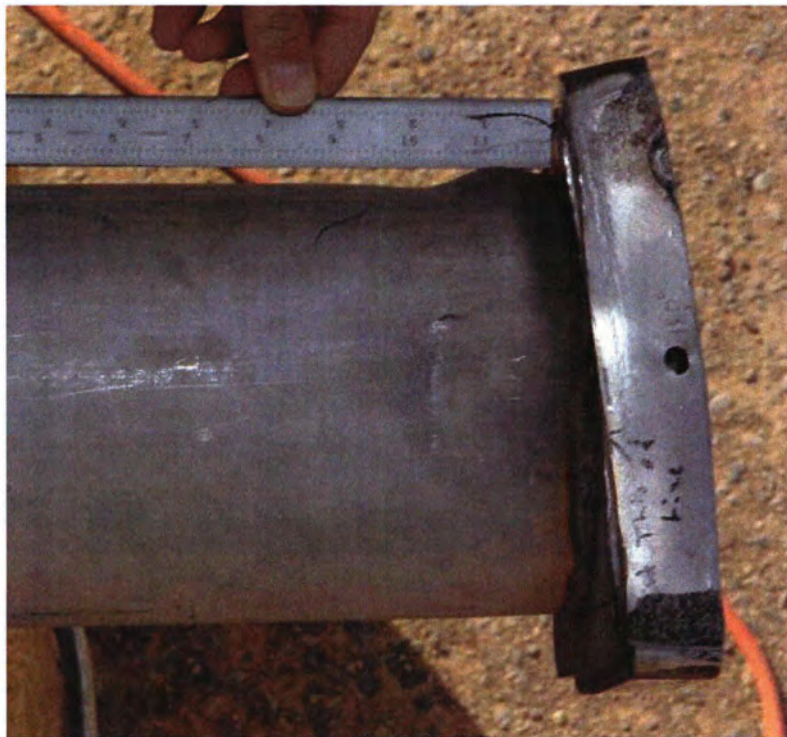


Figure 2.12.1-52 - View of Inner Tube at Closure End



Figure 2.12.1-53 - Inner Tube Deformation at Closure End

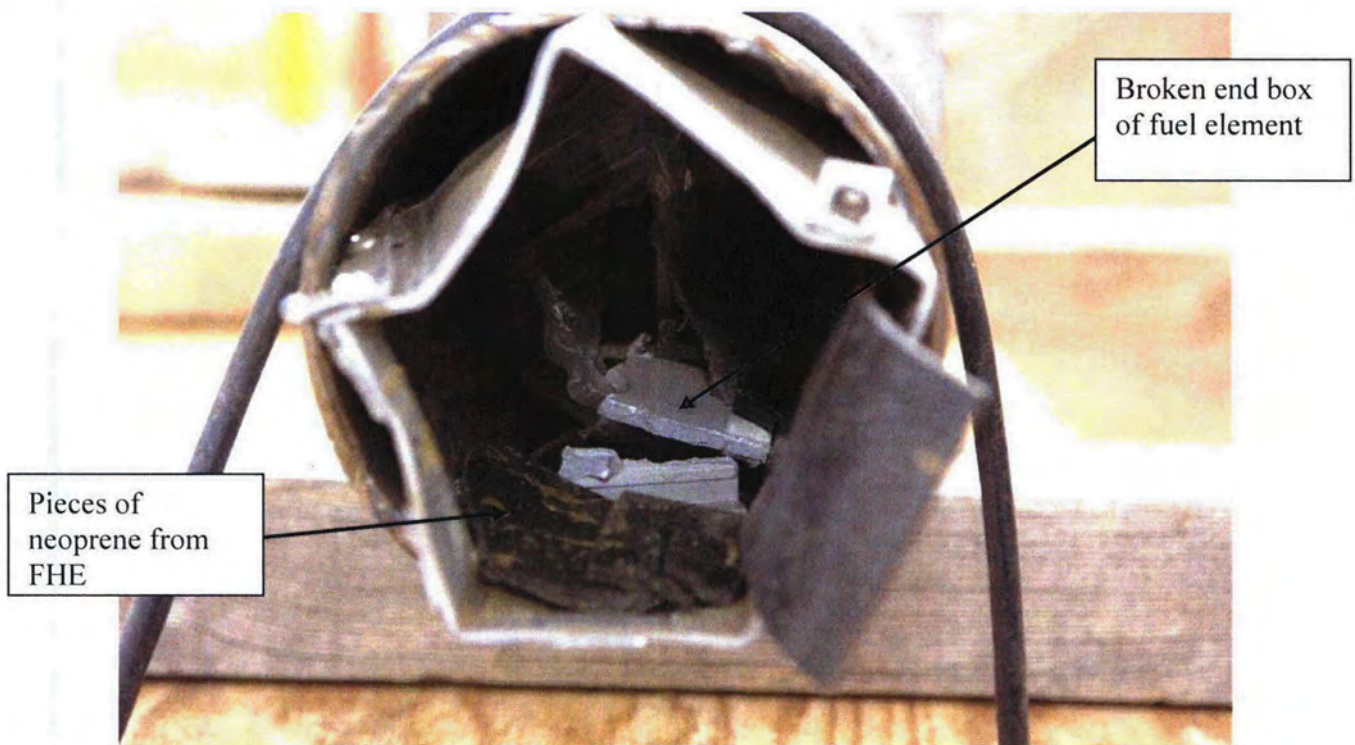


Figure 2.12.1-54 - End View (Bottom) of Opened CTU



Figure 2.12.1-55 - Removal of ATR Fuel Element

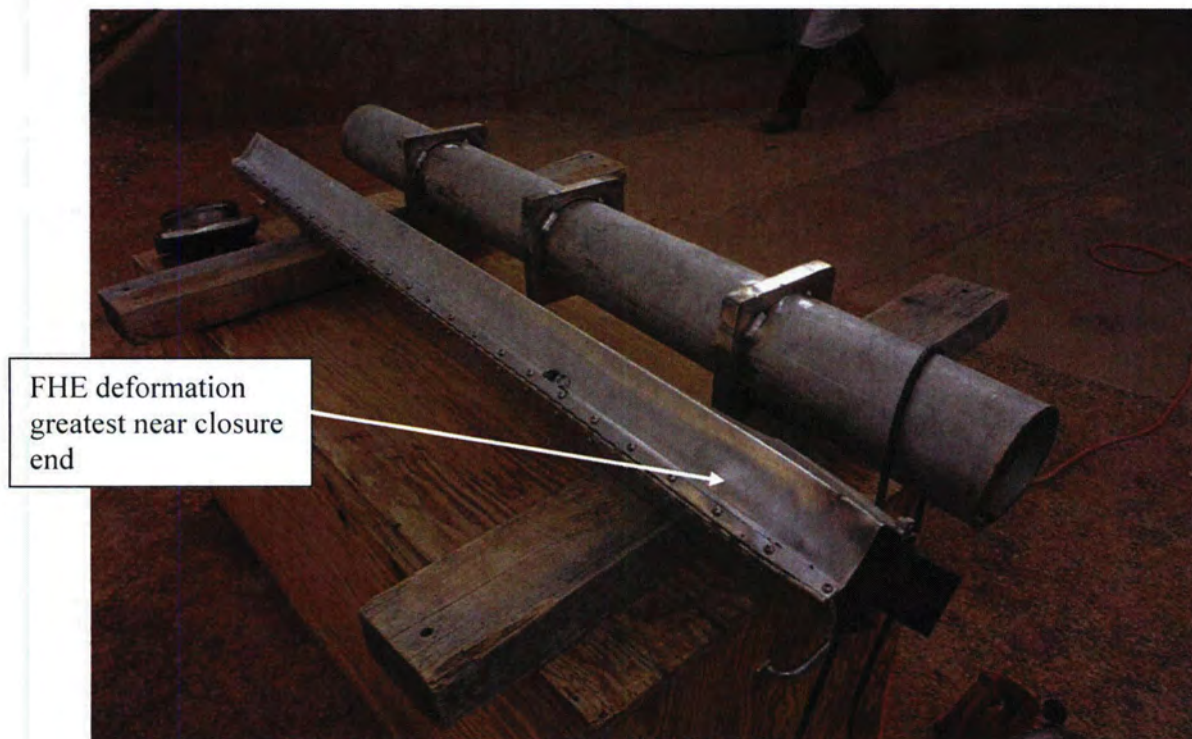


Figure 2.12.1-56 - Fuel Handling Enclosure Deformation



Figure 2.12.1-57 - ATR Fuel Element Inspection

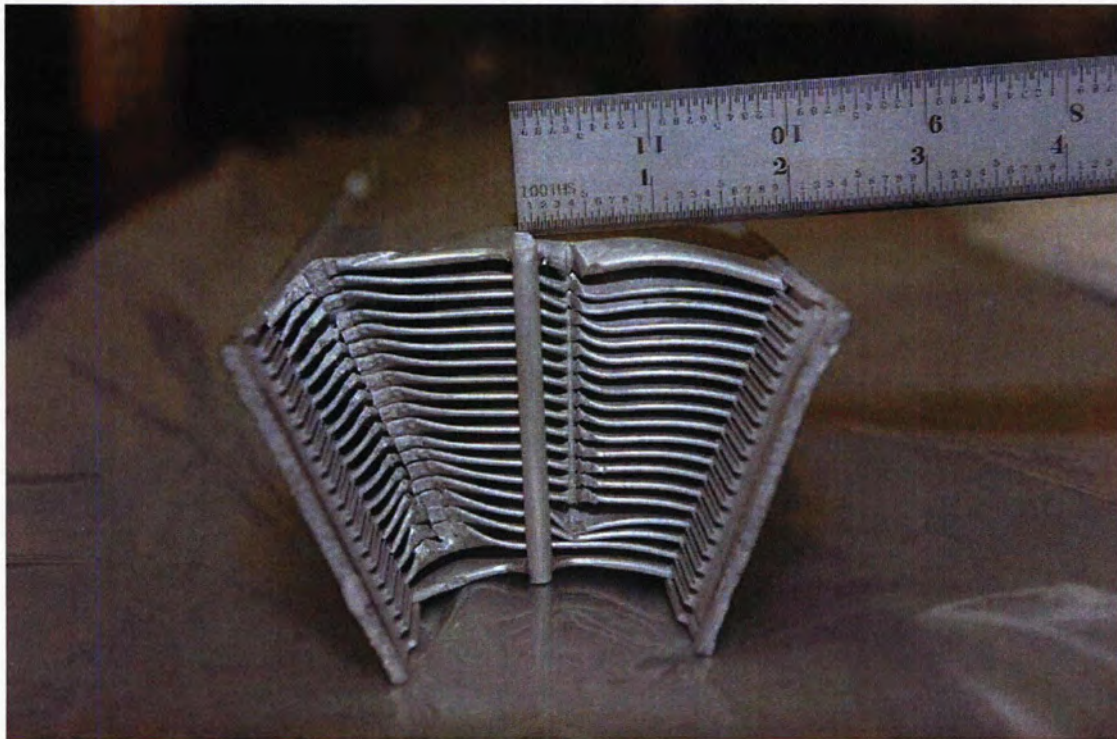


Figure 2.12.1-58 - ATR Fuel Element at Head End

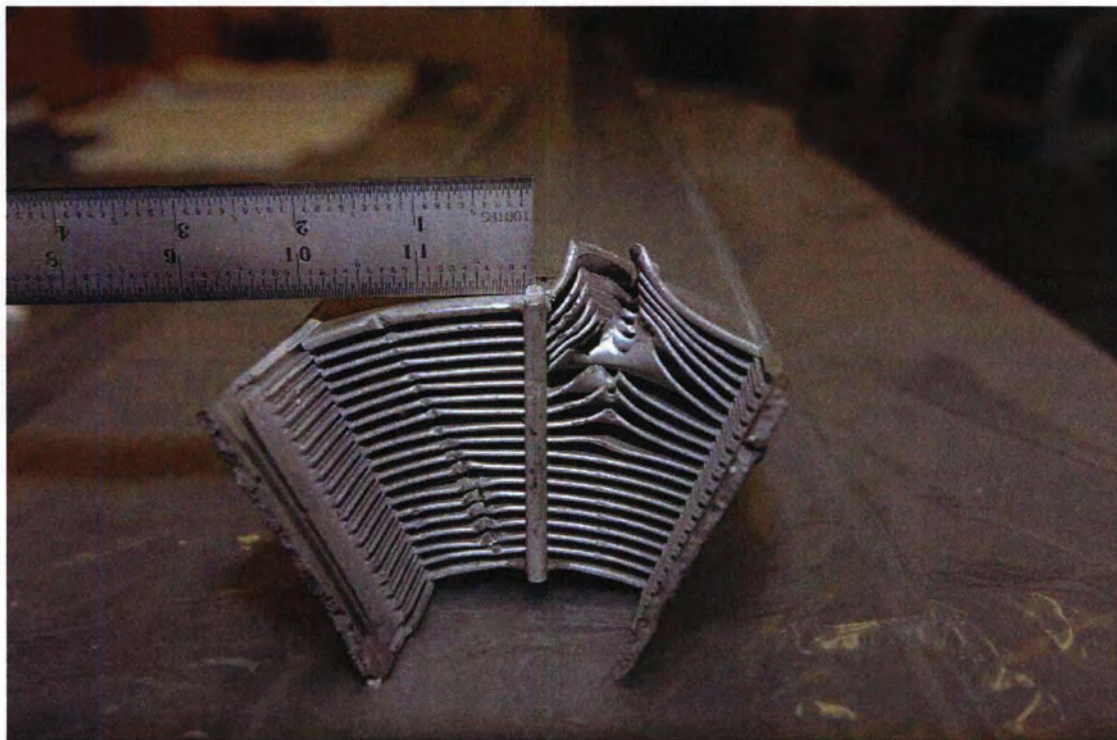


Figure 2.12.1-59 - ATR Fuel Element Damage at Bottom End



Figure 2.12.1-60 - Top View ATR Fuel Element at Bottom End

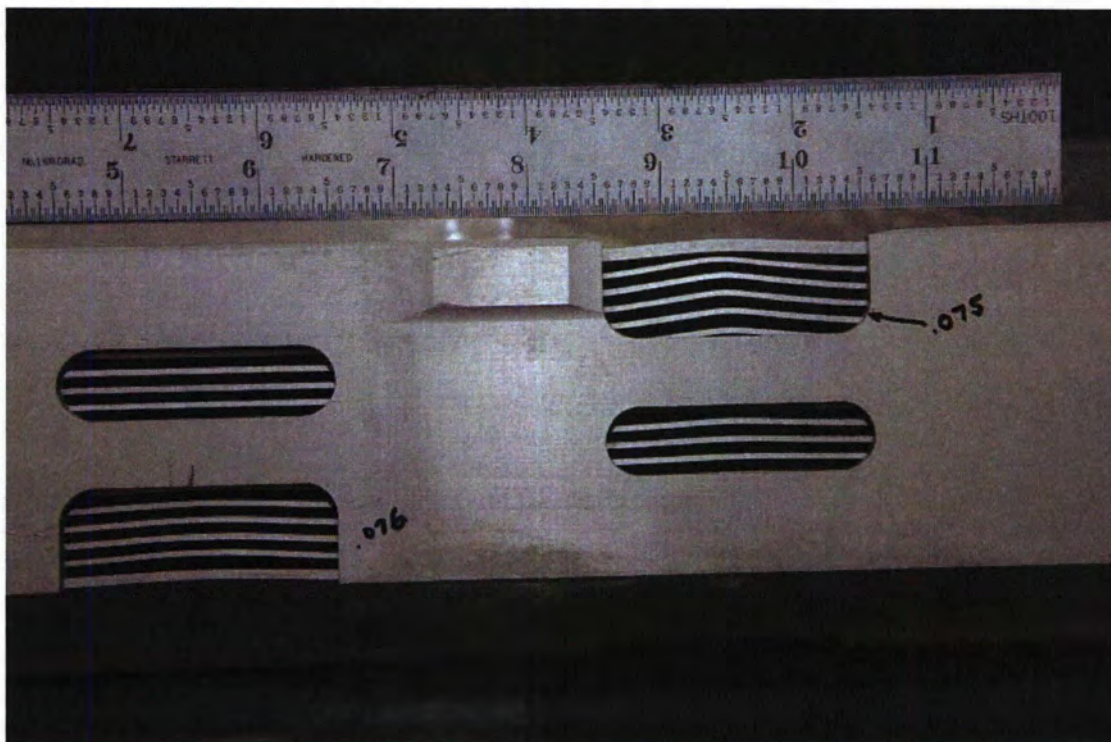


Figure 2.12.1-61 - ATR Fuel Element Fuel Plates Left Side



Figure 2.12.1-62 - ATR Fuel Element Fuel Plates Right Side

2.12.2 Certification Tests on CTU-2

This report describes the methods and results of a series of tests performed on the Advanced Test Reactor (ATR) Fresh Fuel Shipping Container (FFSC) transportation package, shown in Figure 2.12.2-1. The objective of testing was to conduct drop tests in accordance with the requirements of 10 CFR 71, §71.71 Normal Conditions of Transport (NCT), and §71.73 Hypothetical Accident Conditions (HAC). This test was primarily directed at verification of the loose fuel plate basket structural integrity and the performance of the package insulation. The package and ATR fuel element payload performance are supported by the tests described in Section 2.12.1, *Certification Tests on CTU-1*.

Testing was performed at HiLine Engineering in Richland, Washington on May 17, 2007. Color photographs and videos were taken to document the test events and results.

2.12.2.1 Overview

There are three primary objectives for the certification test program:

1. To demonstrate that, after a worst-case series of HAC free drops, the package maintains containment of radioactive contents.
2. To demonstrate that, after a worst-case series of HAC free drops, geometry of both the fuel and package are controlled as necessary to maintain subcriticality.
3. To demonstrate that, after the free drops, the package retains the thermal protection necessary to maintain the fuel below its melting point during the thermal evaluation.

Several orientations were tested to ensure that the worst-case series of free and puncture drop events had been considered. Post-impact examination demonstrated that the package sufficiently met the design objectives. The specific objectives of this test were to demonstrate:

- Any displacement of package insulation and/or thermal shields are bounded in the thermal analysis,
- Reconfiguration of the loose fuel plate basket and/or loose fuel plate payload is bounded in the criticality analysis.

2.12.2.2 Pretest Measurements and Inspections

The ATR FFSC packaging (serial number CTU1), loose fuel plate basket (serial number 1), and simulated ATR loose fuel plates were received at HiLine. The packaging and payload are identified as ATR FFSC Certification Test Unit CTU-2. The components arrived fully constructed and ready for testing.

The ATR loose fuel plates were simulated. The payload was comprised of a combination of 2- and 4-inch wide, .06-inch thick, 5052H32 aluminum flat plates. All plates were 49.5-inches long. There were 15, 2-inch wide plates and 10, 4-inch wide plates making up a total payload weight of 20.7 lbs.

The CTU was dimensionally inspected to the drawings at the fabricator and the fabrication records forwarded to PacTec. A Certificate of Compliance was issued by the fabricator of the CTUs documenting compliance with the fabrication drawings. Minor discrepancies

between the drawings and CTUs were identified and independently evaluated. The evaluations concluded that the discrepancies were minor and would not significantly affect the CTU during testing.

There were five fabrication deviations associated with the S/N CTU1 package fabrication:

- The 3/8-16 UNC index lug screws were obtained without specified ASTM F-879 certifications.
- The #10-24 UNC closure handle screws were obtained without specified ASTM F-879 certifications.
- Chemical overtesting of the package body closure plate material identified a manganese content 0.02% above the ASTM A479 maximum allowable.
- The tap failed when tapping one of the four #10-24 tapped holes for the closure handle screws. As a result, one of the four tapped holes had full threads to a depth of .44-inches rather than the specified .5-inches.
- The handle width is specified to be $7.5 \pm .3$ -inches. When measured in the free state (not secured to the closure), the handle width was undersized by approximately 0.1-inches.

Other deviations relative to the CTU are the absence of the stainless nameplate and the use of temporary rigging attachments. These items are also insignificant relative to the weight of the CTU and their impact upon the drop tests.

2.12.2.2.1 Component Weights

Component weights were measured and recorded as shown in Table 2.12.2-1.

2.12.2.2.2 Drop Test Pad Measurement and Description

The drop pad consists of a 7-foot square x 5-foot thick concrete block covered with a 6-foot square x 2.5-inch thick steel plate. The estimated weight of the pad is greater than 44,000 lbs. Thus the test pad was qualified as an essentially unyielding surface for the approximately 300 lb CTU.

2.12.2.2.3 Equipment and Instruments

Instrumentation used for the component weights and drop tests is given in Table 2.12.2-2. Calibrated test and measurement equipment used were the weight scale and temperature meter. Those two instruments were calibrated in accordance with HiLine procedures. It is noted that the HiLine calibration procedures require National Institute of Standards and Technology (NIST) traceability and that the HiLine records adequately demonstrated that the calibrations were NIST traceable.

A plumb bob with a stretch resistant string was used to determine the appropriate drop height. HiLine project personnel under the supervision of PacTec personnel measured the plumb bob and string using steel tape measures. The angle of the CTU prior to each drop was measured using a mechanical inclinometer.

One low speed digital video camera was used to record the drop events. In addition, color photographs were taken to document the testing.

2.12.2.3 Summary of Tests and Results

2.12.2.3.1 Initial Conditions

All three HAC drops, CD1-2, CD3-2, and CD4-2, were performed at ambient temperature. Ambient temperature and the package surface temperature was recorded before and after each drop. After each drop the closure was removed and the basket inspected. The basket was reassembled (the basket screws tightened to the "finger tight" condition) and the package re-closed for the following test. One tie wrap (securing the loose fuel plate payload) failed in the CD1-2 test and the second tie wrap failed in the CD3-2 test. Neither of the two tie wraps were replaced between tests.

2.12.2.3.2 Summary of Testing

Table 2.12.2-3 identifies the testing performed on the ATR FFSC CTU.

2.12.2.4 Certification Tests

2.12.2.4.1 Drop Tests

The three CTU-2 HAC drop tests were performed to augment the CTU-1 tests for the package, and to demonstrate acceptable performance of the loose fuel plate basket payload. In CTU-1, the package was subjected to end drops on both the closure and the bottom ends of the package. CTU-2 restricted the end drop test to just the bottom end to properly assess axial insulation displacement.

There were no NCT or puncture bar tests performed on the package, since CTU-1 adequately demonstrates acceptable package performance under those conditions. The two side drops subjected the loose fuel plate basket and simulated fuel to worst case impact conditions with the basket oriented perpendicular and parallel to the target surface.

The test identification numbering reflects the same drop orientation as performed in CTU-1. For example, CD3-2 is the same orientation as the third HAC drop in CTU-1, test CD3-1. The "-2" identifies this drop as a CTU-2 test.

2.12.2.4.1.1 CD1-2 –Flat (pocket side down) Side HAC Drop

The CTU was fitted with swivel lift eyes, and the lift eyes were threaded into the package lift points. This configuration oriented the package such that the package pocket side impacted the target surface. Slings were used to rig the CTU from the swivel lift eyes to the crane remote release hook. Figure 2.12.2-5 illustrates the drop orientation. Initial conditions were as follows:

- Ambient temperature: 73 °F
- Avg. surface temperature: 78 °F
- Time: 10:04 a.m. 5/17/2007
- Drop height: 30 ft

Following impact, the CTU bounced slightly and landed on the impact side. There was minor visible exterior damage, principally scuff marks, resulting from the drop. Close examination of

the package, on the impacted surface side, reveals minor distortion of the outer shell localized at the stiffening ribs. Figures 2.12.2-6 and 2.12.2-7 show the CTU prior to and following the drop. There was no bowing or other significant visible deformation. There was no visible deformation or rotation of the closure, and the locking pins condition and function were unaffected by the drop.

The basket was not affected by the drop, however the finger operated screws securing the two basket halves were loosened approximately one turn. One fuel tie wrap was broken but the simulated loose fuel plates were not damaged. The simulated fuel plates were replaced in the basket without installing new tie wraps, and the basket closure screws again tightened to the finger tight condition.

2.12.2.4.1.2 CD3-2 – Flat Side HAC Drop (90° from CD1-2)

Following the CD1-2 drop, lift points were welded to the package to enable a side drop rotated 90° from CD1-2 (Figure 2.12.2-8):

- Ambient temperature: 78 °F
- Avg. surface temperature: 85 °F
- Time: 10:50 a.m. 5/17/2007
- Drop height: 30 ft

The CTU rebounded from the drop pad approximately 1 ft following the 30 ft drop and came to rest on its side (rotated 90° from the drop orientation). As with the CD1-2 event, the outer shell exhibited minor deformation at the stiffening rib locations (reference Figure 2.12.2-9). There was no visible deformation or rotation of the closure, and the locking pins were undamaged and in good working order.

The closure was opened and the basket removed following the drop. The basket exhibited no signs of any deformation but the finger tightened basket screws were loosened approximately 1 turn by the drop.

The basket was opened and it was discovered that the second plastic tie wrap was broken (Figure 2.12.2-10). The simulated fuel plates were found to exhibit no significant damage. The simulated fuel plates were replaced in the basket without installing new tie wraps, and the basket closure screws again tightened to the finger tight condition.

2.12.2.4.1.3 CD4-2 – CG over Bottom End (Vertical)

Following CD3-2, the temporary rigging attachments were removed and the CTU rigged for CD4-2 by lifting the package from the closure handle (Figure 2.12.2-11). Initial conditions were recorded as follows:

- Ambient temperature: 88 °F
- Avg. surface temperature: 90 °F
- Time: 11:20 a.m. 5/17/2007
- Drop height: 30 ft

The CTU appeared to impact slightly off of true vertical; impacting near one corner of the package. This impact dented the lift point feature inward approximately ½-inch, and on one adjacent side, bulged out the square outer tube surface by approximately ½-inch. Following impact, the CTU rebounded vertically approximately 2-feet, tipped over, and landed on the CD3-2 impact side. There was no overall bowing or of the package or other significant visible deformation. There was no visible deformation or rotation of the closure. Figure 2.12.2-12 shows the bottom end of the CTU following the drop.

There was no visible damage to the closure or the locking pins. The closure was removed and the basket extracted following CD4-2. Damaged to the basket was limited to a small dent at the end of the basket that was situated closest to the package bottom. Upon destructive examination of the package, it was discovered that the weld between the package inner shell and the component at the bottom of the payload cavity had intruded into the payload cavity in a localized area (Figure 2.12.2-13). When the package impacted in CD4-2, the basket was partially supported by that weld bead. The end plate of the basket was slightly deformed (Figure 2.12.2-14) as the basket seated on the bottom of the package payload cavity. The damage was minor and did not impair the ability of the basket to retain the fuel plates.

The simulated fuel plates experienced localized deformation at the end of the basket closest to the package bottom (Figure 2.12.2-15 and Figure 2.12.2-16). Above this area the simulated fuel plates were not deformed.

2.12.2.5 Post-test Disassembly and Inspection

The final acceptance criteria for the ATR FFSC package lies with the criticality evaluation. Any increase in reactivity of the contents resulting from the certification tests must not exceed the allowable as defined in the criticality evaluation. The inspections required to support determination of compliance with the acceptance criteria are identified as follows:

- Inspect the outer shell to verify the thermal performance of the package is unimpaired by the free drop events. The thermal analysis assumes that the outer shell is intact such that there is no significant communication between the environment and the outer/inner shell annular space during the thermal event.
- Inspect the insulation to verify compliance with the assumptions of the thermal analysis.

- Inspect the overall package to verify that the package geometry remains within the criticality analyses assumptions.
- Inspect the simulated fuel plate payload to verify that the fuel geometry remains within the assumptions of the criticality analyses.

Any deviation of the test results from these acceptance criteria must be reconciled with the criticality evaluation.

2.12.2.5.1 CTU Inspection

The CTU-2 was disassembled and inspected on May 17, 2007. Prior to disassembly the exterior dimensions were recorded for comparison to the pre-test condition. Table 2.12.2-4 lists the measured dimensions and Figure 2.12.2-17 identifies the location of the identified measurements.

The closure handle was unaffected by the first two drops. In the CD4-2 drop, the handle was dented when it was struck by the rigging shackle. During the CD4-2 CG over bottom (vertical) HAC drop, the outer wall bulged out at the bottom end of the package and caused the width of the package to increase from 8 inches to approximately 8 5/8 inches in that area.

The CTU was disassembled systematically by cutting away the outer layers of the packaging using an abrasive saw. The destructive examination was necessary due to the required inspection of the interior insulation. The package was cut lengthwise along two opposite corners and at the ends to expose the thermal shield.

The stainless steel thermal shields were all intact (Figure 2.12.2-18 through Figure 2.12.2-20). There was minor deformation of the thermal shields at the interface to the stiffening rib. This deformation resulted from the CD4-2 drop and caused the thermal shields to buckle one end and pull away from the stiffening rib at the other end. Figure 2.12.2-21 is typical of this condition. The gap between the thermal shield and the stiffening rib, where the shield pulls away from the rib, is less than 1/16-inch.

Following documentation of the thermal shields the shields were removed to enable examination of the insulation. For reference purposes the ribs are labeled 1 through 3 (Figure 2.12.2-22). The number 1 rib is closest to the bottom end of the package.

As can be seen in Figure 2.12.2-23 through Figure 2.12.2-26 the largest gap occurred at the closure end of the package. The gap ranges from 1-inch to 1 3/4 inches at that location. At the rib 3 and rib 2 locations the gap ranged from 1- to 1 1/2-inches. At the rib 3 location the gap ranged from 1/2- to 1-inch. All gaps are within the 1.85-inch gap assumed in the thermal analysis.

Following thermal shield and insulation removal an abrasive saw was used to separate the bottom end plate from the inner tube. Figure 2.12.2-13 illustrates the condition of the end plate. The endplate showed no drop related deformation and there were no visual indications of broken welds or other damage near the end plate. Using a lathe, the bottom end plate was cut from the insulation pocket to determine the extent of possible insulation compression in the insulation pocket (Figure 2.12.2-27). There was no indication of compression in that region and it was determined that there was no need to open the closure insulation pocket.

The inner tube was inspected and, in general, showed no signs of buckling or large deformations. A minor deformation occurred near the bottom end of the package (Figure 2.12.2-28 and Figure 2.12.2-29) corresponding to the same area of deformation as the outer shell. The tube was bent in that area yielding a slight outward bulge of about 1/16-inch and, closer to the weld between the inner shell and the package bottom, an inward deformation of approximately 1/4-inch. These deformations were localized and did not impair free movement of the basket in the payload cavity. There were no weld failures.

The closure assembly remained fully functional throughout the test series. The only damage to the closure was the handle deformation caused by the rigging shackle. The locking pins and the engagement lugs showed no signs of any deformation. The closure could be freely removed and installed through the tests.

In conclusion, CTU-2 satisfied the acceptance criteria of preventing loss or dispersal of the contents, the outer shell remained intact, the insulation remained within the assumptions of the thermal analysis, and the package and fuel geometry remained greatly unchanged. The deformations of the package and condition of the ATR loose fuel plates were evaluated, against both the criticality evaluation and thermal analysis, and determined to be within the bounds of the assumptions and conditions used to ensure safety.

Table 2.12.2-1 - Component Weights

Component	Weight (lbs)
Body Assembly	224.1
Closure Assembly	8.9
Loose Plate Fuel Basket	29.9
Simulated Fuel Plate Weight	20.7
Package (fully loaded)	283.6

Table 2.12.2-2 - Instrumentation for Drop Tests

Item Description	Model	Serial Number	Calibration Due Date	Comments
Drop Height Indicators	N/A	N/A	N/A	String plumb bobs made specifically for this testing. The length was established using a metal tape measure.
Tape Measure	N/A	N/A	N/A	35-ft. steel tape
Mechanical inclinometer	N/A	N/A	N/A	Used to identify CTU orientation
Weight Scale	Ohaus, Model CD11	0042508-6BD	7/19/2007	Used to measure weights of CTU components. The scale calibration documents included NIST traceable records.
Temperature meter	Carson, Model 4085	41372269	3/1/2008	Handheld temperature reader for measuring ambient temperature and CTU surface temperature. Meter calibration documents included NIST traceable records.

Table 2.12.2.3 - Summary of Testing

Test No.	Test Description	Comments
CD1-2	Flat side drop, pocket side down. Fuel plates oriented perpendicular to target (see Figure 2.12.2-3).	Flat side drop from 30-feet. No visible damage to package. Both closure locking pins remained in the locked position. Closure could be freely opened and payload extracted. The eight hand tightened screws securing the basket halves together were loose (approximately one turn). No visible damage to basket or simulated fuel plates.
CD3-2	Flat side drop, pockets and index lugs on side. Fuel plates oriented parallel to target (see Figure 2.12.2-4).	Flat side drop from 30-feet. No visible damage to package. Both closure locking pins remained in the locked position. Closure could be freely opened and payload extracted. The eight hand tightened screws securing the basket were loose (approximately one turn). The plastic wire ties securing the fuel bundle failed as shown in Figure 2.12.2-10. No significant deformation was observed in the fuel plates.
CD4-2	CG over bottom end (vertical)	<p>Vertical end drop from 30-feet; bottom end of package impacting the target. Both closure locking pins remained in the locked position. Closure could be freely opened and payload extracted. The eight hand tightened screws securing the basket were loose (approximately one turn).</p> <p>The bottom end of the package was deformed on two surfaces (Figure 2.12.2-12). The surface with the threaded hole was dented inward and the adjacent surface 90° apart was bulged outward.</p> <p>The surface of the basket end plate contacting the bottom of the package was slightly dented.</p> <p>The simulated fuel plates were deformed at the bottom end of the basket (Figure 2.12.2-15 and Figure 2.12.2-16).</p>

Table 2.12.2-4 - Package Length Measurements

Test ID	1	2	3	4	5	6	7	8
Pre-Test (in.)	72 7/16	72 1/2	72 7/16	72 1/2	72 7/16	72 7/16	72 7/16	72 1/2
CD1-2 (in.)	72 7/16	72 1/2	72 7/16	72 1/2	72 7/16	72 7/16	72 7/16	72 7/16
CD3-2 (in.)	72 7/16	72 1/2	72 7/16	72 1/2	72 7/16	72 7/16	72 7/16	72 7/16
CD4-2 (in.)	72 7/16	72 1/2	72 3/8	72 7/16	72 5/16	72 5/16	72 3/16	72 3/8



Figure 2.12.2-1 - ATR FFSC CTU-2
(CTU-2 uses package S/N CTU1)

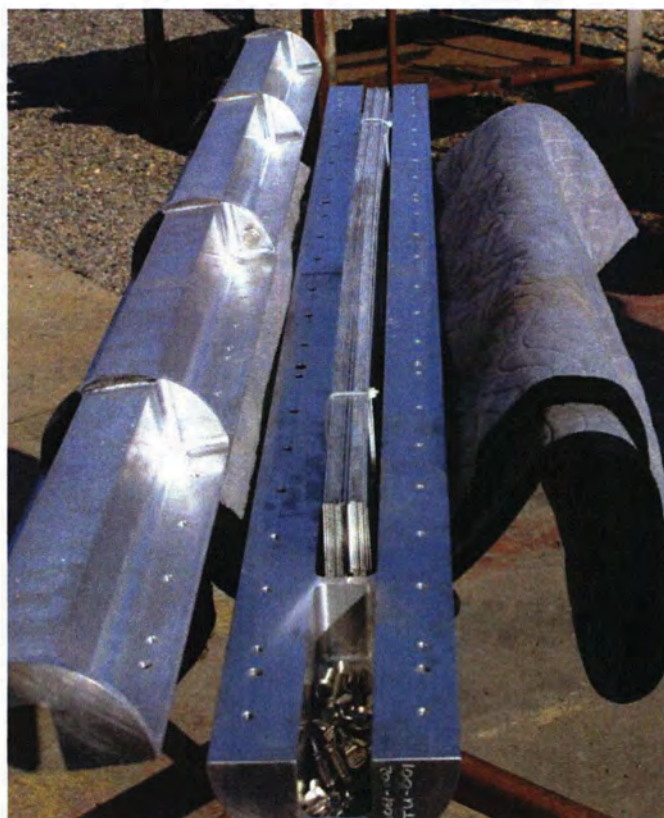


Figure 2.12.2-2 - Loose Fuel Plate Basket and Simulated Fuel Plates

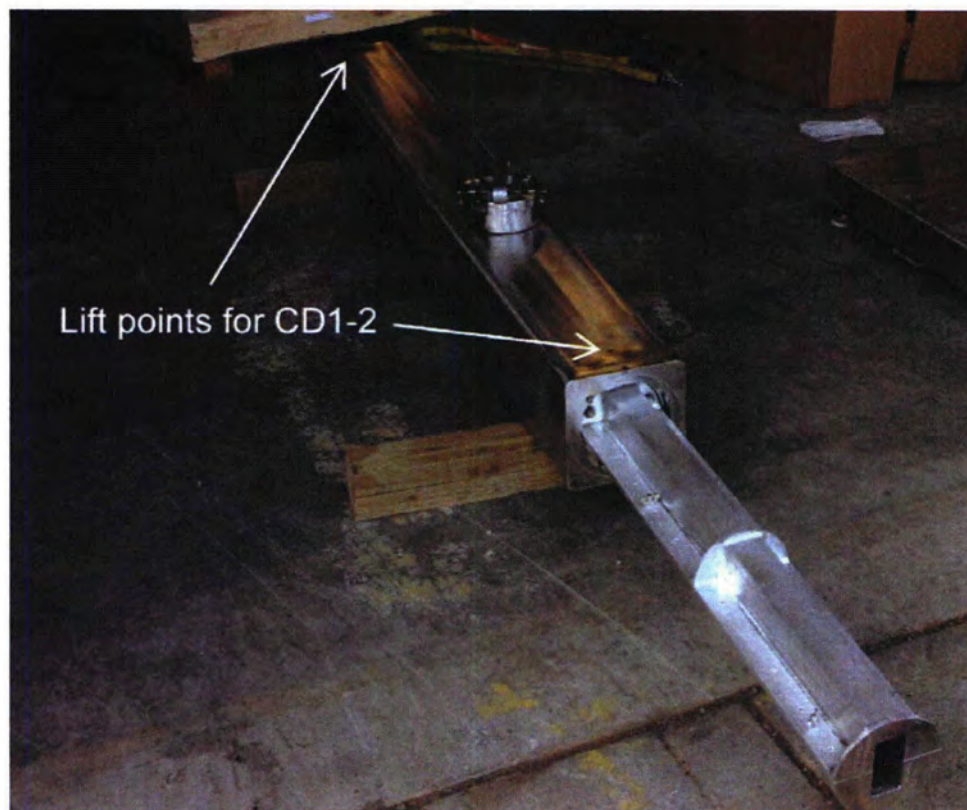


Figure 2.12.2-3 - Basket Orientation in CD1-2



Figure 2.12.2-4 - Basket Orientation in CD3-2



Figure 2.12.2-5 - CD1-2 Drop Orientation



Figure 2.12.2-6 - CTU Following CD1-2 Impact
(impact side facing up)

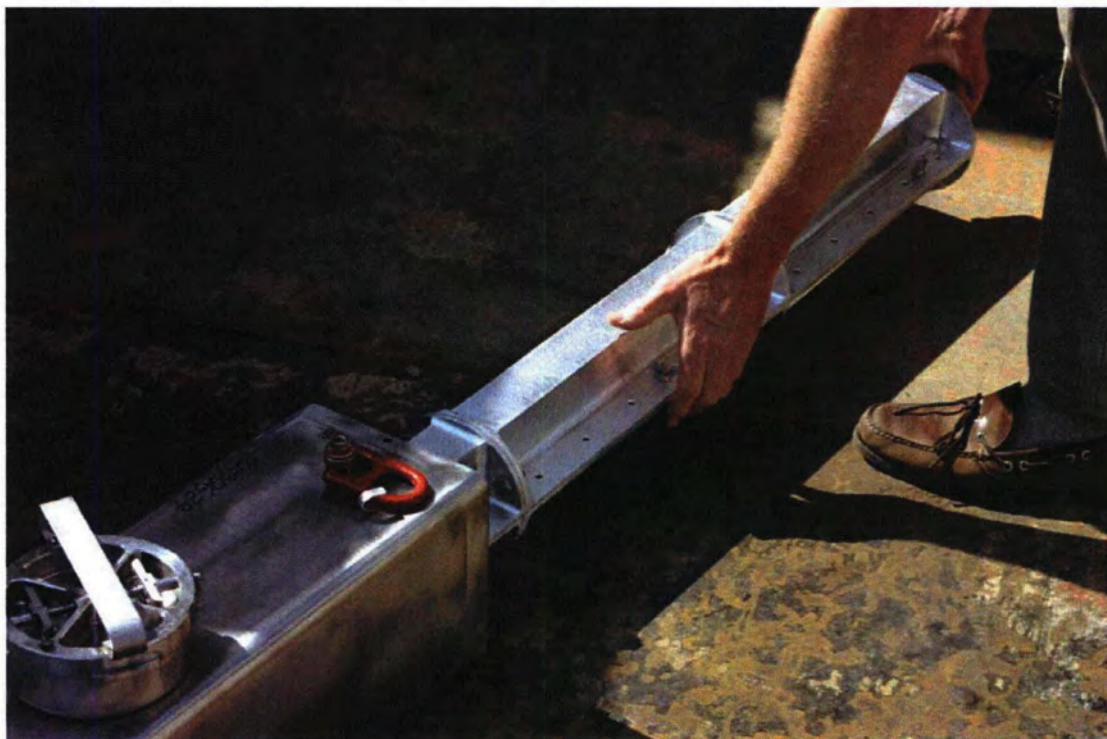


Figure 2.12.2-7 - CD1-2, Extracting Basket Following Drop



Figure 2.12.2-8 - CD3-2 Drop Orientation

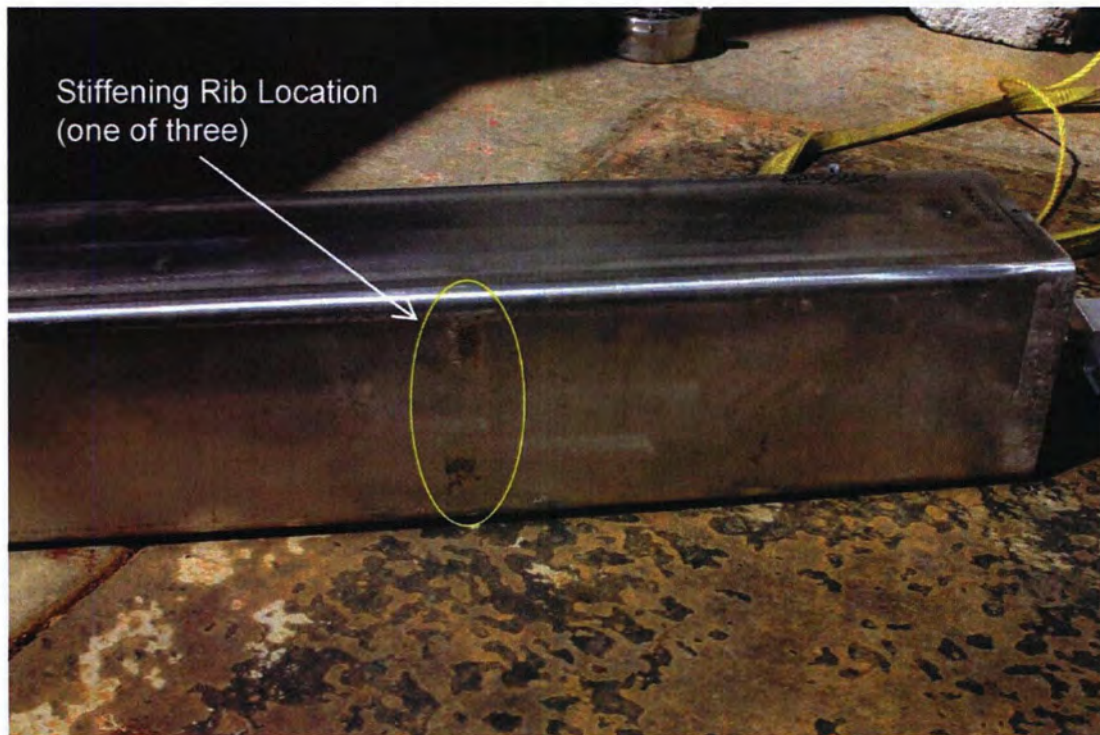


Figure 2.12.2-9 - CD3-2 Deformation at Stiffening Rib Location

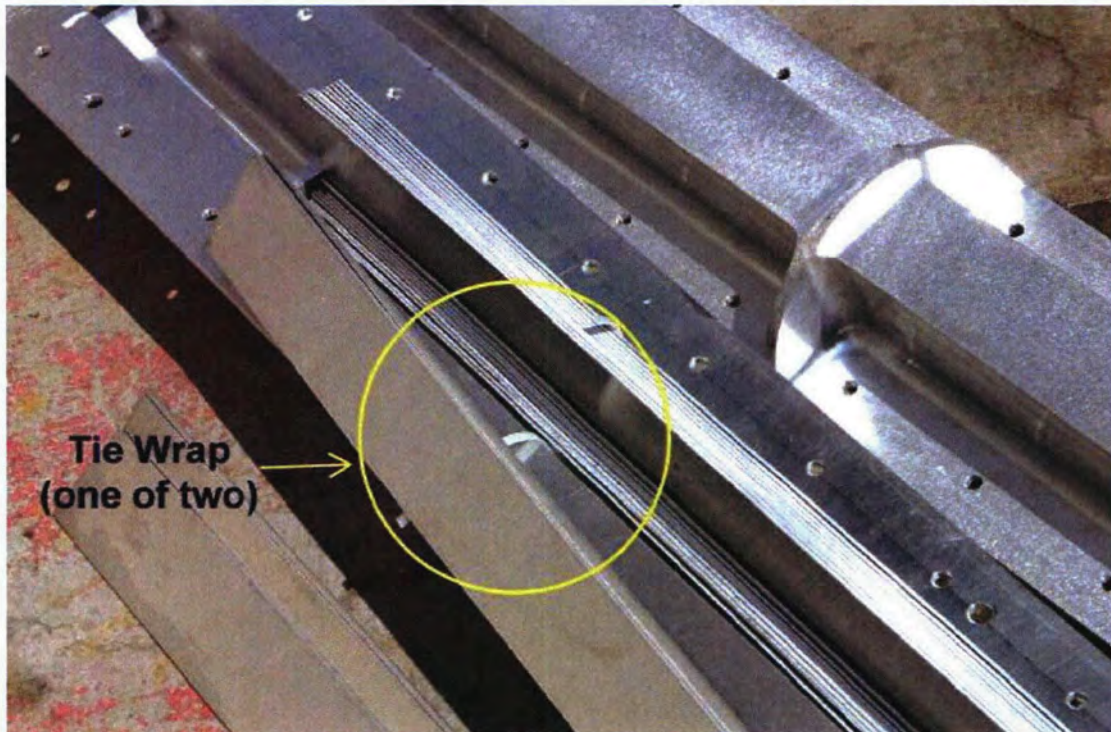


Figure 2.12.2-10 - CD3-2 - Failed tie wraps



Figure 2.12.2-11 - CD4-2 – Drop Orientation

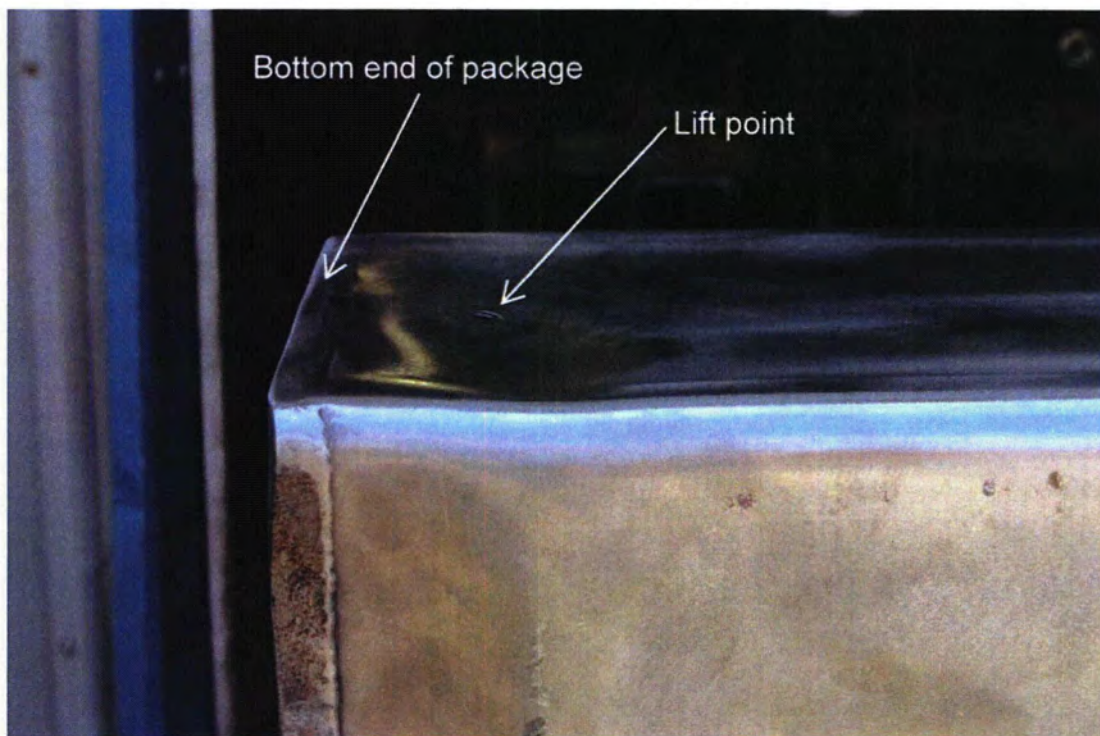


Figure 2.12.2-12 - CD4-2 Impact Damage to Package

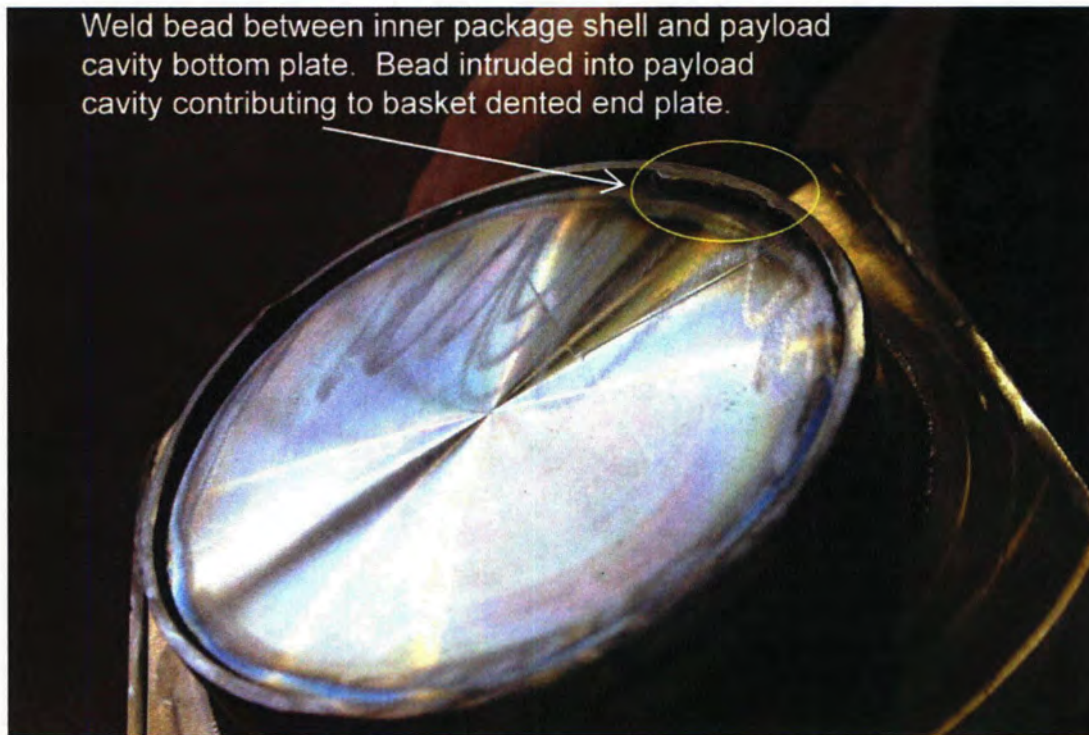


Figure 2.12.2-13 - Weld bead protruding into package payload cavity (inner shell has been removed in this photo)

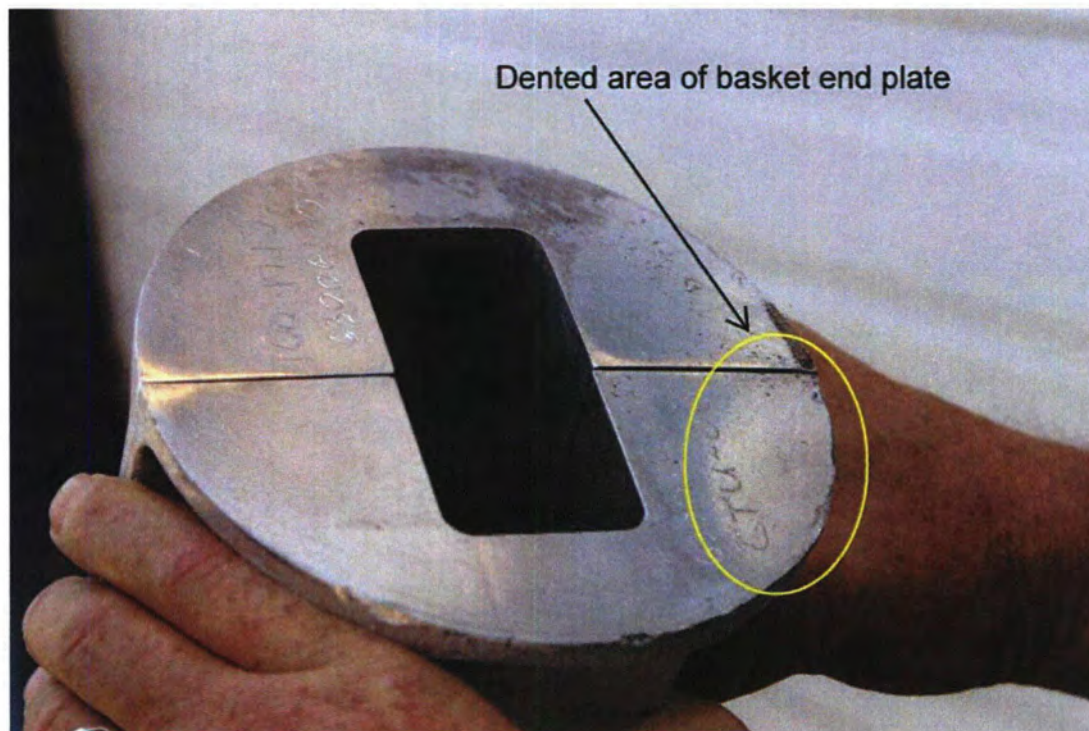


Figure 2.12.2-14 - Dented area – basket end plate



Figure 2.12.2-15 - CD4-2 Impact Damage to Simulated Fuel Plates



Figure 2.12.2-16 - CD4-2 Impact Damage to Simulated Fuel Plates (close up view)

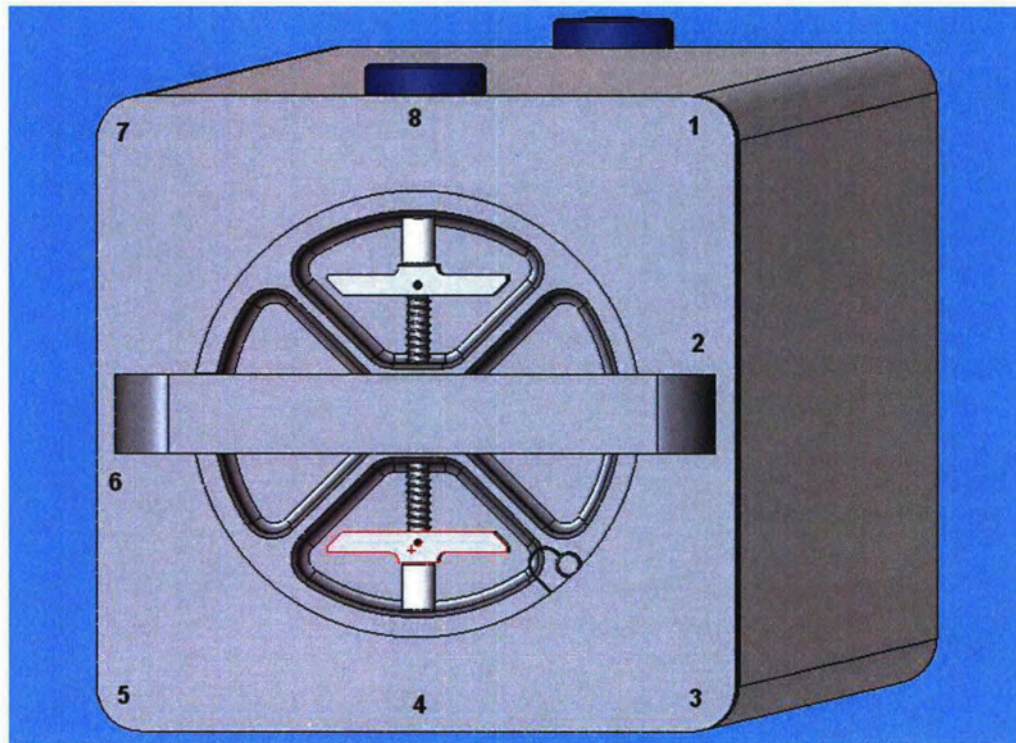


Figure 2.12.2-17 - CTU Measurement Locations



Figure 2.12.2-18 - Thermal Shield Condition, View 1

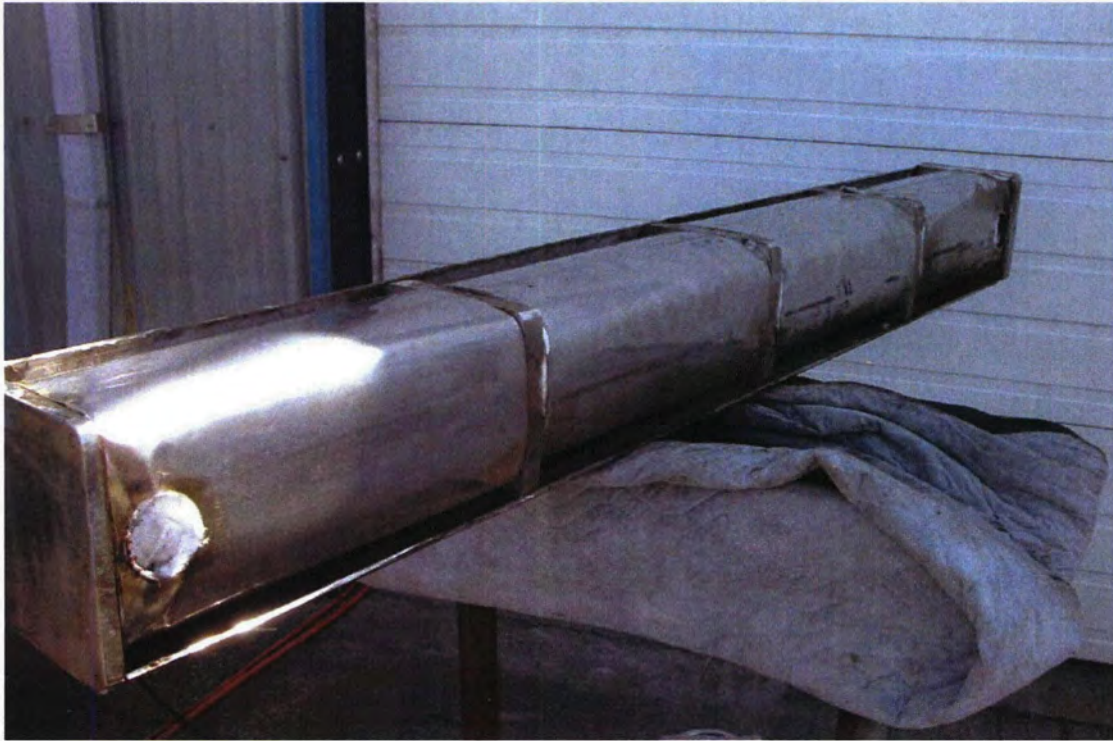


Figure 2.12.2-19 - Thermal Shield Condition, View 2



Figure 2.12.2-20 - Thermal Shield Condition, View 3

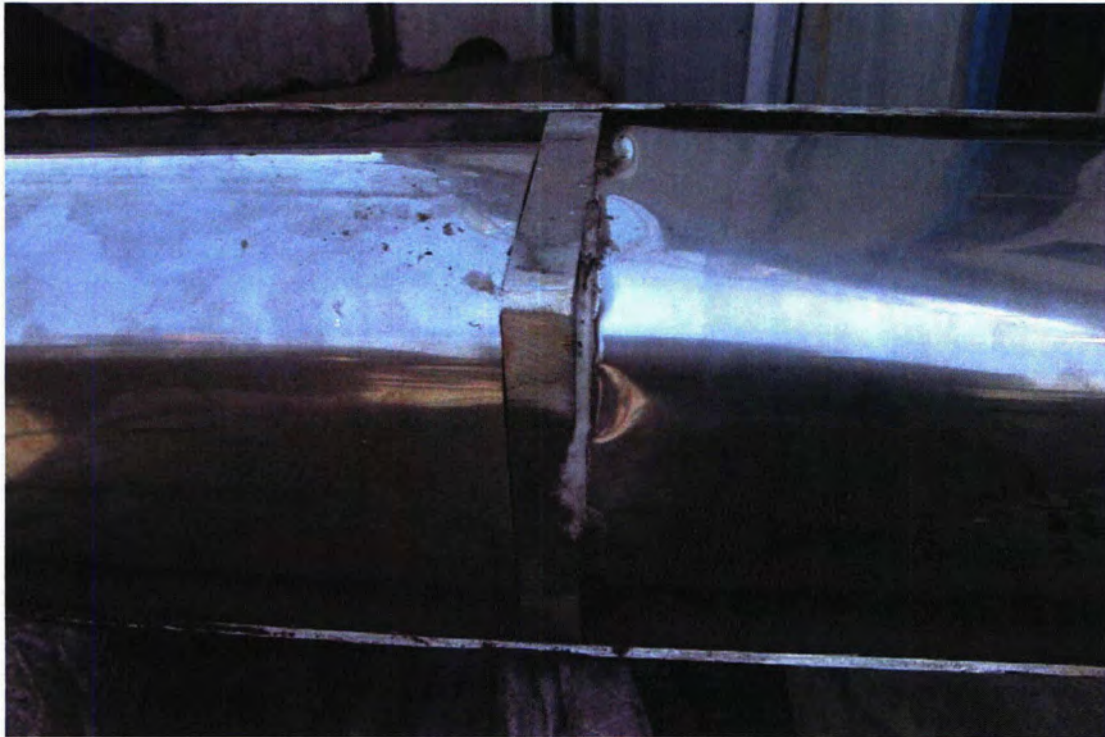


Figure 2.12.2-21 - Thermal Shields at Interface to Stiffening Rib

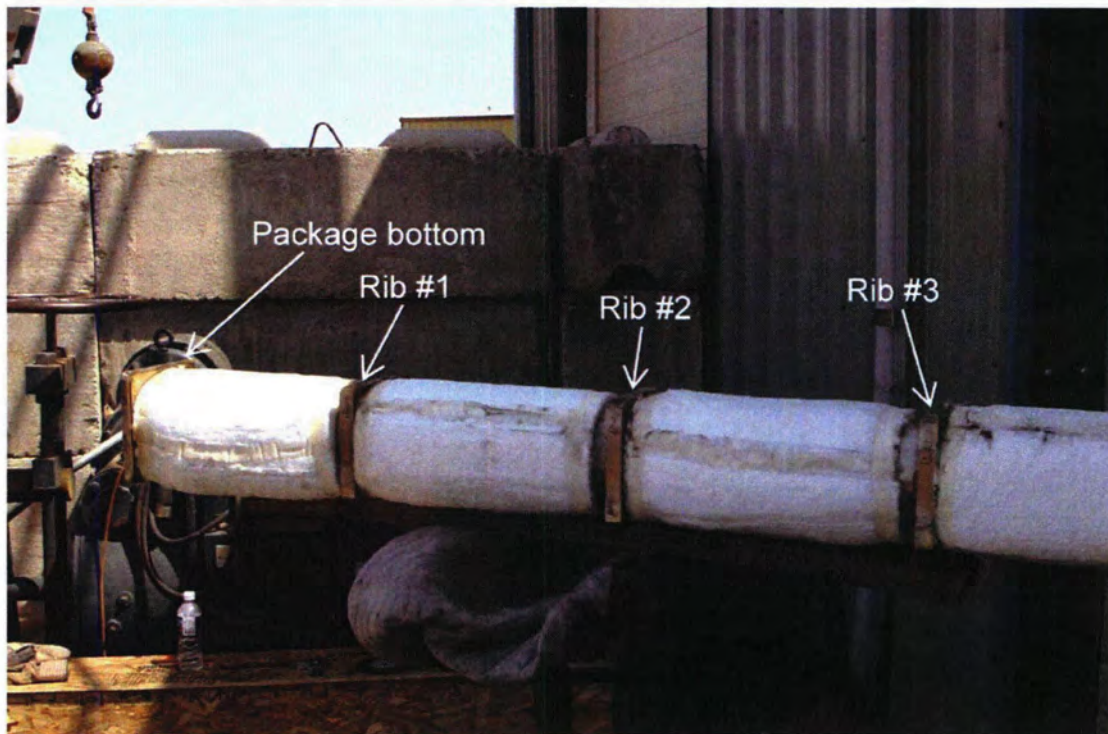


Figure 2.12.2-22 - Exposed Insulation - Overview

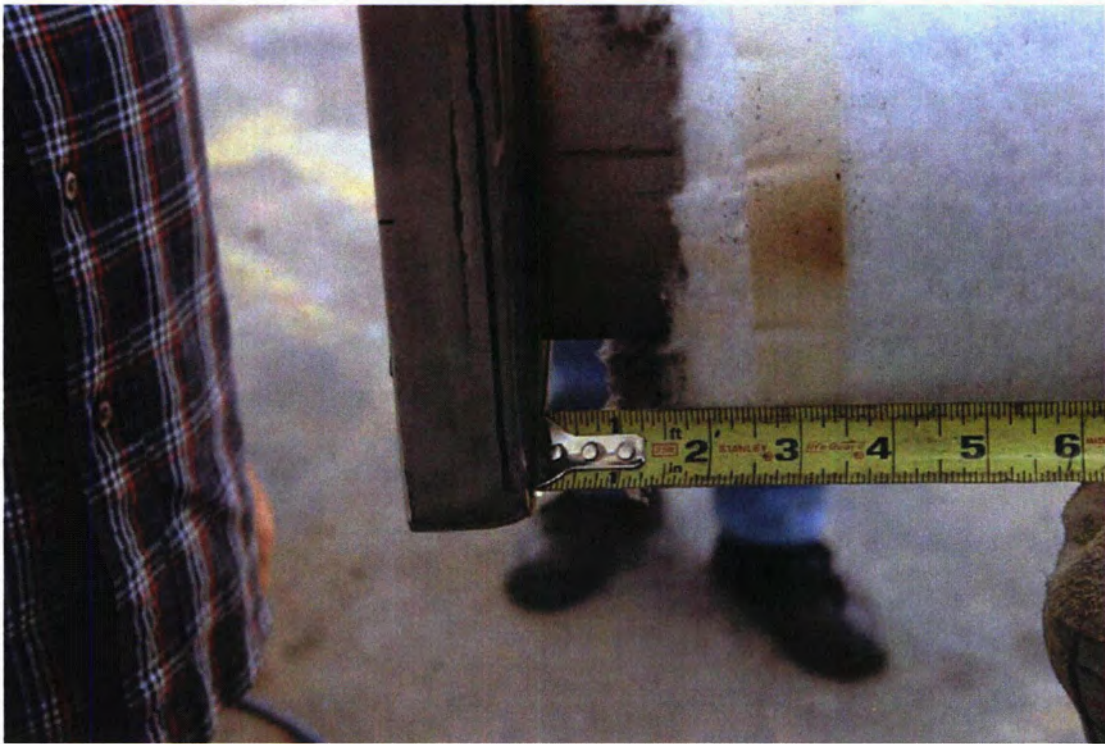


Figure 2.12.2-23 - Insulation Gap at Package Closure End



Figure 2.12.2-24 - Insulation Gap at Rib #3

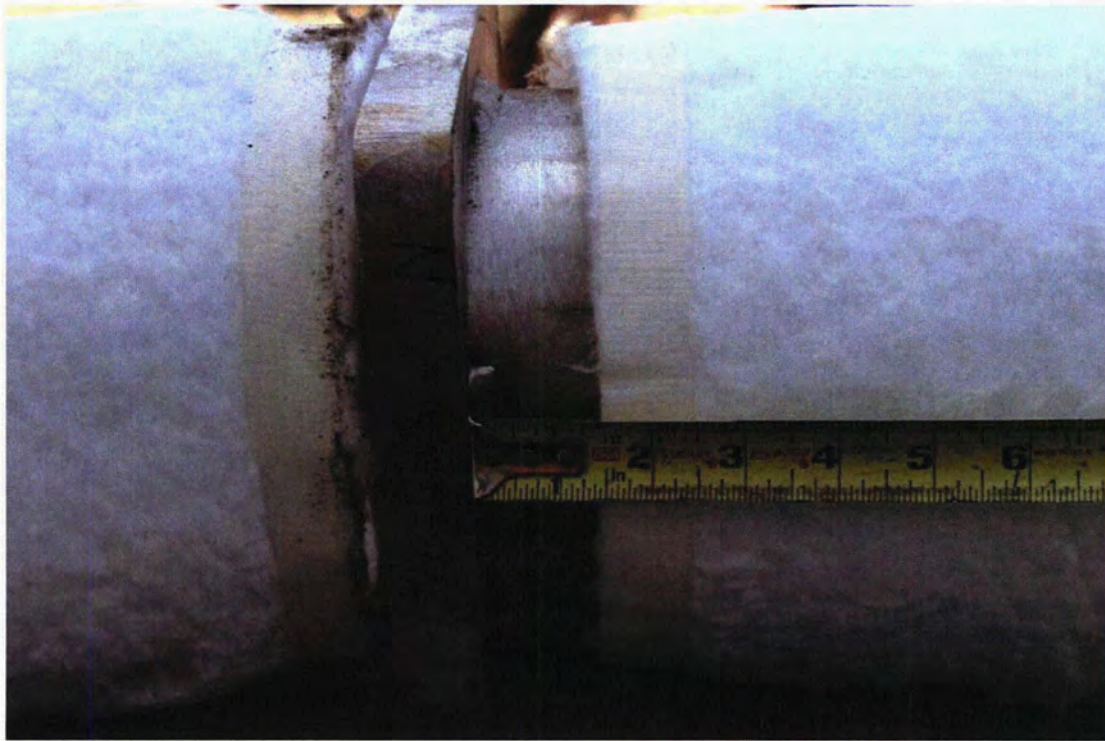


Figure 2.12.2-25 - Insulation Gap at Rib #2

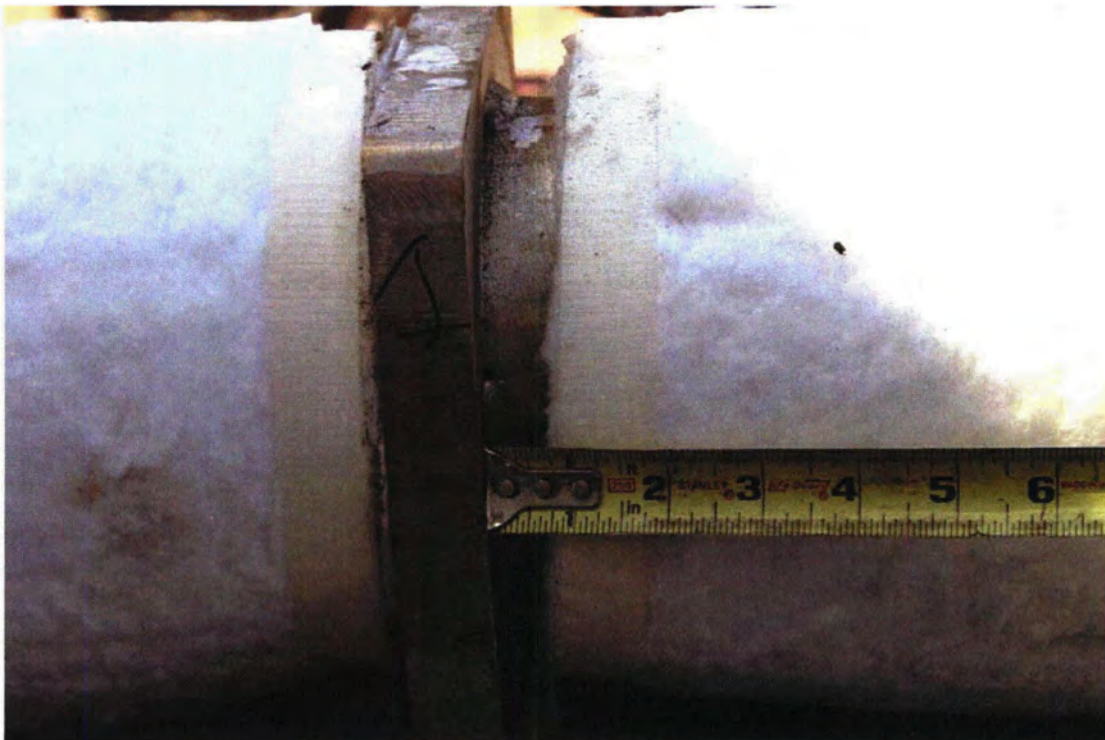


Figure 2.12.2-26 - Insulation Gap at Rib #1 (nearest impact)



Figure 2.12.2-27 - End Plate Insulation Condition

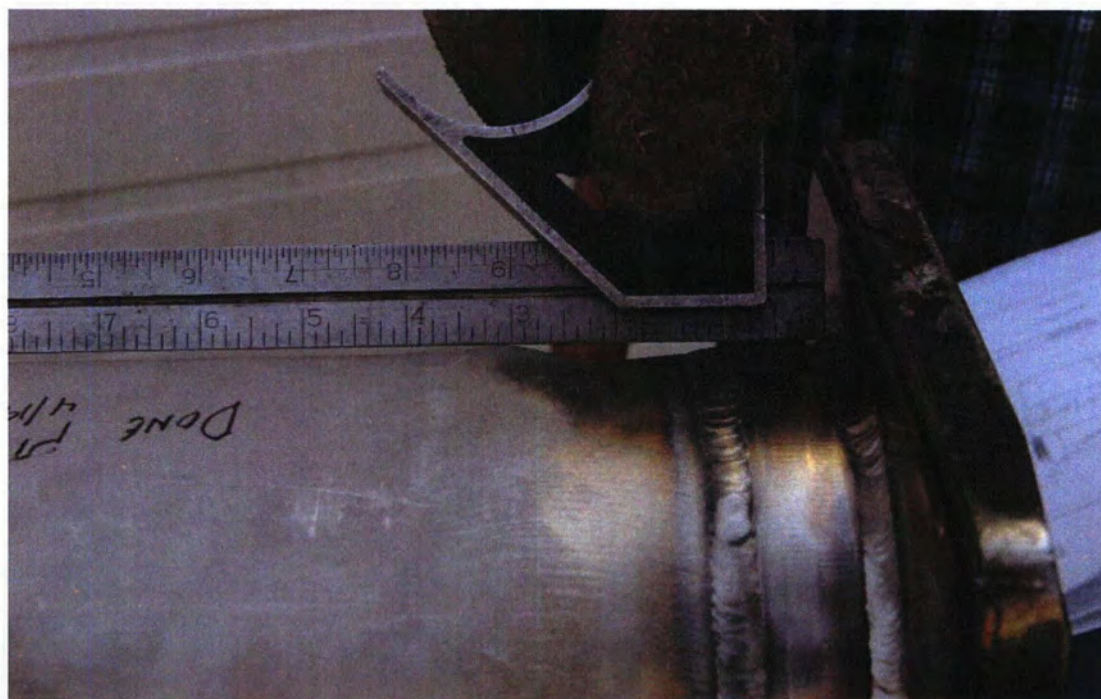


Figure 2.12.2-28 - Tube to Bottom End Plate – View 1



Figure2.12.2-29 - Tube to Bottom End Plate – View 2